DISSERTATION

Department of Earth Sciences
Freie Universität Berlin

Weichselian phases and ice dynamics of the Scandinavian Ice Sheet in northeast Germany

—

A reassessment based on geochronological and geomorphological investigations in Brandenburg

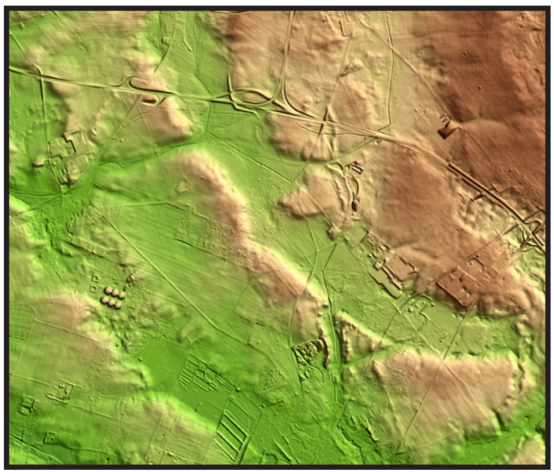

Jacob Hardt

Freie Universität Berlin

Berlin, 2017

Weichselian phases and ice dynamics of the Scandinavian Ice Sheet in northeast Germany

—

A reassessment based on geochronological and geomorphological investigations in Brandenburg

Dissertation

zur Erlangung des Doktorgrades
der Naturwissenschaften (Dr. rer. nat.)

am Fachbereich Geowissenschaften
der Freien Universität Berlin

vorgelegt von
Jacob Hardt

Berlin, 2017

First Supervisor

Prof. Dr. Margot Böse
Freie Universität Berlin
Institute of Geographical Sciences
Physical Geography
Malteserstraße 74-100
12249 Berlin
Germany

Second Supervisor

Prof. Dr. Markus Fuchs
Justus-Liebig-Universität Gießen
Department of Geography
Physical Geography
Schlossgasse 7
35390 Giessen
Germany

Date of Disputation

February 10, 2017

I ACKNOWLEDGEMENTS

First I want to thank Prof. Dr. Margot Böse, my supervisor. Her outstanding knowledge and her ideas were a major source of inspiration for me throughout the whole project. I greatly acknowledge her support and patience. Apart from my dissertation project, she triggered my fascination for Taiwanese landscapes and cultures, which I regard as a great gift.

I want to thank Ass. Prof. Dr. Christopher Lüthgens. His ideas, his knowledge, and his great talent to make difficult aspects of, e.g., luminescence, understandable to me were of an inestimable value and kept me motivated throughout the whole project. I am very thankful for his continuous support and also for his hospitality in Vienna.

I want to thank Dr. Robert Hebenstreit, who always had a sympathetic ear and helped me with good thoughts throughout my whole project. Our expedition to the Taiwanese high mountains was certainly a highlight I will never forget.

During my research project I had the opportunity to meet great researchers, who were willing to share ideas and knowledge with me. I am afraid this list will not be complete. Dr. Sven Lukas is thanked for, e.g., his tips concerning sediment description. Prof. Dr. Henrik Rother is thanked for inspiring discussions. Thanks to Dr. Jan Lentschke for introducing me into the ERT method. Prof. Dr. Manfred Frechen, Dr. Tony Reimann, Dr. Andreas Börner, Dr. Olaf Juschus, and Dr. Peter Gärtner are thanked for their advice during different stages of this project.

My dear colleagues at the Institute of Geographical Sciences made the last years very pleasant and scientifically inspiring! Thank you! Especially I want to mention Marc Bauersachs, Johanna Stößel, Dr. Michael Thelemann, and Dr. Chia-Han Tseng.

I want to thank all the students who participated in my project during the last years. In particular Sarah Mosser, Carolin Nitzsche, and Marc Becker are thanked for their efforts, help during fieldworks and in the laboratory, and inspiring discussions.

Thanks to Sven Ziegler for his firm will to undertake geophysical field measurements.

My friends Antonia Müller and Sebastian Emmerich are deeply thanked for proof reading this thesis.

With all my heart I want to thank my friends and family for their presence in my life. My parents Cornelia Dreves-Hardt and Prof. Uwe Dreves have always been supporting my studies. My wife Maria is my most important source of bliss. Thank you!

II ABSTRACT

The glacial formation of the young morainic landscape of northeast Germany has been investigated for more than 100 years. Different Weichselian advances of the Scandinavian Ice Sheet into northeast Germany were differentiated on basis of morphological and sedimentological findings. The chronology of the different phases was mostly based on long-distance correlations of radiocarbon ages or estimates. In recent years, a number of studies have shown that these traditional models require revision. Modern dating methods allow for direct dating of glaciofluvial or glacigenic deposits and high resolution digital elevation models reveal morphological details of the glacial landscape, which give new insights in the dynamics of the inland ice.

In this study, Optically Stimulated Luminescence (OSL) dating was applied to determine depositional ages of glaciofluvial sediments belonging to the Weichselian Brandenburg and Frankfurt phases at study sites in Brandenburg. The ice advance during the Brandenburg phase was dated to 34.1 ± 4.6 ka. The formation of the Brandenburg ice marginal position was dated to 30 ± 4 ka. For the first time the Frankfurt phase, the succeeding meltdown phase, was dated to 26.3 ± 3.7 ka. A landscape stabilization phase, as indicated by recalibrated exposure ages of glacigenic boulders, set in at around 24 ± 2 ka in middle Brandenburg. A phase of aeolian activity, possibly triggered by medieval human activity, was dated to ~1 ka.

Previously published cosmogenic exposure ages from erratic boulders were recalculated with an up-to-date ^{10}Be production rate, which significantly increased the ages. After recalculation, the cosmogenic exposure and OSL ages provide a consistent geochronological data base, which confirms a two-fold last glacial maximum in Brandenburg. The largest Weichselian ice-extent occurred during the Brandenburg phase in late marine isotope stage 3. This advance correlates with the Klintholm advance in Denmark and possibly an advance in middle Poland. At the time of the global last glacial maximum, the Pomeranian ice marginal position was formed (~20 ka).

The Barnim plateau, a till plain of the Brandenburg young morainic landscape, was reassessed concerning its glacial geomorphology. A qualitative geomorphological analysis of a laser scan digital elevation model revealed a succession of parallel, arcuate ridges in the middle Barnim region. According to outcrop studies and geophysical investigations, they consist of fine-grained, diamictic material. Their lengths vary up to 15 km and their widths are up to 1.5 km. They are interpreted as ice marginal fans, which were formed during the Frankfurt phase (the downwasting phase after the Brandenburg phase) around 26.3 ± 3.7 ka by an oscillation of the ice margin.

III ZUSAMMENFASSUNG

Die glaziale Entstehungsgeschichte der nordostdeutschen Jungmoränenlandschaft wird seit über 100 Jahren erforscht. Mehrere weichselzeitliche Vorstöße des Skandinavischen Inlandeises nach Nordostdeutschland konnten anhand von morphologischen und sedimentologischen Befunden nachgewiesen werden. Die Zeitstellung der verschiedenen Phasen beruhte hauptsächlich auf Verknüpfungen von entfernten Radiokohlenstoffaltern oder Schätzungen. In den letzten Jahren haben Studien gezeigt, dass die traditionellen Modelle revisionsbedürftig sind. Moderne Datierungsmethoden ermöglichen das direkte Datieren glazifluvialer oder glazigener Ablagerungen und mithilfe hochaufgelöster digitaler Geländemodelle können bisher unerkannte Glazialformen detektiert werden, die neue Einblicke in die Dynamik der Inlandvereisungen geben.

Im Rahmen dieser Arbeit wurden mittels Optisch Stimulierter Lumineszenz (OSL) Ablagerungsalter von glazifluvialen Sedimenten ermittelt, die den weichselzeitlichen Brandenburg- und Frankfurt-Phasen angehören. Der Eisvorstoß während der Brandenburg-Phase wurde auf 34.1 ± 4.6 ka datiert. Die Bildung der Brandenburger Randlage wurde auf 30 ± 4 ka datiert. Erstmalig wurde die Frankfurt-Phase, die anschließende Niederschmelzphase, auf 26.3 ± 3.7 ka datiert. Eine Phase der Landschaftsstabilisierung setzte ab 24 ± 2 ka im mittleren Brandenburg ein, was aus rekalibrierten Oberflächenexpositionsaltern von Findlingen hervorgeht. Eine Phase äolischer Aktivität, möglicherweise ausgelöst durch mittelalterlichen menschlichen Einfluss, wurde auf ~1 ka datiert.

Bereits veröffentlichte Oberflächenexpositionsalter erratischer Blöcke wurden mit einer modernen ^{10}Be-Produktionsrate neu berechnet, was zu einer signifikanten Erhöhung der Alter führte. Mit der Neuberechnung ergeben beide Methoden eine solide geochronologische Basis, die bestätigt, dass das letztglaziale Maximum in Brandenburg zweigeteilt war. Die größte weichselzeitliche Eisausdehnung fand in der Brandenburg-Phase im späten marinen Isotopenstadium 3 statt. Dieser Vorstoß korreliert zeitlich mit dem Klintholm-Vorstoß in Dänemark und einem möglichen Eisvorstoß im mittleren Polen. Zur Zeit des globalen letztglazialen Maximums wurde die Pommersche Eisrandlage gebildet (~20 ka).

Das Barnimplateau, eine Grundmoränenplatte der Brandenburgischen Jungmoränenlandschaft, wurde hinsichtlich seiner glazialen Landformen neu untersucht. Durch eine qualitative geomorphologische Analyse eines hochaufgelösten laserscanbasierten digitalen Geländemodells wurde eine Abfolge von parallelen, bogenförmigen Rückenstrukturen im Bereich des mittleren Barnim detektiert. Aufschlussstudien und geophysikalische Untersuchungen ergaben, dass die Rücken aus feinkörnigem, diamiktischem Material bestehen. Ihre Längenausdehnung beträgt bis zu

15 km und ihre Breite bis zu 1.5 km. Die Rücken werden genetisch als „eisrandliche Fächer“ (ice marginal fans) interpretiert, deren Anlage durch eine Oszillation des Eisrandes während des Niederschmelzens des Eises während der Frankfurt Phase um 26.3 ± 3.7 ka einzuordnen ist.

IV TABLE OF CONTENTS

V LIST OF FIGURES

VI LIST OF TABLES

VII LIST OF UNITS AND ABBREVIATIONS

a	*Year*
AMS	*Accelerator Mass Spectrometry*
asl	*Above Sea Level*
BP	*Before Present (1950)*
CAM	*Central Age Model*
D_e	*Equivalent Dose*
D_r	*Dose Rate*
DEM	*Digital Elevation Model*
DRA	*Dynamic Range Adjustment*
ERT	*Electrical Resistivity Tomography*
GIS	*Geographic Information System*
Gy	*Gray*
ibid.	*Ibidem, "see preceding reference"*
IMP	*Ice Marginal Position*
IRSL	*Infrared-Stimulated Luminescence*
IR-RF	*Infrared Radiofluorescence*
ka	*Thousand years*
LiDAR	*Light Detection And Ranging*
LGM	*Last Glacial Maximum*
MAM	*Minimum Age Model*
MIS	*Marine Isotope Stage*
Ωm	*Ohm meter*
OSL	*Optically Stimulated Luminescence*
σ	*Sigma*
S1	*(Saalian) Drenthe phase*
S2	*(Saalian) Warthe phase*
SAR protocol	*Single-Aliquot Regenerative-dose protocol*
SED	*(cosmogenic nuclide) Surface Exposure Dating*
SIS	*Scandinavian Ice Sheet*
SRTM	*Shuttle Radar Topography Mission*
TL	*Thermoluminescence*
W_{1B}	*(Weichselian) Brandenburg phase*
W_{1F}	*(Weichselian) Frankfurt phase*
W_2	*(Weichselian) Pomeranian phase*

1 INTRODUCTION

1.1 MOTIVATION AND AIMS OF THIS STUDY

„Noch starrt das Land von fremden Zentnermassen;
Wer gibt Erklärung solcher Schleudermacht?
Der Philosoph, er weiß es nicht zu fassen,
Da liegt der Fels, man muß ihn liegen lassen,
Zuschanden haben wir uns schon gedacht.“

“Those foreign boulders scattered through the land:
Who knows what forces left them high and dry?
Philosophers all have failed to understand,
The rocks are there, and we must let them stand,
We’ve damaged them, already, where they lie.”

Mephistoteles says to *Faust* in: Johann Wolfgang von Goethe: Faust - Part II, act IV, scene I.
English translation by A.S. Kline.

This quote from one of the most famous plays of Goethe (Faust II, 1832) is a good starting point to introduce this thesis. Goethe himself speculated about the occurrence of erratic boulders in the German lowlands and in the Alps, and some even refer to him as the “discoverer of the ice age” (Cameron, 1965). At that time, erratic boulders seemed to be inexplicable natural phenomena. Nowadays we know about past inland glaciations and glacial transport processes, which explain their occurrence in the lowland areas.

The first considerations about extensive glaciations in the beginning of the 19th century (Bernhardi, 1832) were followed by the *concept of polyglaciations* (Penck, 1879). Nowadays, new methods allow for discovering and investigating new details on very different scale levels – from luminescence properties of single sand grains to kilometer-wide geomorphological features to the formation of complex landscapes.

Knowledge about past glacier dynamics, i.e., the timing of glacier advances and meltdown phases as well as the behavior of ice streams and ice margins, are important proxies. They are necessary to reconstruct the palaeoclimate of a certain region and to understand the mechanisms that trigger the movement of glaciers and ice sheets. In a further perspective, this knowledge is an important component regarding the prediction of future climate fluctuations and future glacier dynamics.

In very recent years, a number of studies were published, which address the ice-sheet-wide dynamics of the Scandinavian Ice Sheet (SIS) at different time slices (Hughes et al., 2015; Stroeven et al., 2016). These are built upon comprehensive databases that were published in individual papers over the last decades containing geomorphological, stratigraphical, and geochronological data. Looking at the amount of up-to-date data available for the north of Germany, information is comparably sparse.

Although the northeast German lowland has a long research history in Quaternary geology and glacial geomorphology, there is still a lack of robust numerical chronologies for various Quaternary

periods. This study aims to provide new geomorphological and geochronological data, especially for the Frankfurt phase of the Weichselian glaciation.

The dissertation project of Christopher Lüthgens, which was finished in 2011 at the Freie Universität Berlin, was a major source of inspiration for this thesis. The work of Lüthgens deals with optical dating of sandur deposits in the foreland of Weichselian ice marginal positions from the Brandenburg phase and the Pomeranian phase. The interjacent Frankfurt phase was not investigated in these preceding works and some questions remained concerning the geochronology of the Brandenburg phase. As a part of this thesis, sediments from both, the Frankfurt and the Brandenburg phase, were dated with optically stimulated luminescence.

In literature, the end moraines of the Frankfurt phase are subject to controversial debate. Some authors assume an advance of the SIS during the Frankfurt phase and describe a consecutive line of end moraines or end moraine like features. Other authors question whether an ice advance occurred during the Frankfurt phase. In order to contribute to this discussion, a high resolution digital elevation model was analyzed with focus on the glacial landforms.

Modern dating methods such as optically stimulated luminescence (OSL) and cosmogenic surface exposure dating allow for obtaining direct ages of glacigenic or glaciofluvial sediments. Especially in the case of cosmogenic exposure dating, a comprehensive database has been developed over the last decade. Compared to the OSL data, an age gap is often observed, which can not only be explained by the sampling of different kinds of landforms. Another aim of this study is to review existing geochronological data and to understand the apparent age gap between different methods.

1.2 Selection of the research area

While the research area in a broader sense is the northeast German lowland area, most of the detailed analyses were carried out on the Barnim plateau, a till plain to the north of Berlin. The Barnim plateau is traditionally correlated with the Frankfurt phase and was thus favored for the investigations. The long glacial-geomorphological research history offered the chance to reassess existing models and to integrate new results into the current state of research.

1.3 Remarks about the structure of this thesis

This doctoral thesis is mainly based on three research articles, which have already been published in international, peer-reviewed journals. Furthermore, one previously unpublished case study is contained in this thesis. I am the first author of the three previously published papers, planned and

conducted the field work, performed the analyses, wrote the manuscripts, and prepared all figures and maps. All co-authors contributed to different aspects of the workflow.

The first paper (chapter 4; Hardt et al., 2015) mainly deals with geomorphological investigations on the Barnim plateau. Analyses of maps and literature, combined with the analysis of a LiDAR (Light detection and ranging) digital elevation model (DEM) led to new results about the glacial geomorphology and especially the ice dynamics during the downwasting period of the Brandenburg phase in the study area.

The second paper (chapter 5; Hardt and Böse, 2016) reviews a set of geochronological data, which has been compiled from literature. Especially from cosmogenic exposure dating, a relatively large number of ages were published during the last decade dealing with the formation of Weichselian ice marginal positions south of the Baltic Sea and the onset of the succeeding downwasting phase. Recalculation of the previously published cosmogenic exposure ages resulted in a significant shift, which requires a different ice-dynamic and palaeoclimatic interpretation than stated in the original papers.

The third paper (chapter 6; Hardt et al., 2016) builds up on both previous papers. For the first time numerical OSL ages are presented for deposits correlated with the Frankfurt phase of the Weichselian glaciation. The determined ages are also connected to the geomorphological findings presented in paper 1. The results are integrated in a wider context, also regarding the recalculated ages introduced in paper 2.

In the case study (chapter 7), newly derived OSL ages from glaciofluvial deposits of the Brandenburg phase of the Weichselian glaciation are presented and discussed. The samples originate from a key site of the Brandenburg ice marginal position – the *Taubendorfer sandur*. The results are integrated into the other results of this thesis and into the state of research. Although this study site lies outside the main research area of this work, the results are crucial because they strengthen the previous findings and complete the picture of a new Weichselian ice-dynamic model in northeast Germany.

Table 1 lists the applied methods and their importance to each individual paper and the case study.

Table 1: Applied methods and their importance to each paper and the case study. **+++** main method of the paper; ++ important method of the paper; + method relevant to the paper.

	field work	*geophysics*	*GIS analyses*	*DEM interpretation*	*OSL dating*	*literature review*	*statistical analyses*
Paper 1	++	++	++	**+++**		++	
Paper 2			+	+		**+++**	**+++**
Paper 3	++	+		+	**+++**	++	++
Case study			+		**+++**	++	++

2 RESEARCH AREA

2.1 A BRIEF SUMMARY OF THE HISTORY OF ICE AGE RESEARCH

In 1832, Bernhardi articulated the possibility that ice, originating in the polar regions, had extended into northern Germany and the neighboring countries. He based his theory on the abundance of erratic boulders found in northern Germany, which could be explained as morainic material. Louis Agassiz and Karl Friedrich Schimper collected and published evidence of a former more extensive glaciation in the Alps in the 1830ies. The term *Die Eiszeit (the ice age)* was used by Schimper in written form for the first time in 1837 (summarized in Woodward, 2014).

However, it was not before the findings of Swedish geologist Otto Torell (1875) and the book *The Great Ice Age* by Geikie (1874) among others, that the formerly predominant *drift ice theory* was consequently replaced by the *glacial theory*. The drift theory goes back to Lyell who interpreted erratics as ice rafted debris in a sea (e.g., Lyell, 1853: 155). In the limestone quarry Rüdersdorf, located in the south of the Barnim plateau, Torell observed striations in bedrock, which were indicative of erosion by active glacier ice (Fig. 1).

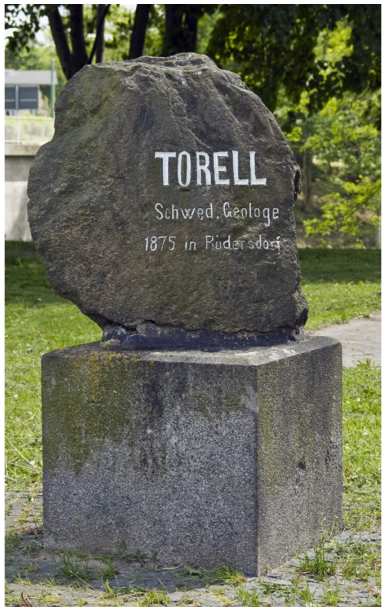

Fig. 1: Memorial stone dedicated to Swedish geologist Otto Torell in Rüdersdorf, where he observed glacial striations in bedrock in 1875.

Penck and Brückner (1909) set up a stratigraphical framework in the Alps, differentiating between four glacial and four interglacial stages. Their work paved the way for the so-called concept of poly-glaciations (summarized in Woodward, 2014). In the north of Germany, three different glacial stages have subsequently been identified; named Elsterian, Saalian, and Weichselian (summarized in Ehlers et al., 2011). Milutin Milankovitch (1879 – 1958) carried on the work of James Croll (1821 – 1890),

and explained changes in the earth's climate by astronomical factors. Milankovitch showed that the sunlight intensity had varied significantly over the last 600 ka and he identified low points which would correlate with the glacial stages of Penck and Brückner (1909) (summarized in Berger, 1988; Bard, 2004; Paillard, 2015). Additional to these extraterrestrial factors, tectonic processes were also an important factor triggering the onset of the ice age. As an example, the drift of Antarctica toward the South Pole in the Paleogene, the Alpine orogeny in Europe and Asia, and the Pliocene closing of the Isthmus of Panama, influenced the global oceanic circulation and the global climate significantly (Raymo and Ruddiman, 1992; Smith and Pickering, 2003).

2.2 The Pre-Quaternary evolution of northeast Germany

During the Paleogene and Neogene, the north of Germany was an accumulation area, dominated by the deposition of a variety of marine and perimarine sediments (Standke, 2015). Brandenburg was situated in the southeast of the *Northwest European Tertiary Depression*, which was influenced by several sea-level changes (trans- and regression cycles) of the Palaeo North Sea (ibid.). The widespread occurrence of lignite, especially in the south of Brandenburg, is a result of the repeated existence of coastal bogs in this area (ibid.). Toward the end of the Neogene, the environmental conditions changed drastically and big parts of northern Germany were dominated by terrestrial, especially fluvial, processes (Lippstreu et al., 2015).

2.3 The Quaternary of northeast Germany

The *Quaternary*, the youngest geological system, is subdivided into the series *Pleistocene* and *Holocene* (Cohen and Gibbard, 2011). The northeast of Germany was glaciated by the Scandinavian Ice Sheet (SIS) repeatedly during the glacial stages (Elsterian, Saalian, Weichselian; Table 2) of the Pleistocene. The names date back to the Prussian geological survey, which first used them on map sheets in the beginning of the 20th century (Ehlers et al., 2011). Figure 2 gives an overview of the Pleistocene main ice marginal positions in northeast Germany.

Although several cold- and warm-phases occurred during the early Pleistocene, the first clear glacial deposits are documented from the Elsterian glaciation (Ehlers et al., 2011). Whether the Elsterian ice advances took place in marine isotope stage (MIS) 10 or MIS 12 is still up for debate (Lippstreu et al., 2015). The maximum extent of the Elsterian glaciation is indicated by the so-called flint line (*Feuersteinlinie*) in Saxony-Anhalt, Thuringia, and Saxony (Litt et al., 2007). In some places two Elsterian till layers were found, which correspond to two different ice advances. The till layers are occasionally embedded in varved clay layers. Those clay layers are relicts of lakes, which were dammed by the SIS (Junge and Eissmann, 2000). During the downwasting of the first Elsterian ice

advance, subglacial meltwater runoff coupled with neotectonic subsidence of central Europe, was causing deep incision (up to 500 m) into Weichselian, Tertiary, and also pre-Tertiary layers. As a result, a system of elongated deep channels with a general northeast-southwest orientation developed in northeast Germany (Stackebrandt, 2009).

Table 2: Stratigraphical chart of the Pleistocene of Brandenburg. Simplified and modified after Lippstreu et al. (2010). Note: The positions of the W_1 and W_2 phases have been placed according to the outcome of this thesis. All other information is based on the stratigraphical chart of Brandenburg. In some stratigraphical charts, e.g., Pillans and Gibbard (2012), the boundary between Middle and Late Weichselian is placed at the beginning of MIS 2.

<table>
<tr><th>MIS</th><th>System</th><th colspan="4">Series</th></tr>
<tr><td>1</td><td rowspan="13">Quaternary</td><td colspan="4">Holocene</td></tr>
<tr><td rowspan="3">2</td><td rowspan="11">Pleistocene</td><td rowspan="8">Weichselian glacial</td><td>Late Weichselian</td><td>Younger Dryas
Alleröd interstadial
Older Dryas
Bölling interstadial
Oldest Dryas
Meiendorf interstadial</td></tr>
<tr><td rowspan="2">Middle Weichselian (Weichselian Pleniglacial)</td><td rowspan="2">Mecklenburg phase W_3
Pomeranian phase W_2

Frankfurt phase W_{1F}
Brandenburg phase W_{1B}</td></tr>
<tr><td></td></tr>
<tr><td>3</td><td></td><td rowspan="2">Early Weichselian</td><td rowspan="2"></td></tr>
<tr><td>4</td></tr>
<tr><td>5a

5d</td><td></td><td></td></tr>
<tr><td>5e</td><td colspan="3">Eemian interglacial</td></tr>
<tr><td>6</td><td rowspan="2">Saalian glacial</td><td>Upper Saalian</td><td rowspan="2">Warthe phase S2
Drenthe phase S1</td></tr>
<tr><td>?</td><td>Lower Saalian</td></tr>
<tr><td>9? / 11?</td><td colspan="3">Holstein interglacial</td></tr>
<tr><td></td><td colspan="3">Elsterian glacial</td></tr>
</table>

Deposits of the succeeding Holstein interglacial can be found in those Elsterian channels. During the Holstein interglacial (Holsteinian), a marine transgression occurred in Mecklenburg-Vorpommern (Ehlers et al., 2011). Several limnetic-terrestrial archives were investigated with palynological methods. The climate first changed from subarctic to boreal, to temperate conditions – and then back to subarctic conditions (Litt et al., 2007). The duration of the vegetation period during the Holstein interglacial was estimated to 15000 - 16000 years, according to varve chronologies (Meyer,

1974). Based on ^{230}U/Th dating of peat layers (Bossel site, northern Germany), Geyh and Müller (2005) correlate the Holstein interglacial with MIS 9. However, other authors correlate the Holsteinian with MIS 11 (e.g., Grün and Schwarcz, 2000; Candy et al., 2014; Szymanek, 2016; Tye et al., 2016) or consider the occurrence of more than one temperate stages with Holsteinian vegetational sequences (Scourse, 2006).

The Saalian glacial is divided into a lower and an upper stage. The Lower Saalian was characterized by several climatic fluctuations. The Saalian ice advances into the research area occurred during the Upper Saalian (Lippstreu et al., 2010).

Fig. 2: Overview map of Quaternary main ice marginal positions in northeast Germany and adjoining areas. Ice marginal positions compiled from Ehlers and Gibbard (2004) and Liedtke (1981). The white line represents the maximum ice extent during the Elsterian glacial. Map based on SRTM data (Jarvis et al., 2008).

During the Lower Saalian, the deposition of fluvial material prevailed in the study area. From the ('southern') mineral composition of fluvial deposits it could be reconstructed that the Elbe river took its course into the Berlin area from the late Elsterian on up to the early Saalian (summarized in Thieke, 2010). The formation of the so-called *Tranitzer Fluviatil* in southern Brandenburg, which is also characterized by a certain component of minerals originating from the lower mountain ranges, took place during the Lower Saalian, too (Lippstreu et al., 2015; see chapter 7 for details).

The two major ice advances of the Upper Saalian are named *Drenthe stadium* and *Warthe stadium*. Both advances probably occurred in MIS 6 (Litt et al., 2007). Glaciofluvial sediments (fine to middle sands; gravelly sands) deposited in the foreland of the advancing Drenthe stadium are widespread in Brandenburg and can be distinguished from the Lower Saalian fluvial deposits by its lithology (Lippstreu et al., 2015). The first Drenthe advance covered all of Brandenburg and reached into Thuringia, Saxony-Anhalt and Saxony but was less extensive than the preceding Elsterian advances (Fig. 2). Subglacial erosion was less intensive than during the Elsterian glacial, indicated by the lower frequency and lower depth of respective subglacial channels (ibid.). In the region of Barnim and Lebus, till layers with a thickness of 10 – 20 m are reported for this phase (Lippstreu and Zwirner, 1972). The youngest Saalian ice advance, the Warthe stadium (Warthanian), reached into the south of Brandenburg (Fläming, Lusatia) and was less extensive than the Drenthe advance. Again, till layers and glaciofluvial sediments were deposited. The corresponding till is widely found in Brandenburg and its thickness usually ranges between 30 – 40 m (Lippstreu et al., 2015). The deformation of older landforms caused by oscillations of the inland ice complicate the exact localization of a terminal position. The Saalian Late Glacial is documented in the onset of limnetic sedimentation in kettle holes (e.g., Kühner and Strahl, 2008). Palynological analyses revealed a succession of four different vegetational phases (Hermsdorf and Strahl, 2008).

The Eemian interglacial occurred in MIS 5e (Shackleton et al., 2003) and lasted from 127.2 ka to ~115 ka (Litt et al., 2007; Litt and Gibbard, 2008). According to palynological analyses, the climatic changes were comparable to those of the Holsteinian. Compared to the Holocene, the climate was probably a bit warmer, along with a higher global sea level (Ehlers et al., 2011). Terrestrial Eemian sediments can be frequently found in northeast Germany. For example, in Berlin and Brandenburg, 566 (limnetic) Eemian sites have so far been mapped (Hermsdorf and Strahl, 2008). Unlike the Holsteinian interglacial deposits, the Eemian deposits are not connected to glacial or subglacial channels, but rather occur in isolated small scale basins (ibid.).

The Weichselian glacial lasted from the end of the Eemian until the end of the Pleistocene, i.e. from MIS 5d to the onset of MIS 1 (~115 ka to 11.7 ka; Cohen and Gibbard, 2011). Although northern Europe was glaciated during the Early Weichselian, northeast Germany was not glaciated before the

Middle Weichselian (MIS 4 – 3). An early ice advance into Schleswig-Holstein (*Ellund* advance), which correlates with the *Ristinge* advance in Denmark at ~50 ka (Houmark-Nielsen, 2010), was reconstructed from sedimentological data and OSL/TL dating (summarized by Stephan, 2011). On basis of facies analyses, Müller (2004) identified a specific early Weichselian till in northwest Mecklenburg (termed *Warnow* phase), which might also occur in the north of Brandenburg (Perleberg). The deposition of this till could correlate with the Ellund advance. However, robust ages and further evidence of such an extensive early Weichselian advance still need to be provided (Lippstreu et al., 2015).

The Brandenburg (W_{1B}), Frankfurt (W_{1F}), and Pomeranian (W_2) phases are the three most important phases of the Weichselian in northeast Germany. Most of the present landforms were shaped or modified during these glacial events. The main geomorphological structure of Brandenburg with its plateaus and depressions (‘*Platten und Niederungen’*) is a result of the Weichselian glaciations. As an outcome of this study, parts of the ‘traditional’ geomorphological-geochronological state of research have to be reassessed. The results are presented and discussed in the following chapters. To avoid confusion and repetitions, only a brief overview of the Weichselian main advances is given in the following paragraphs.

The Brandenburg phase represents the most extensive ice advance of the Weichselian (Fig. 2). Its ice marginal position is located to the north of the Glogow-Baruth ice marginal valley in Brandenburg. The localization is equivocal because clear end moraine-like features are scarce (Lippstreu et al., 2015). Juschus (2010) summarized evidence of a maximum W_{1B} advance 2 – 12 km south of the main IMP. Till of the W_{1B} advance is frequently found at the surface in middle Brandenburg, especially on the different plateaus (e.g., Barnim plateau, Nauener plateau, Teltow plateau, Glien; Lippstreu et al., 2015). A thickness of the till up to 30 m has been reported, but it usually ranges below 10 m (ibid.). According to the comparably low thickness of the till and a limited glacigenic deformation of underlying sediments, Brose (1995) infers a relatively low thickness of the ice sheet in this area. In the Polish Quaternary stratigraphy, the Leszno phase is parallelized with the W_{1B} phase (Börner, 2007).

The Frankfurt phase is regarded as a longer lasting recessional halt of the W_{1B} ice masses, at least in northeast Germany (Cepek, 1965). In Poland, the corresponding Poznan phase (Börner, 2007) is interpreted as a readvance of the SIS (Marks, 2012). Morphological evidence for a distinct IMP is scarce (Liedtke, 1981; Gärtner, 1993; Bussemer, 1994) and the IMP is sometimes predefined by older (Saalian) landforms (Hannemann, 2005).

In contrast, the IMP of the Pomeranian phase can mostly be well recognized by distinct ice-marginal landforms, which were formed by a strong readvance of the SIS (Liedtke, 1981). In the hinterland of the Pomeranian IMP, a till with an average thickness of 20 m was deposited (in Brandenburg). Tertiary or Cretaceous blocks (*Schollen*), relocated by the SIS, can be found (Lippstreu et al., 2015). A hummocky topography characterizes the young morainic landscape of the W_2 phase.

In the Late Glacial, after the final downwasting of the SIS in the research area, several changes of colder and warmer phases occurred. During this period periglacial-fluvial processes modified the glacial landscape. Present-day dry valleys were incised, the infill of basins set in, and alluvial fans were deposited. Deflation holes, dunes and cover sands are relicts of Late Glacial aeolian processes, which are typical for the young morainic landscapes. Another paraglacial modification of the landscape originated from delayed melting of buried dead ice, resulting in the development of kettle holes and lakes of different sizes (Lippstreu et al., 2015).

Table 3 lists a summary of existing geochronological data for the Weichselian main IMPs of northeast Germany. The chronologies are discussed in later sections of this thesis. The table is intended to give a brief overview of published ages. The presented ages, derived by different methods (or estimates), should not be taken as face values and are not necessarily comparable, because different processes, landforms and materials have been dated. This issue is also discussed in other sections of this thesis.

Table 3: Summary of geochronological data for Weichselian main IMPs of northeast Germany. *Radiocarbon ages recalibrated with OxCal 4.2 (c14.arch.ox.ac.uk/oxcal/) and the IntCal13 atmospheric curve (Reimer et al., 2013). ^Cosmogenic exposure ages (SED) were recalibrated with a recent ^{10}Be production rate – see sections 3.2 and 5 for details.

Phase	Age	Method	Reference
Pomeranian W_2	20.1 ± 1.6 ka	OSL	Lüthgens et al., 2011b
	19.4 ± 2.4 ka	OSL	Lüthgens et al., 2011b
	17.7 ± 0.9 – 15.4 ± 0.6 → 19.5 ± 1.4 – 17 ± 1.1^	SED (^{10}Be) SED (^{10}Be) recalibrated	Heine et al., 2009 Hardt & Böse, 2016
	15.6 ± 0.6 → 17.3 ± 1.6^	SED (^{10}Be) SED (^{10}Be) recalibrated	Rinterknecht et al., 2014 Hardt & Böse, 2016
	17.6 → 19.7 – 19.4 cal ka BP*	Radiocarbon	Kozarski, 1995
Frankfurt W_{1F}	18.8 → 22.8 – 22.4 cal ka BP*	Radiocarbon	Kozarski, 1995
Brandenburg W_{1B}	~20 ka BP	estimate	Liedtke, 1981; Kozarski, 1995
	21 ka → 25.5 – 25.2 cal ka BP*	Radiocarbon	Marks, 2002
	<34.1 ± 3.0	OSL	Lüthgens et al., 2010b
	<34.4 ± 7.0	OSL	Lüthgens et al., 2010a
	27.7 ± 4.0	OSL	Lüthgens, 2011

2.4 Introduction into the study area – The Barnim plateau

The Barnim plateau is a till plain in the federal states of Brandenburg and Berlin with a size of some 1900 km². Within the geomorphological structure of Brandenburg, it represents one major morphogenetic unit. The main morphogenetic units of Brandenburg are the (glacio-)fluvial lowlands and the glacigenic plateaus (Stackebrandt and Lippstreu, 2010).

The name *Barnim* probably goes back to the Polabian (Slavic) language where *Barnim* was a documented person's name. Less likely is that the name is derived from the old Polabian term *bara*, which can be translated into English as *swamp* (Fritze, 1987). Apart from the plateau, *Barnim* is nowadays also the name of a district of the federal state Brandenburg. With a size of roughly 1500 km² it is not congruent with the till plain, extends farther to the north and is less extensive to the east.

The Berlin city districts Reinickendorf, Mitte, Friedrichshain-Kreuzberg, Pankow, Lichtenberg, and Marzahn-Hellersdorf are - at least partially - located on the Barnim plateau. However, the biggest proportion of the plateau (~90 %) is situated in Brandenburg.

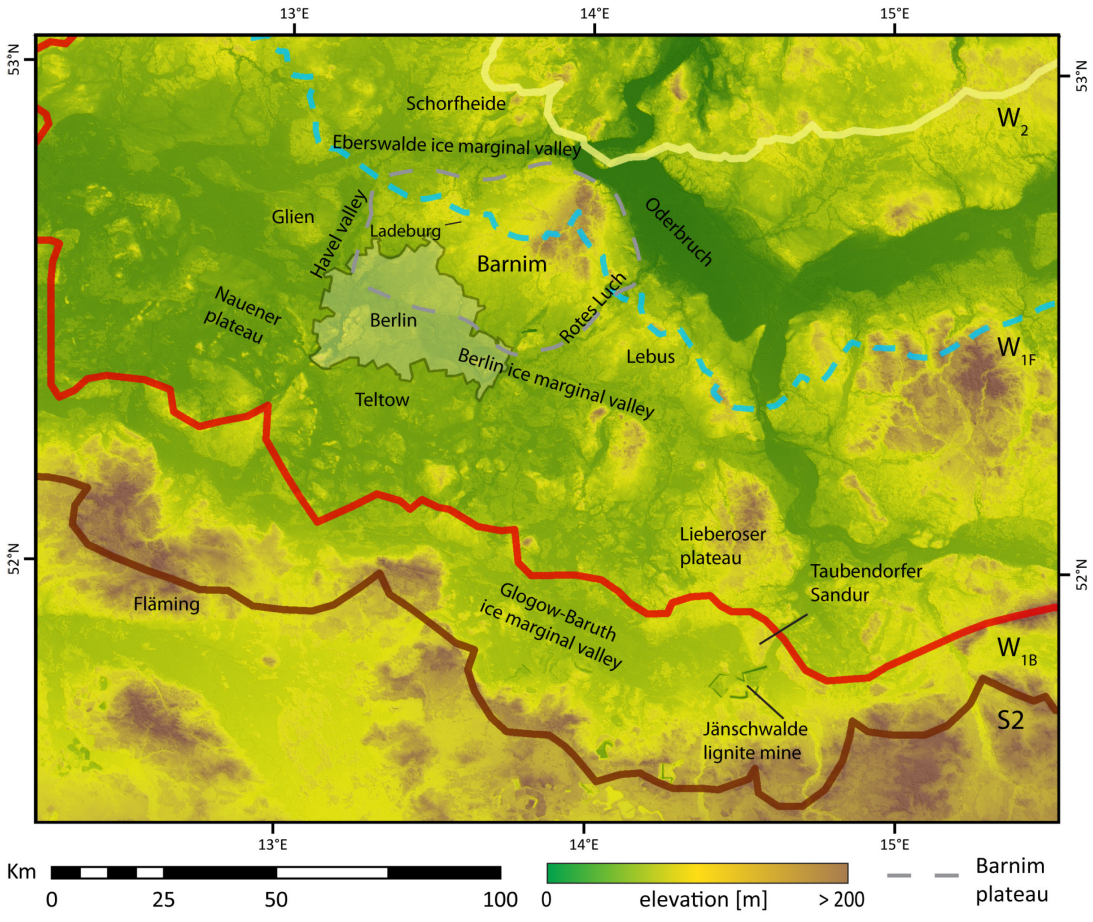

Fig. 3: Overview map of the Barnim plateau and surrounding landscape elements. See Fig. 4 for a more detailed map of the Barnim plateau. Map based on SRTM data (Jarvis et al., 2008).

To the north, the plateau is bounded by the Thorn-Eberswalde ice marginal valley. To the east the Oderbruch depression and to the west the Havel valley represent its natural limits. To the south, the border is the Warsaw-Berlin ice marginal valley. To the south-east, the Barnim plateau is separated from the Lebus plateau by the Rotes Luch valley (Fig. 3).

The present-day land use of the Barnim plateau is heterogeneous. Urban areas mostly occur in and around the city of Berlin. Rural areas spread over the plateau. Forestry and agriculture are carried out on large proportions of the plateau. Some parts of the plateau are under the protective rules of the *Naturpark Barnim* (nature park) administration.

Geomorphologically, the Barnim plateau can be divided into three units: the western, middle, and eastern Barnim (Fig. 4). The Weichselian outwash plains of the western Barnim are relatively flat. The middle Barnim is characterized by several till islands and intermediate depressions. Gärtner (1993) described the middle Barnim topography as a 'garland-like structure of flat undulating ridges and depressions' (German: "[…] Struktur girlandenförmig angeordneter, flachwelliger Schwellen und Becken […]"; Gärtner, 1993: 6), without further interpretation of these landscape elements. The description and interpretation of these landforms (Fig. 4) is one major topic of this thesis (see sections 4; 6; 8). The eastern Barnim has the highest elevations. Here, Tertiary and Quaternary material form a push moraine complex, which was shaped by Saalian ice advances (Hannemann, 2005).

According to, e.g., Woldstedt (1925), Schneider (1965), and Liedtke (1981), the Frankfurt IMP traverses the Barnim plateau, although the exact localization varies according to each author (Fig. 18).

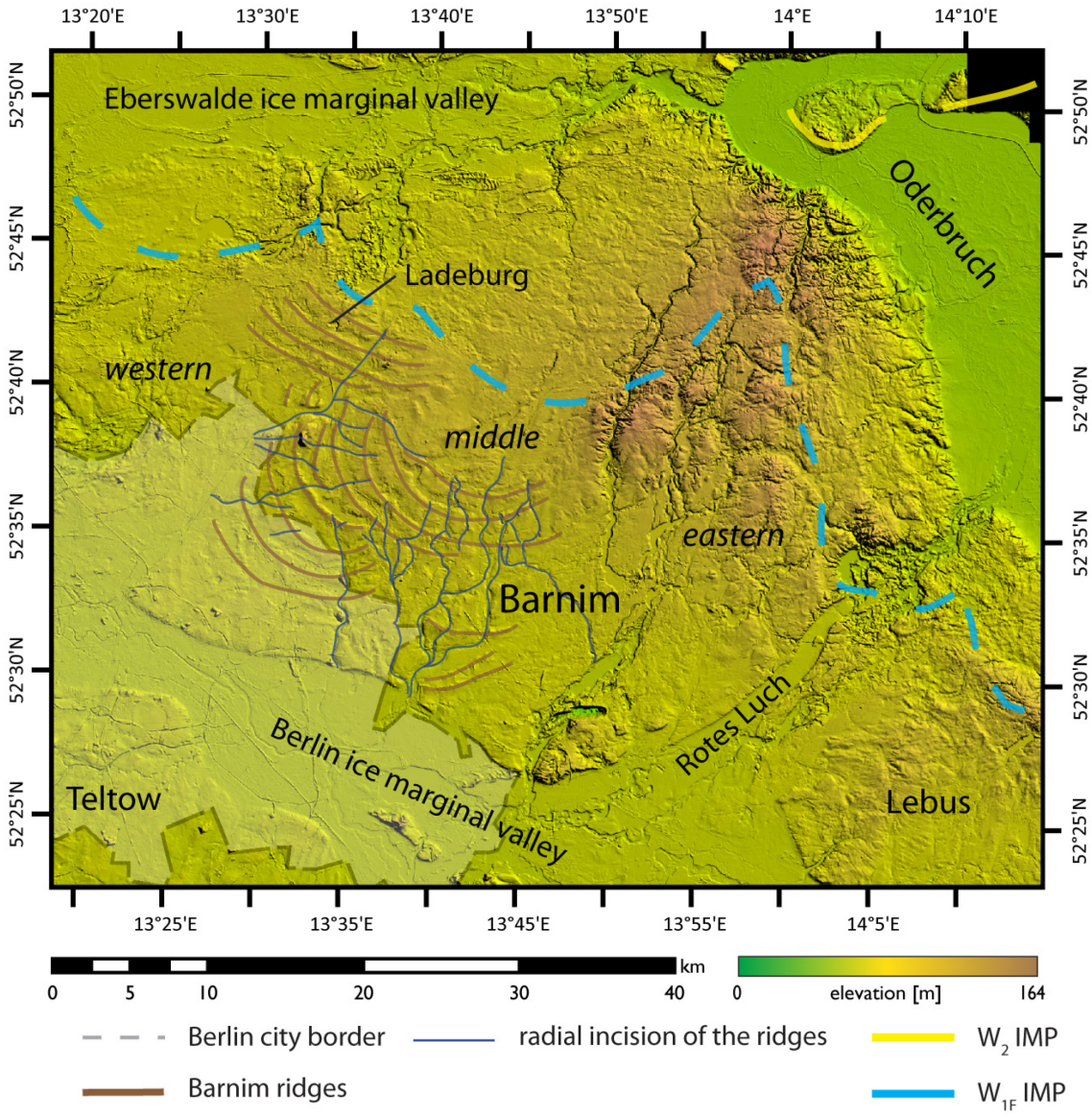

Fig. 4: Color coded hillshade map of the Barnim plateau. The ridge structures are indicated by brown lines. The radial incision of the ridges is indicated by dark blue lines – these lines do not represent the present-day drainage network. Ice marginal positions after Liedtke (1981). Map based on LiDAR data (Geoportal Berlin and Federal Institute for Geosciences and Natural Resources Brandenburg).

3 METHODS

In the following, a detailed overview of the applied geomorphological and geochronological methods is given. As the methods are only briefly described in the respective papers, this chapter provides some more fundamental information about source, analysis, and interpretation of the data presented in this thesis.

3.1 TERRAIN ANALYSIS WITH HIGH RESOLUTION DIGITAL ELEVATION DATA

3.1.1 DATA ACQUISITION AND PROPERTIES

The Light Detection and Ranging (LiDAR) digital elevation model (DEM) used in this study was acquired from the *Federal Institute for Geosciences and Natural Resources Brandenburg* and the *Senate Department for Urban Development and the Environment Berlin (Geoportal Berlin)*. As part of the border between the federal states Berlin and Brandenburg lies in the southwest of the Barnim plateau, data acquisition from both respective federal agencies was necessary.

The LiDAR data was obtained from airborne measurements, which took place during the years 2007 – 2008 (Berlin) and 2009 (Brandenburg). The DEM data for all areas in Brandenburg has a horizontal resolution of 1 m and the DEM data of Berlin has a horizontal resolution of 2 m. The respective metadata for both DEM are listed in table 4.

Table 4: Metadata of acquired DEM. Data collected from the respective providers.

Federal state	**Provider**	**Creation date**	**Horizontal resolution**	**Vertical accuracy**	**Reference frame**	**Height reference**
Brandenburg	*Federal Institute for Geosciences and Natural Resources Brandenburg*	2009 (for research area)	1 m	0.3 – 0.5 m	ETRS89 - UTM Zone 33N	DHHN92
Berlin	*Senate Department for Urban Development and the Environment Berlin (Geoportal Berlin)*	2007 - 2008	2 m	not stated by the provider	ETRS89 - UTM Zone 33N	DHHN92

For airborne laser scanning, the LiDAR system is mounted on an airplane, helicopter or unmanned aerial vehicle. The LiDAR system, which has an integrated global positioning system (GPS), transmits light pulses toward the ground (Wehr and Lohr, 1999; Rutzinger et al., 2011). The light is scattered and reflected by the earth's surface or objects on the earth's surface (Liu, 2008). The LiDAR system

receives the reflected return signals and calculates the distance between sensor and object by the time it took to receive the return signal. The data is saved in a so-called point cloud, where the measured points are stored inside a three-dimensional coordinate system (Otepka et al., 2013). The point cloud can finally be used to generate a raster grid DEM (Leberl et al., 2010) for further processing in a geographic information system (GIS).

In vegetated areas, a LiDAR sensor can receive multiple return signals from one single emitted pulse because the laser is able to penetrate vegetation (Fig. 5). In this case the first return signal represents the top of the plant material and the last return signal represents the bare earth surface (Leberl et al., 2010; Oguchi et al., 2011; Tarolli, 2014). By using the last return signal for DEM generation, the vegetation can be excluded from the DEM. This is a big advantage over, e.g., the spaceborne SRTM (Shuttle Radar Topography Mission) DEM, which includes vegetation. In Hardt et al. (2015) it was shown that forested areas in the middle Barnim region obscure landforms in the SRTM DEM, which could only be recognized in the LiDAR DEM.

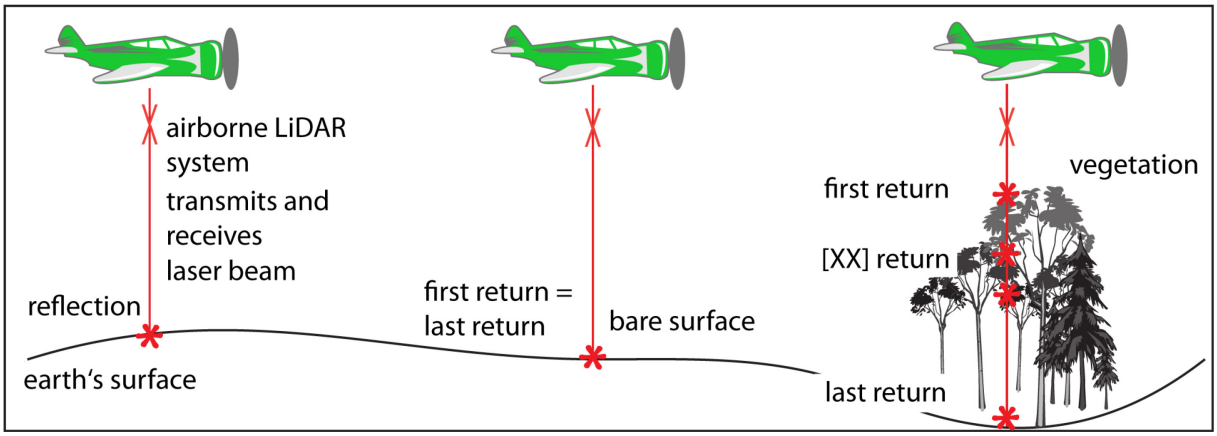

Fig. 5: Basic principles of airborne LiDAR.

Apart from the advantage of representing the bare earth surface, another advantage of the LiDAR data is its higher ground resolution. The ground resolutions of the freely available DEM, such as SRTM (90 m), ASTER (30 m, Advanced Spaceborne Thermal Emission and Reflection Radiometer), and XSAR SRTM (25 m), are still far above the 10 m-threshold. However, a horizontal resolution of <10 m is usually recommended for the analysis of geomorphic processes (Zhang and Montgomery, 1994; Tarolli and Tarboton, 2006). A comparison of the resolution between the different mentioned DEM is given in Fig. 6.

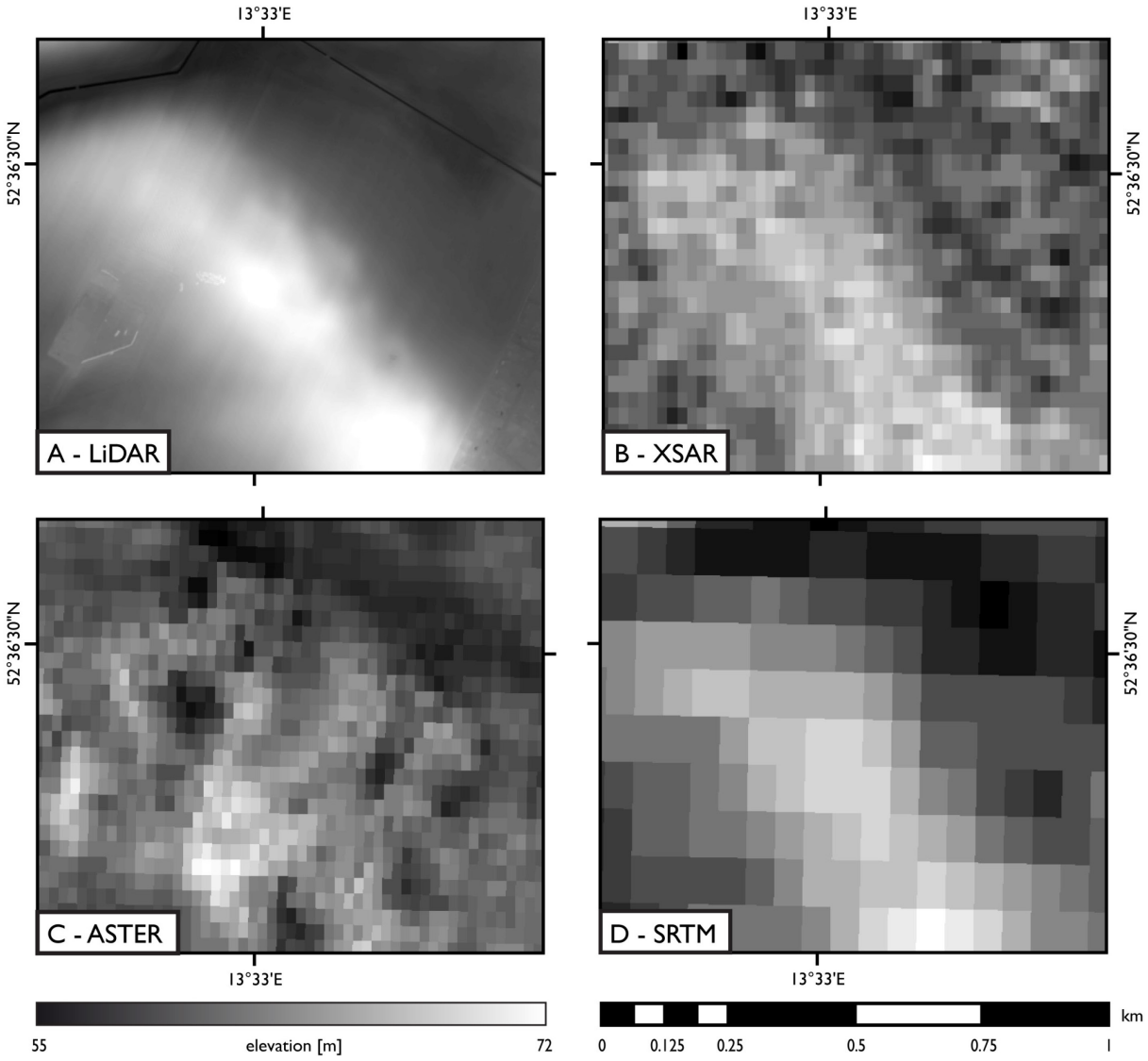

Fig. 6: Comparison of different digital elevation models available for this study.

3.1.2 PROCESSING AND ANALYSIS OF THE DATA

All GIS analyses were operated in an ESRI ArcGIS 10.1 environment. Additional cartographic refinements were subsequently done in Adobe Photoshop CS4 and Adobe Illustrator CS4.

The LiDAR data of the Barnim region in Brandenburg were obtained in a total of 5674 tiles in ASCII format. The tiles were mosaiced stepwise into one raster dataset using the *workspace to raster* function in ArcMap.

The basic visualization method for DEMs in a GIS is the application of a greyscale palette to the pixel values. The pixel values represent the elevation above a fixed datum (as in Fig. 6 and 7) (Smith, 2011). In order to enhance the contrast for qualitative analysis of the DEM, the *Dynamic Range Adjustment* (DRA) function proved to be useful for feature detection. The DRA function stretches the pixel values only over the pixels which are actually displayed and not over all pixels of the dataset.

This dynamic setting achieves a good contrast between different landscape elements even when the overall relief intensity is low (Fig. 7).

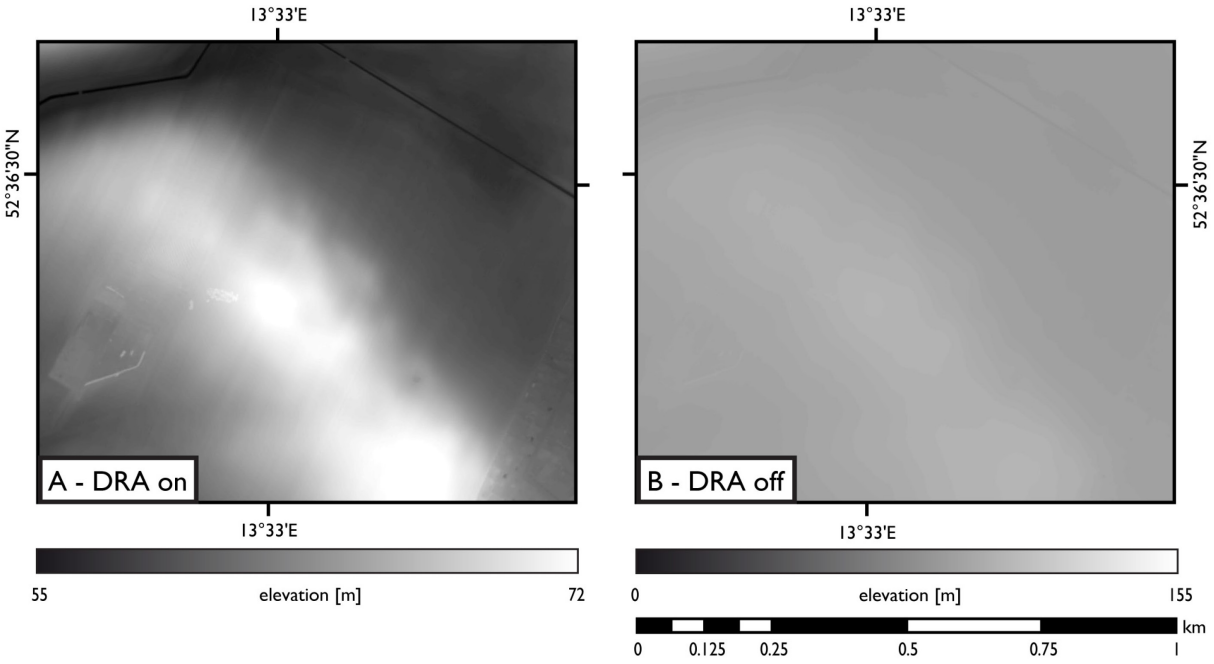

Fig. 7: Comparison between DRA on and DRA off. DRA: Dynamic Range Adjustment.

For further improvement of the visualization, a hillshade function was applied to the DEM. The hillshade function simulates an artificial light source at a user specified azimuth and elevation to illuminate the DEM. The output appears as a plastic landscape, which can be helpful for identification and interpretation of single landforms. To enhance the hillshade effect, a tenfold vertical exaggeration was applied to the function throughout the GIS analyses, which proved to be useful for the dataset of the study area (Fig. 8).

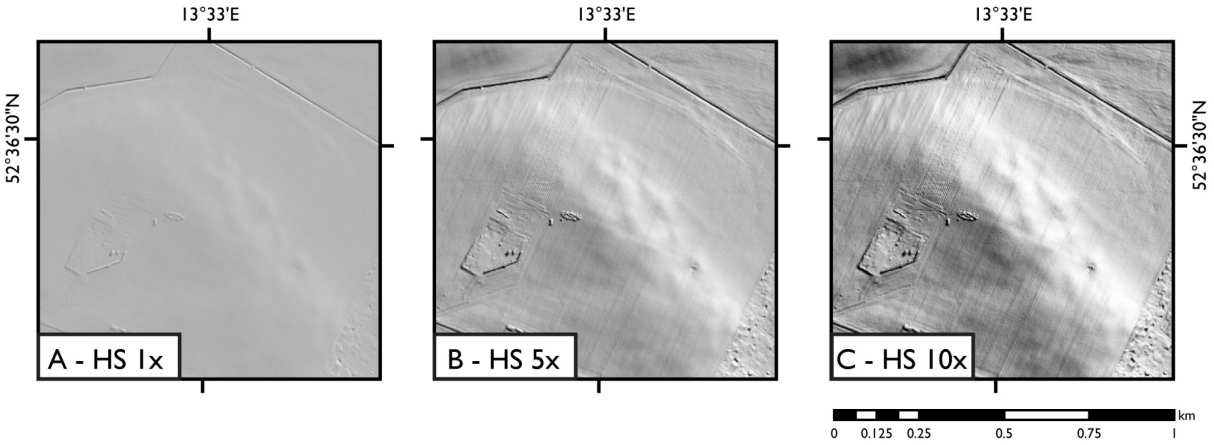

Fig. 8: Comparison of different vertical exaggeration factors for the hillshade function. HS: Hillshade factor.

However, the hillshade function is prone to azimuth biasing. According to the setting of the azimuth, certain existing lineaments may be concealed or lineaments may appear, which do not exist (Smith

and Clark, 2005; Smith and Wise, 2007). Thus, while an azimuth of 45° and an elevation of the light source of 45° proved to be the most favorable for the visualization of DEM data in this study, it was necessary to reassess the results with different azimuth settings during the analyses.

In order to increase the information content of hillshaded DEM images, additional data layers - such as geology or elevation - can be added in the GIS and displayed with a certain transparency. Due to the transparency, both, the hillshade layer and the top layers are visible. A problem of this method is the loss of color intensity and the overall slightly dull appearance of the resulting cartographic output (Fig. 9 A). Therefore, all hillshade-based images presented in this study were created by using the *pansharpening function* in ArcMap. This way, the overlaid layer is draped over the hillshade image by retaining the full color information, resulting in a well perceivable output image (Fig. 9 B).

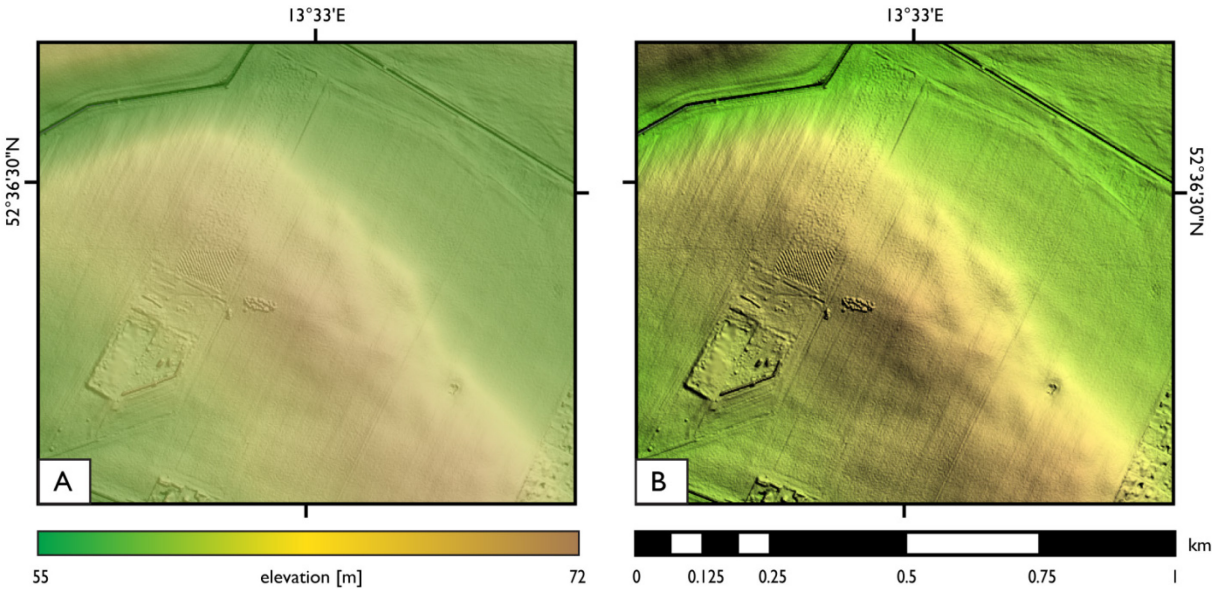

Fig. 9: Comparison of color coded shaded relief images. A - Hillshade overlain with elevation tint with 30% transparency. B - Elevation tint draped over hillshade with the pansharpening function.

3.2 Recalibration of cosmogenic nuclide surface exposure ages

3.2.1 Background

In recent years, a considerable number of studies were carried out aiming at the dating of the retreat of the SIS with *in situ cosmogenic nuclide surface exposure dating* (in the following termed *cosmogenic exposure dating*) (Rinterknecht et al., 2005; Rinterknecht et al., 2006a; Rinterknecht et al., 2007; Rinterknecht et al., 2008; Heine et al., 2009; Rinterknecht et al., 2012; Rinterknecht et al., 2014). Cosmogenic exposure dating allows determining the duration of a rock surface's exposure to cosmogenic nuclides (Gosse and Phillips, 2001).

Cosmogenic nuclides, such as ^{10}Be or ^{26}Al, are produced in minerals at or very near (several dm) the earth's surface under the influence of cosmic radiation (Nishiizumi et al., 1993). The amount of

cosmogenic nuclides produced in the mineral is indicative of the time spent at the surface (Granger, 2013). The cosmogenic nuclides are usually measured with accelerator mass spectrometry (AMS) (Ivy-Ochs and Kober, 2008). Given a glacigenic boulder was transported and deposited by the inland ice, this method allows determining the timing of the downwasting of the ice, which is – ideally – synchronous with the exposition of the boulder (Cockburn and Summerfield, 2004).

In order to obtain reliable ages it is important that the sampled surface has *no preexposure* (no inherited nuclides), was *not covered* during the exposure and has *not moved* after deposition (Ivy-Ochs and Kober, 2013). In the case of glacial boulders, inherited nuclides may occur when the surface of the boulder was not sufficiently eroded during transport (Bierman and Nichols, 2004). Inherited nuclides will lead to an overestimation of the deglaciation age. Both, covering (e.g. by vegetation or snow) and postdepositional movement of a boulder affect the cosmic-ray flux and will result in an age underestimation (Dunai, 2010).

The determined age depends on the production rate of the respective cosmogenic nuclide that is investigated. The production rate is a function of a number of factors such as the geographical position (variations of the geomagnetic field), the time (e.g., variations in cosmic-ray flux), the elevation (atmospheric shielding), and the topography (topographic shielding) (summarized in Cockburn and Summerfield, 2004). On basis of these factors, the production rate can be scaled for a specific sample at a specific location (Lifton et al., 2014).

3.2.2 REASONS FOR RECALIBRATION

For this method, the determination of the production rate of cosmogenic nuclides is the most crucial step toward reliable age calculation (Dunai, 2010). Production rates have been derived either by experiments with artificial or natural materials, or on a theoretical basis (summarized in Cockburn and Summerfield, 2004). Since 2008, the CRONUS-Earth online calculator (http://hess.ess.washington.edu) provides users with an easily accessible interface for the calculation of exposure ages (Balco et al., 2008). The calculator includes different scaling models and is commonly used by the scientific community (Schaefer and Lifton, 2013). In 2016, a new calculation tool was presented, which includes new functions for the growing number of applications in cosmogenic nuclide research (Marrero et al., 2016).

During the last years, several calibration studies were carried out all over the world to obtain local or regional production rates (e.g., Balco et al., 2009; Putnam et al., 2010; Fenton et al., 2011; Briner et al., 2012; Goehring et al., 2012; Young et al., 2013; Kelly et al., 2015; Stroeven et al., 2015). In these studies it was commonly observed, that regional ^{10}Be production rates are 5 – 15 % lower than the

reference production rate implemented in the CRONUS online calculator (Heyman, 2014; Stroeven et al., 2015). When calculating an age, a lower production rate will result in an older age.

Heyman (2014) compiled an updated global reference ^{10}Be production rate, which includes 24 calibration sites. This updated ^{10}Be production rate reflects the very recent progress in cosmogenic exposure research. It can be used as an alternative calibration data set within CRONUS-Earth online (http://hess.ess.washington.edu/math/al_be_v22/alt_cal/Heyman_compilation_input_aspublished.html). In this study, cosmogenic exposure data was collected from a number of studies and recalculated with the updated production rate (see chapter 5).

3.3 OPTICALLY STIMULATED LUMINESCENCE DATING

Optical sediment dating with optically stimulated luminescence (OSL) provides the possibility to determine depositional ages of minerogenic sediments. Quartz or feldspar grains are used as natural dosimeters, which were exposed to natural ionizing radiation. Due to the natural radiation a time-dependent signal builds up in the grains, which is depleted by exposure to sunlight during, e.g., a transport process. Thus, in an idealized model, sediment grains are reset during their last transport cycle. After their subsequent deposition and coverage a signal builds up, which is proportional to the duration of burial and can be measured in the laboratory (Preusser et al., 2008; Rhodes, 2011).

There is a variety of Quaternary environments in which OSL has been successfully applied (Lian and Roberts, 2006). The glaciofluvial process area is among those and numerous studies have dealt with the application of OSL and the improvement of the technique in this environment (summarized in Fuchs and Owen, 2008; Thrasher et al., 2009).

The OSL samples were taken in opaque plastic cylinders. In the laboratory, they were treated to be free of organic and carbonate matter, and the mineral fractions were separated. The grains were etched in order to exclude alpha radiation effects (Preusser et al., 2008). More details about the sample preparation are given in section 6.3.3.

3.3.1 BACKGROUND OF THE TECHNIQUE

The term *luminescence* describes the effect of matter emitting light (photons) when externally stimulated. If the wavelength of the external stimulation is in the spectrum of the visible light, it is termed OSL; if the wavelength of the stimulation is, e.g., in the far-infrared spectrum it is called infrared-stimulated luminescence (IRSL). Although the complex physical processes behind luminescence have not been completely understood yet, there are models which briefly explain the physical background and the possibilities for sediment dating (Preusser et al., 2009; Lian, 2013).

During this project, all OSL analyses were performed with quartz minerals. Although other minerals, such as feldspar, can also be used for luminescence dating, the following passages refer to quartz minerals or quartz OSL.

One advantage of quartz over feldspar is that it is faster bleached. The luminescence signal of quartz can be reset within some minutes of exposition to sunlight (Preusser et al., 2009). This is highly advantageous in environments where incomplete bleaching has to be expected (Lüthgens, 2011). Additionally, quartz is not affected by anomalous fading (a signal loss over time), eliminating the need for respective correction (summarized in Thrasher et al., 2009). Quartz (SiO_2) is the second most frequent mineral occurring in the Earth's continental crust (Preusser et al., 2009). It is abundant in igneous, metamorphic and sedimentary rocks. Accordingly, it is frequently present in loose rock, too.

Within the crystal lattice of quartz minerals impurities or structural defects can cause the occurrence of so-called electron traps. Ionizing radiation leads to excitation of free electrons and free holes in the crystal lattice (Bøtter-Jensen et al., 2003b). These excited electrons and holes can be transferred to the electron traps and remain there in a metastable state (Preusser et al., 2009). Optical energy, such as sunlight, stimulates relaxation of the system and the trapped electrons transfer to holes, which are called recombination centers or luminescence centers (Bøtter-Jensen et al., 2003b). If the recombination of electron and luminescence center is radiative, luminescence is emitted in the form of photons (Fig. 10) (Aitken, 1998). The photons can be counted with help of a photomultiplier tube built in the measurement device (Preusser et al., 2008).

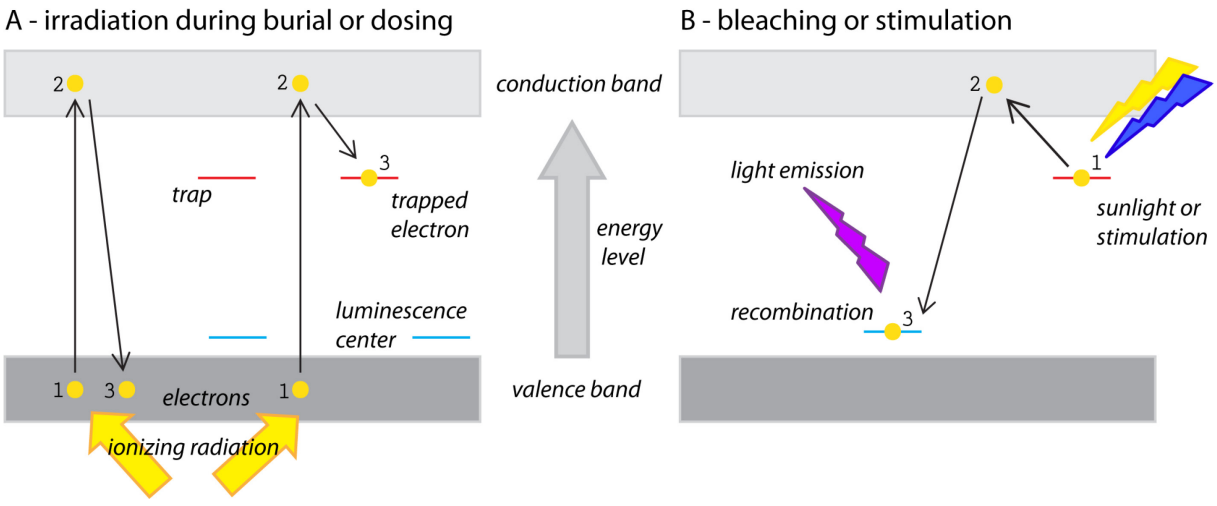

Fig. 10: Schematic band energy model of a crystal based on Aitken (1998) and compiled and modified after (Lüthgens, 2011; Rhodes, 2011). A: (from left to right) an electron is excitated by ionizing radiation either during burial or laboratory dosing. Due to the external energy input it is lifted to a higher energy level at the conduction band and immediately moves back to its initial state at the valence band – this is the most frequent case. Another electron is lifted to the conduction band, too. It does not move back to its initial state but is caught in an electron trap, where it remains in a metastable state. B: (from right to left) Sunlight or laboratory stimulation cause eviction of the electron from the trap and subsequent recombination in a luminescence center, which causes emission of light.

While some traps are emptied quickly during stimulation (within few seconds), some traps need a longer exposure, thus resulting in a number of components that contribute to the OSL signal (Lian, 2013). The so-called fast component, which is measured immediately after stimulation, is usually used for age determination (Bailey, 2010). The longer a quartz grain is exposed to ionizing radiation, the more electron traps will be filled, the stronger is the measured OSL signal. At a certain point, an additional dose will not result in a stronger OSL signal because all traps are full - the grain is saturated. This point represents the method's upper age limit (Rhodes, 2011).

In the laboratory, the radiation dose received by a certain grain is determined (equivalent dose, D_e) in *gray* [Gy; 1 Gy = 1 J/kg]. In another step the intensity of the surrounding ionizing radiation per time is determined (dose rate, D_r) in gray per thousand years [Gy/ka]. If both values are known, a depositional age can be calculated with the following equation:

$$age\ [ka] = {}^{equivalent\ dose\ [Gy]}\Big/_{dose\ rate\ \left[\frac{Gy}{ka}\right]}.$$

3.3.2 DOSE RATE DETERMINATION

The dose of ionizing radiation depends on alpha and beta particles as well as gamma rays from the decay of ^{235}U, ^{238}U, ^{232}Th, ^{40}K, ^{87}Rb, and their daughter nuclides (Lian, 2013). The radiation comes either from the mineral grain itself or from other minerals of the surrounding sediment body. In the case of quartz minerals there is no significant internal dose rate contribution. Cosmic radiation also contributes to the total dose rate (Rhodes, 2011). While the cosmic dose rate can be calculated according to the geographic position, elevation, and the thickness and density of the overlying material (Prescott and Hutton, 1994), the dose rate emitted from the sediment body must be determined in the laboratory. The contribution of alpha irradiation can be excluded when the grains used for OSL are etched before the measurements (Aitken, 1998).

The water content (or moisture content) of a sedimentary layer affects the dose rate. Water absorbs radiation, thus attenuating the dose effectively reaching the grain. Therefore, the water content is an important factor which has to be addressed in the age calculation (Aitken, 1998).

In the field, samples for dose rate determination were taken from the surrounding 30-40 cm of the OSL sample. To avoid inhomogeneities, samples were only taken from layers which were at least 50 cm thick. The bulk samples were sealed in *Marinelli* beakers and the respective external radiation was determined by high resolution gamma spectrometry (for details see chapter 6.3.3.4) (Preusser et al., 2008).

The results from the gamma spectrometry were combined with the results of the cosmic dose rate calculation and yielded the total dose rate (D_r [Gy/ka]). The dose rate was ascertained with the software ADELE (Kulig, 2005).

3.3.3 EQUIVALENT DOSE DETERMINATION

The equivalent dose (D_e [Gy]) is determined by comparing a sample's OSL characteristics in response to gradually increasing laboratory doses with its natural luminescence signal (Lian, 2013). Two Risø TL-DA 20 readers (Bøtter-Jensen et al., 2010) were used for the measurements in the Vienna Luminescence Laboratory (VLL). Several subsamples (aliquots) of one sample were analyzed. The *single-aliquot regenerative-dose* (SAR) protocol (Murray and Wintle, 2000, 2003; Wintle and Murray, 2006) is currently the most frequently used measurement routine for equivalent dose determination (Preusser et al., 2009; Lian, 2013). With this protocol it is possible to detect different dose populations within one sample (if the aliquot size and number of aliquots are appropriate), which is a great advantage for incompletely bleached material. Furthermore, there are a number of built-in tests that are used to correct the results of each individual aliquot (Fig. 11).

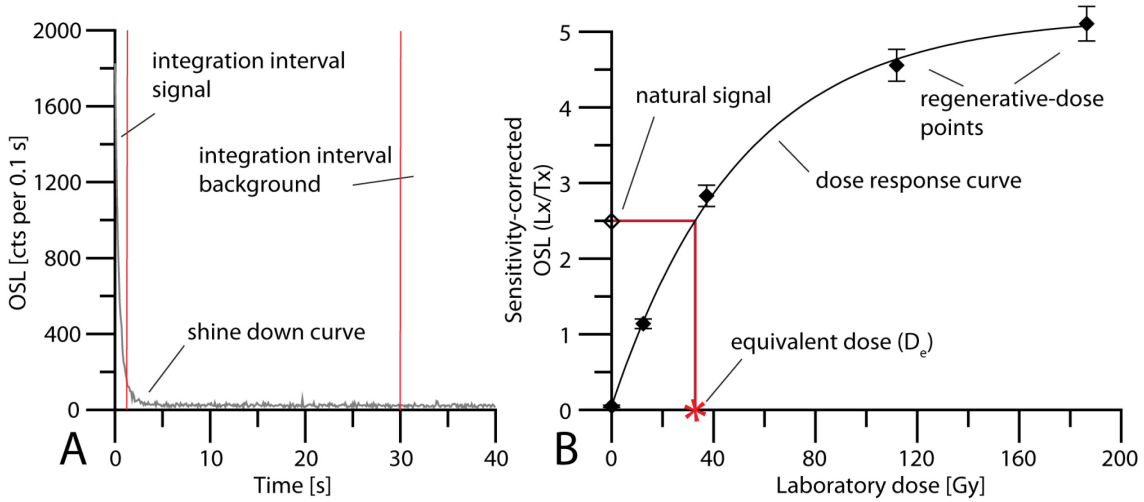

Fig. 11: OSL shine down curve (A) and growth curve resulting from the SAR protocol (B). A: the shine down curve displays the photon counts captured by the photomultiplier during 40 s of optical stimulation. The red lines indicate the signal integration interval and the background integration interval. The background interval is being subtracted from the signal interval. B: The dose response curve (or growth curve) is being interpolated between the regenerative-dose points in order to determine the equivalent dose. The OSL signal is sensitivity corrected by an aliquot's individual response to the test dose.

The protocol is described in detail in Wintle and Murray (2006), a brief overview is given in the following (Fig. 12).

Before every single measurement, the respective aliquot is preheated to empty unstable traps (called cutheat before test dose), which might erratically influence the signal (step 2 + 5). In the beginning of the first SAR cycle the natural luminescence signal is being recorded (step 3). In all subsequent cycles a gradually increasing laboratory dose is given to the aliquots (step 1); afterwards the respective

luminescence signal is measured (step 3). In the second part of each SAR cycle, a so-called test dose is given to the aliquots (step 4). The test dose stays constant over the whole measurement process and is used to identify sensitivity changes of the aliquots. If an aliquot varies its sensitivity during the measurements (e.g., an aliquot's luminescence intensity increases after each cycle), the sensitivity can be mathematically corrected unless a threshold is exceeded. The number of SAR cycles depends on the number of selected dose points.

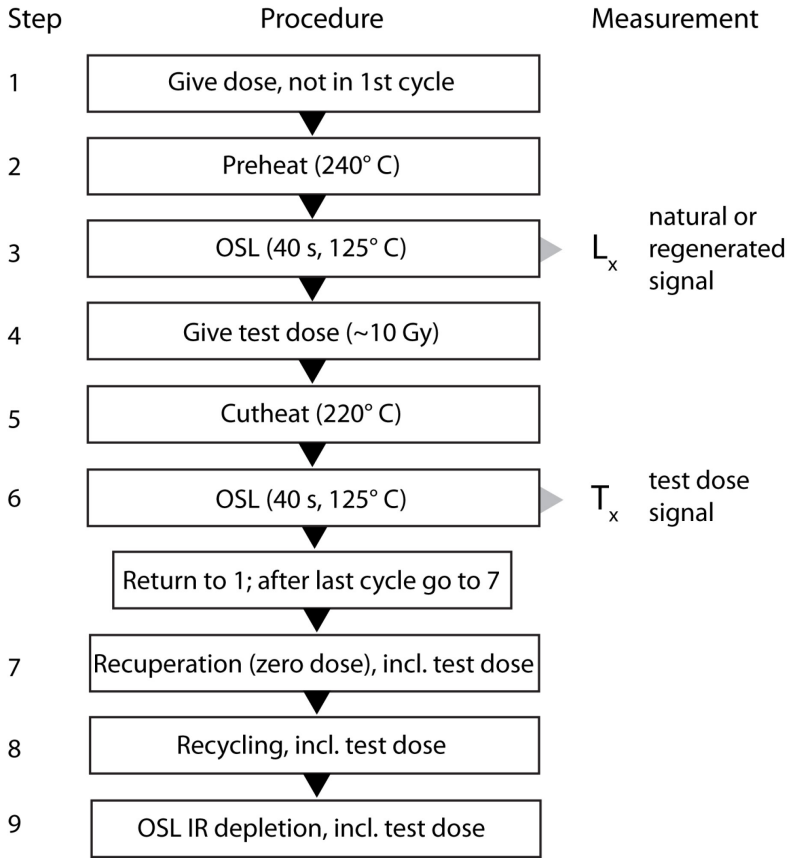

Fig. 12: Basic diagram of the single-aliquot regenerative-dose (SAR) protocol after Murray and Wintle (2000). Figure compiled and modified after Preusser et al. (2009) and Lian (2013). The preheat and cutheat temperatures as well as the test dose are according to the settings used in this study.

After the last SAR cycle, two quality checks are routinely performed in the protocol. First, a recuperation test is done, in which the reaction of the aliquots to a zero dose is measured (which should be zero). Second, a recycling ratio is measured by repeating a dose point from one SAR cycle. The tested aliquot should ideally show the same luminescence signal. Threshold values are selected for both tests and the test dose deviation, which should not be exceeded (Table 5). Otherwise the aliquot will be removed from the population (Wintle and Murray, 2006).

Table 5: Rejection criteria of quality tests during the SAR protocol.

Recycling ratio limit	15 %
Recuperation	< 5 % of the natural signal

Additionally, a test for feldspar contamination was performed with infrared stimulation (IRSL). Unlike feldspar, quartz aliquots should not respond to IRSL. If aliquots could be significantly stimulated by IRSL, they were subsequently removed (OSL IR depletion ratio after Duller, 2003).

The SAR results were analyzed with the software Analyst 4.12 (Duller, 2007). As most of the samples were affected by incomplete bleaching, subsequent steps were necessary before depositional ages could be estimated.

To test the overall suitability of the sampled material for OSL dating, a combined dose recovery/preheat test and thermal transfer tests were carried out (Wintle and Murray, 2006). The results are described in section 6.4.3.

3.3.4 INCOMPLETE BLEACHING

Turbid water streams frequently occur in the glaciofluvial environment owing to a large amount of available sediment volume and more or less high flow velocities. Gemmell (1985) proved experimentally that high flow speed along with turbid water significantly decreases the chance of transported grains to be bleached because the light intensity in the water is reduced. In an underwater bleaching experiment, Rendell et al. (1994) determined that up to a water depth of 12 - 14 m the quartz OSL signal can be reset within 3 h. However, the suspended load of glaciofluvial streams can be highly variable (Clifford et al., 1995). As a result, it has to be expected that a sample from a glaciofluvial layer consists of heterogeneously bleached grains. This is also referred to as *incomplete bleaching* – only a proportion of grains was completely bleached prior to the last deposition (Olley et al., 1998; Olley et al., 1999).

Incomplete bleaching can be detected by analysis of the determined D_e distribution. A mixture of bleached and poorly bleached grains from one sample results in an asymmetric, positively skewed D_e distribution (Fig. 13) (Thrasher et al., 2009). An important prerequisite for detecting incomplete bleaching is measurement of single grains or small aliquots consisting of few grains. If the aliquot size is too big, signal averaging can occur, obscuring the heterogeneously bleached populations. Another parameter indicative of incomplete bleaching is the so-called overdispersion, which describes the spread of the D_e values which cannot be explained by the D_e errors only (Galbraith et al., 1999). Well bleached samples can have overdispersion values around 10 %, whereas incompletely bleached samples can have overdispersion values of > 10 % to > 100 % (Rhodes, 2011). If incomplete bleaching is unambiguously detected, it is reasonable to apply age models for the D_e determination (see next section) (Thrasher et al., 2009).

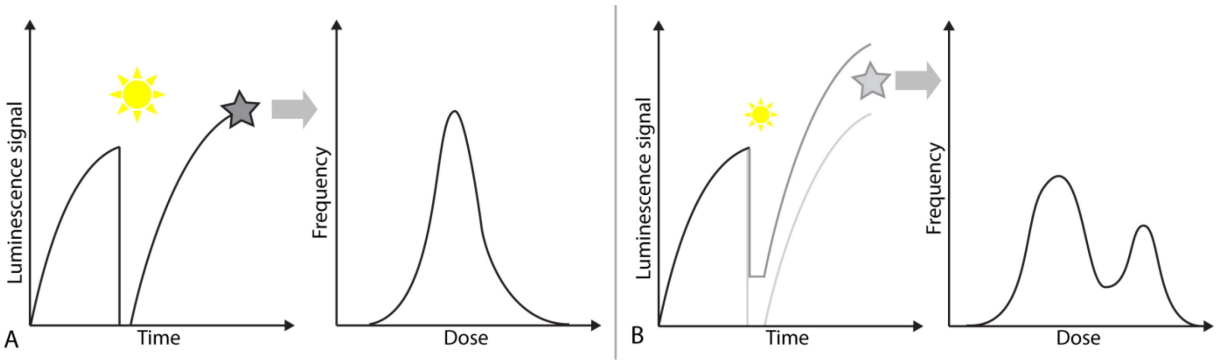

Fig. 13: Schematic comparison of complete and incomplete bleaching with corresponding schematic dose distribution curves. A: During a transport process sufficient exposure to sunlight resets the luminescence signal prior to the next burial. A luminescence signal builds up subsequently, which is represented by a unimodal dose distribution curve. B: During a transport process only parts of the material were sufficiently exposed to sunlight and residual signals remain, resulting in a positively skewed, bimodal dose distribution curve. Compiled and modified after Lüthgens (2011) and Reimann (2012).

3.3.5 Age determination

For a well bleached sample, the *true* D_e, which represents the whole sample, can be derived by applying the Central Age Model (CAM, Galbraith et al., 1999). The CAM calculates a weighted mean of the determined D_es (Lian and Roberts, 2006).

For a heterogeneously bleached sample, the Minimum Age Model (MAM, Galbraith et al., 1999) is preferable to determine the D_e. The MAM mainly incorporates the lowest-dose population of aliquots, thus calculating a D_e representative for the well bleached population of the distribution. The overdispersion is an important input parameter for this age model and it should be calibrated according to a well bleached sample of the same material (Lian and Roberts, 2006). The MAM was used for final D_e calculation of heterogeneously bleached samples in this study. More details are given in section 6.4.3.

There are several more age models specialized for different applications. A decision tree for selecting the appropriate model based on statistical parameters has been proposed by Bailey and Arnold (2006). The statistical analyses were performed using the R-Luminescence package (Dietze et al., 2013; Fuchs et al., 2015) in R Studio.

3.4 Electrical resistivity tomography

Geophysical methods can be very powerful tools for geomorphological research including subsurface structures. The non-destructive data-acquisition and the possibility to map the subsurface in 2D or 3D expand the information gained from drillings, outcrop studies, or geomorphological mapping. Although the data acquisition is relatively easy, the data processing and interpretation can be challenging because the results are not necessarily biunique (Schrott and Sass, 2008).

During the dissertation project, electrical resistivity tomography (ERT) was applied at several sites. The method was favored for the exploration of the Barnim ridge structures to map the transition between the different geological units and their respective thickness. In the following subsections some more methodological details are given, which could not be included in Paper 1 and 3 (chapter 4 and 6) due to space restrictions.

3.4.1 BASIC PRINCIPLE

With the ERT method, subsurface structures can be mapped by injecting electrical current into the ground via two current electrodes (A, B) and measuring the voltage difference between two potential electrodes (M, N) (Loke, 2014). The measurement values represent an apparent resistivity value. The electrical properties of the ground allow geological interpretations concerning the pore value, the geochemical composition, the water content, the grain size, etc. The resistivity is measured in ohm-meters [ohm m] (Kearey et al., 2002).

In a 2-D survey, horizontal and vertical variations of the electrical resistivity can be detected by moving the positions of the electrodes along a line at a fixed inter-electrode spacing (Samouëlian et al., 2005). After one line of measurements is finished, the inter-electrode spacing is increased by a certain factor. The bigger the electrode spacing, the bigger the penetration depth (Schrott and Sass, 2008). After the next line is finished, the spacing is increased again. This procedure is repeated until the maximum electrode spacing is reached or the measurement is stopped by the user (Fig. 14).

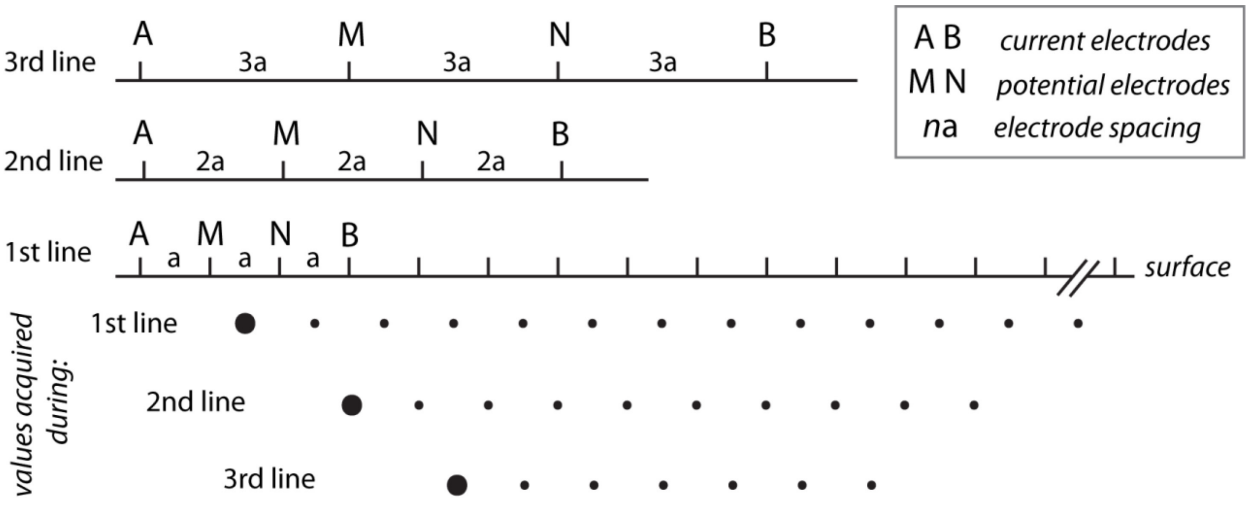

Fig. 14: Schematic illustration of the electrode configuration with a Wenner array. Modified after Griffiths and Barker (1993).

There are several measurement protocols, which determine the electrode configuration. In case of the *Schlumberger* array, the potential electrodes remain in the center of the profile and the current electrodes move stepwise to the sides. This array is sensitive to lateral inhomogeneities. The *Wenner* array is characterized by an equal spacing of the current and potential electrodes, which is gradually

increased after each reading (Kearey et al., 2002) (Fig. 14). The Wenner array is particularly useful for the detection of horizontal structures (Smith and Sjogren, 2006) and is relatively unsusceptible against resistivity variations at the near-surface, which can cause scatter (Griffiths and Barker, 1993).

3.4.2 Field application

A total of three different multi-electrode systems were used in the field campaigns: a *Syscal Pro* (Iris instruments; 96 electrodes; Fig. 15), a *Campus Tigre Resistivity Meter* (64 electrodes), and a *GeoTom* system (Geolog; 75 electrodes). Three different ridge structures were investigated with ERT: Albertshof (see section 4.4.13), Ladeburg (see section 6.4.2; Appendix 3) and Neulindenberg (see Appendix 2). In most cases the investigated profile line was longer than the maximum electrode spread. Consecutive measurements were performed as a *roll along procedure* with an overlap of 33 % (Ladeburg) to 50 % (Albertshof, Neulindenberg). An overlap of at least 33% is necessary to ensure continuity of the ERT data because the maximum penetration depth is only reached at the middle point of the array.

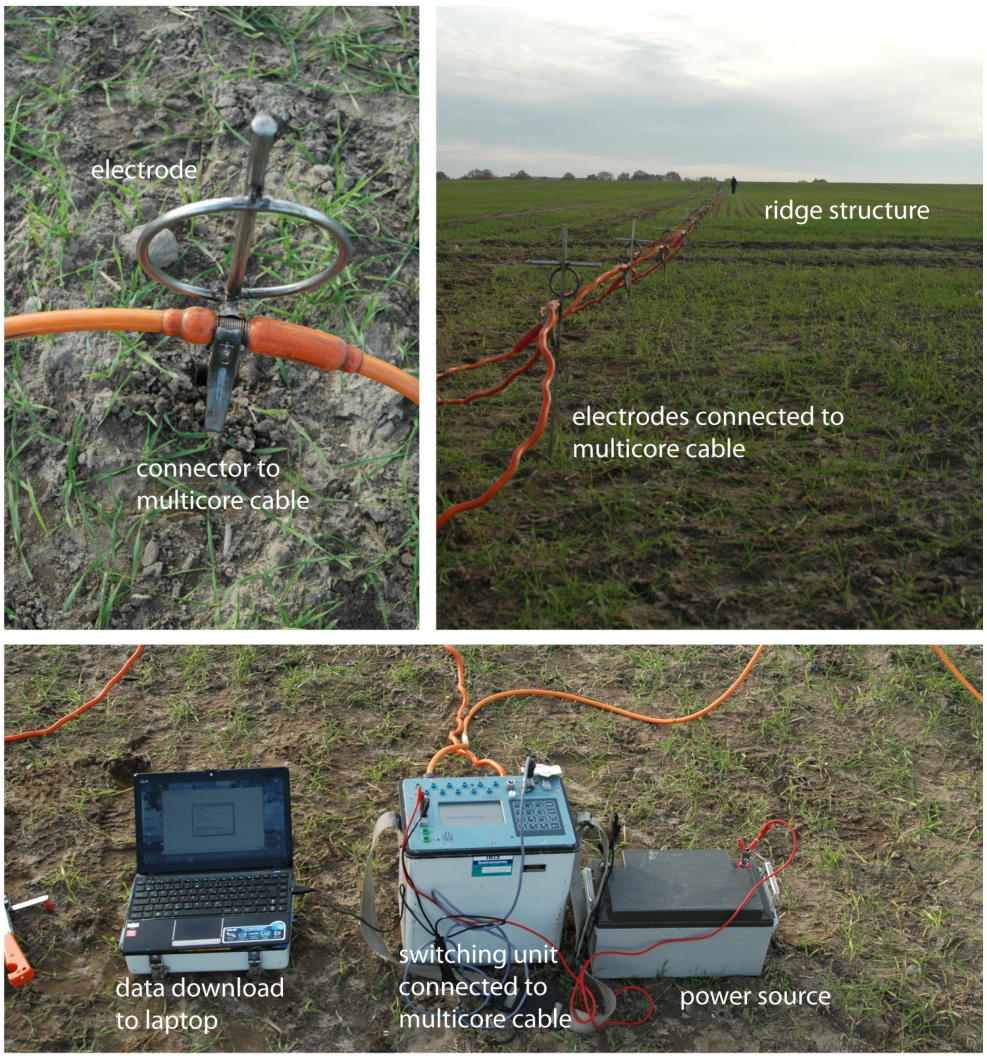

Fig. 15: Impressions of the fieldwork with a Syscal Pro ERT device.

3.4.3 DATA PROCESSING AND INTERPRETATION

Depending on the different measurement devices, several steps were necessary to process the data. In case of the *Syscal Pro* (Iris instruments) device used in Albertshof, the elevation values were added and the data was transformed with the *Prosys II* software. The data acquired with the *Campus Tigre Resistivity Meter* and *GeoTom (Geolog)* devices could directly be imported into *Res2Dinv*.

The Res2Dinv software (Loke and Barker, 1995, 1996) is the most commonly used computer program for processing electrical resistivity data (Schrott and Sass, 2008) and for creating the so-called pseudo-sections. A pseudo-section is the common way to present ERT data (Griffiths and Barker, 1993) in an illustrative form that allows for interpretation (Loke, 2014). In a stepwise iteration process – termed inversion – the program applies a least squares fit to the measured apparent resistivity values (Smith and Sjogren, 2006). During the inversion process the apparent resistivity values are converted to true resistivity values with depth information (Samouëlian et al., 2005). The results of roll along measurements were combined using the *concatenate* function in Res2Dinv.

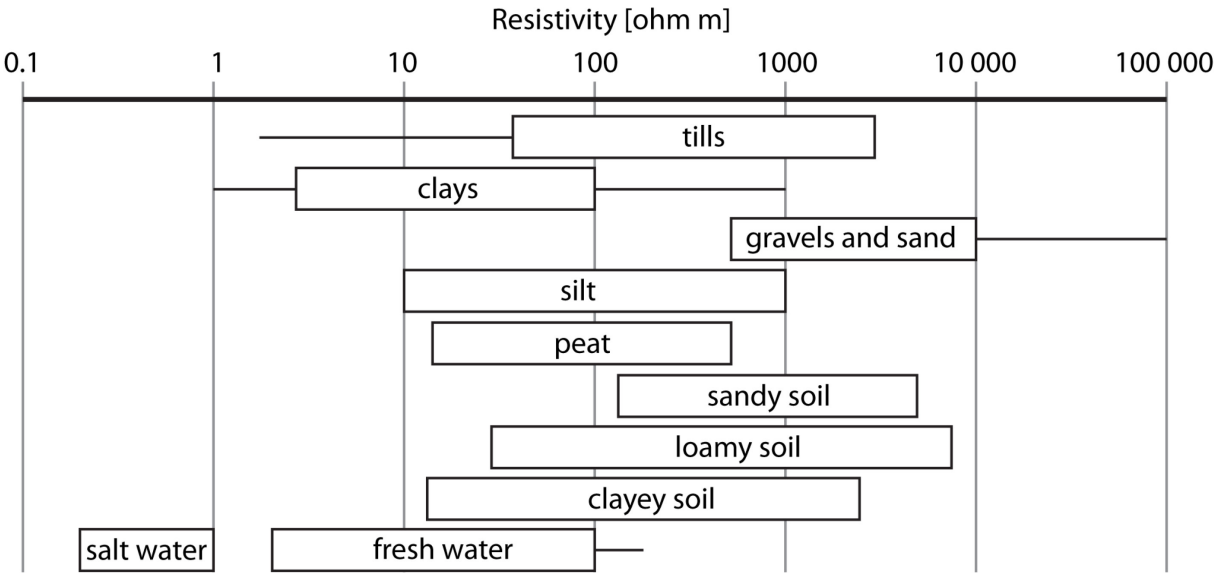

Fig. 16: Typical electrical resistivities of sediments, soils, and water in morainic landscapes. Compiled after Greinwald and Thierbach (1997), Kearey et al. (2002), and Samouëlian et al. (2005). The resistivity values highly depend on the water content of the material and are highly variable according to different literature sources.

As mentioned above, the results presented in the pseudo-section are not biunique. Thus, a certain resistivity value can correlate to a number of different geological units. In Figure 16 a number of typical resistivity ranges were compiled for sediments expectable in the study region. The values are highly dependent on the water content of the subsurface because water modifies the electrical properties of the material. For example, water-saturated clay has resistivity values below 10 Ohm m, whereas dry clay has a much higher resistivity up to 1000 Ohm m (Greinwald and Thierbach, 1997).

For a reliable interpretation of the ERT pseudo-sections it is necessary to compare the results to field data such as drillings and outcrops, and geological maps. In combination with these data, simplified models were created which illustrate the 2-D distribution of geological units (e.g., Fig. 24).

4 HIGH-RESOLUTION MAPPING OF ICE-MARGINAL LANDFORMS IN THE BARNIM REGION, NORTHEAST GERMANY

This section has already been published. For copyright reasons, the text is not included in the published version of this thesis. Bibliographical data is listed below.

Title	High-resolution mapping of ice-marginal landforms in the Barnim region, northeast Germany
Journal	Geomorphology
Issue	250
Year	2015
Pages	41-52
First Author	Jacob Hardt
Co-Authors	Robert Hebenstreit, Christopher Lüthgens, Margot Böse
Accepted	29 July 2015
Available online	1 August 2015
Weblink	http://www.sciencedirect.com/science/article/pii/S0169555X15301094
DOI	http://dx.doi.org/10.1016/j.geomorph.2015.07.045

5 THE TIMING OF THE WEICHSELIAN POMERANIAN ICE MARGINAL POSITION SOUTH OF THE BALTIC SEA: A CRITICAL REVIEW OF MORPHOLOGICAL AND GEOCHRONOLOGICAL RESULTS

This section has already been published. For copyright reasons, the text is not included in the published version of this thesis. Bibliographical data is listed below.

Title	The timing of the Weichselian Pomeranian ice marginal position south of the Baltic Sea: A critical review of morphological and geochronological results
Journal	Quaternary International
Issue	XXX (in press)
Year	2016
Pages	1-8
First Author	Jacob Hardt
Co-Author	Margot Böse
Accepted	27 July 2016
Available online	17 August 2016
Weblink	http://www.sciencedirect.com/science/article/pii/S1040618216301872
DOI	http://dx.doi.org/10.1016/j.quaint.2016.07.044

6 GEOCHRONOLOGICAL (OSL) AND GEOMORPHOLOGICAL INVESTIGATIONS AT THE PRESUMED FRANKFURT ICE MARGINAL POSITION IN NORTHEAST GERMANY

This section has already been published. For copyright reasons, the text is not included in the published version of this thesis. Bibliographical data is listed below.

Title	Geochronological (OSL) and geomorphological investigations at the presumed Frankfurt ice marginal position in northeast Germany
Journal	Quaternary Science Reviews
Issue	154
Year	2016
Pages	85-99
First Author	Jacob Hardt
Co-Authors	Christopher Lüthgens, Robert Hebenstreit, Margot Böse
Accepted	26 October 2016
Available online	15 November 2016
Weblink	http://www.sciencedirect.com/science/article/pii/S0277379116304772
DOI	http://dx.doi.org/10.1016/j.quascirev.2016.10.015

7 CASE STUDY: NEW OSL AGES FROM THE W_{1B} ICE MARGINAL POSITION AT JÄNSCHWALDE

7.1 INTRODUCTION AND STATE OF RESEARCH

This study site in question is located to the north of the *Glogow-Baruth ice marginal valley* close to the German-Polish border in Lusatia on the *Lieberoser plateau* (Fig. 43). The ice marginal valley is correlated with the Brandenburg (Leszno) phase of the Weichselian glaciation. The *Taubendorfer Sandur,* named after the village *Taubendorf*, was deposited in front of the Brandenburg IMP. The IMP is represented only by fragments of end moraine deposits. To the south of the sandur, remnants of Saalian Warthanian till are found at the surface (Fig. 44; Lippstreu et al., 2001).

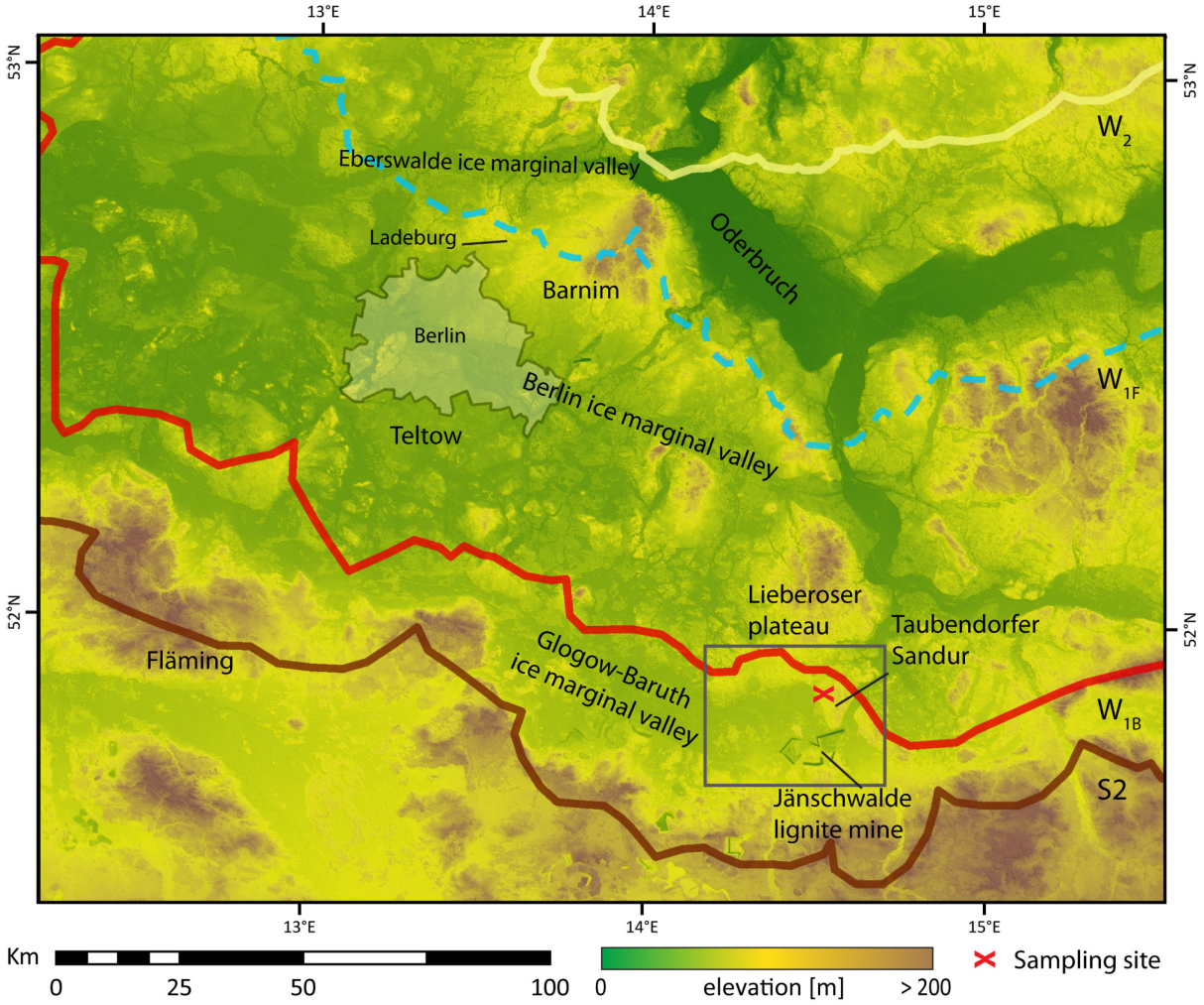

Fig. 43: Physical overview map of east Brandenburg showing the main ice marginal positions and landscape units mentioned in the text. The grey box marks the extent of Fig. 44. Ice marginal positions according to (Liedtke, 1981), map based on SRTM data (Jarvis et al., 2008).

Nevertheless, the maximum extent of the SIS during the Brandenburg phase is debatable. Some authors found geomorphological evidence for a Weichselian ice advance south of the main Brandenburg IMP, which is referred to as *maximum extent* in the following sections (summarized in Juschus, 2010). It is assumed that numerous pits found at the sandur surface are remnants of formerly buried dead ice (Brose and Marcinek, 1995). This theory has been rejected by Liedtke (1981), as the pits could also be preserved by *aufeis* (also: *naled* or *icings*; frozen meltwater that collected in proglacial depressions and was subsequently buried). However, during detailed geomorphological investigations, Juschus (2003) identified several landforms indicative of a maximum extent in the southeast of Brandenburg some kilometers south of the main Brandenburg IMP.

7.2 STUDY SITE

Located in the Glogow-Baruth ice marginal valley and on the Taubendorfer sandur (Fig. 43 + 44), the active lignite opencast mine *Jänschwalde* exposes a complex sequence of Quaternary and Tertiary material. The ongoing excavation, which started lignite production in 1976, has repeatedly been investigated with respect to the Quaternary, especially Saalian, deposits (Cepek et al., 1994; Kühner, 2003; Lippstreu and Stackebrandt, 2003; Nowel, 2003b; Degering and Krbetschek, 2007; Preusser et al., 2008; Kühner, 2013; Zöller and Schmidt, 2016).

The so-called *Tranitzer Fluviatil*, a sediment layer of fluvial deposits which are classified as Lower Saalian (MIS 7 - 9), has been of special interest for the Quaternary stratigraphy in the study area. This layer is composed of fine to middle grained sand with varying gravel contents. Silty or clayey mud layers and ice cast wedges can occur (summarized in Lippstreu et al., 2015). The mineralogical composition of the gravel fraction, at least for the upper part of this layer, is representative of the *Neiße* and *Spree* river catchments (Kühner et al., 2008; Lippstreu et al., 2015).

It has been questioned, whether the Tranitzer Fluviatil is in fact older than the Saalian Drenthe glaciation (Lippstreu and Stackebrandt, 2003), or whether it was deposited between the Saalian Drenthe and Warthe glaciations (Nowel, 2003a, b). Krbetschek et al. (2008) dated samples of the *Tranitzer Fluviatil* from Jänschwalde with infrared radiofluorescence of feldspar (IR-RF) to 149 ± 8 - 171 ± 15 ka (Jae 2-1, 2-2 and 3 in Krbetschek et al. 2008), corresponding to MIS 7. Two samples of the Tranitzer Fluviatil from the nearby *Klinge* (Degering and Krbetschek, 2007) were dated to 272 ± 23 and 268 ± 20 (KLT 1 and 4 in Krbetschek et al. 2008), corresponding to MIS 8. These geochronological results support the theory of Lippstreu and Stackebrandt (2003), as the onset of the first Saalian glaciation (Drenthe) in Brandenburg occurred in the MIS 6 at around 150 ka (Litt et al., 2007; Lippstreu et al., 2010). Nevertheless, IR-RF dating of feldspar is not a routinely applied method and is

still considered highly experimental. In an accuracy test of this method with independent age control, Buylaert et al. (2012) observed a significant age under estimation (~30 ka) of samples with a known age of 130 ka.

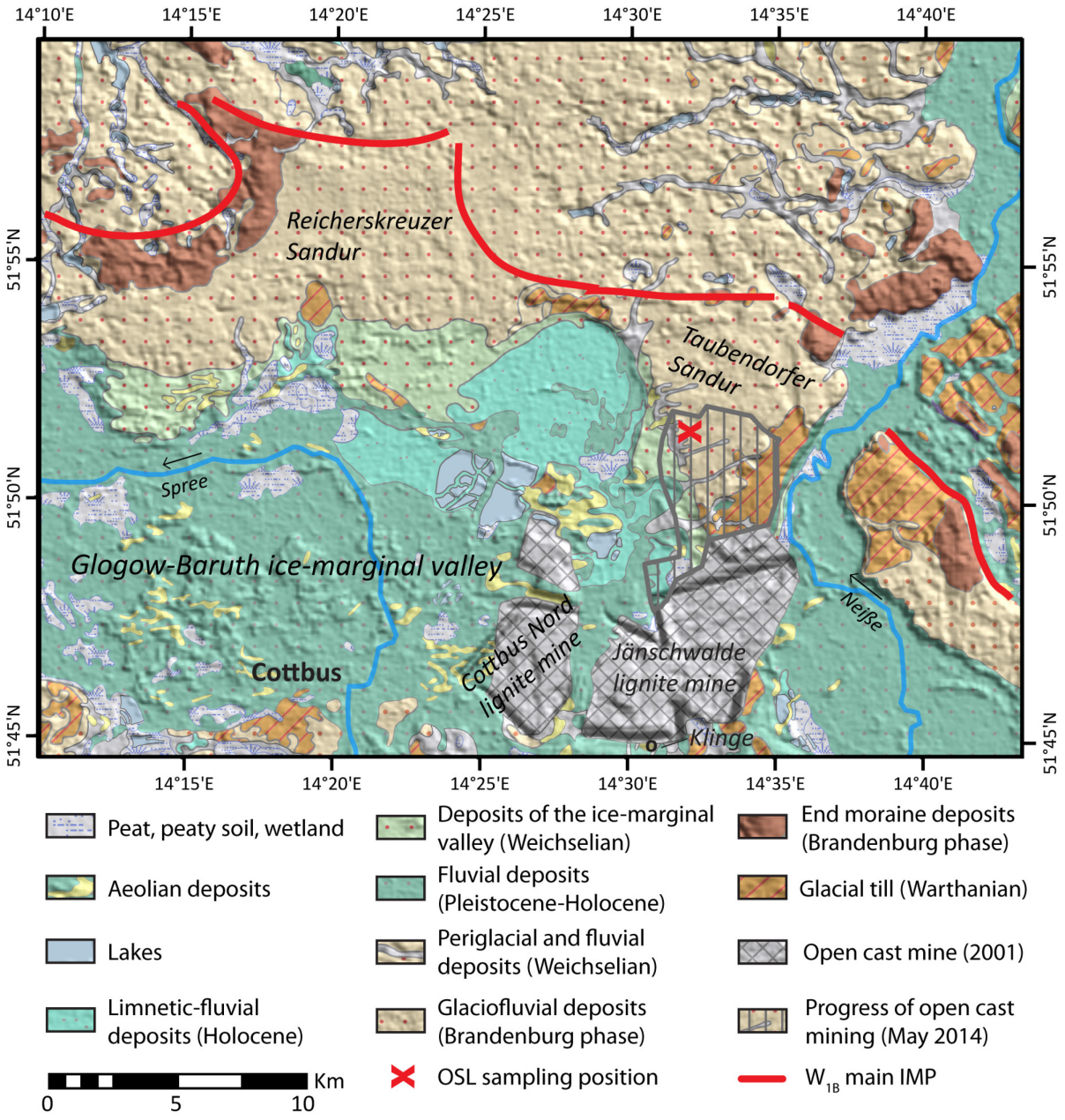

Fig. 44: Geological overview map of the study area. Geological data simplified after Lippstreu et al. (2001). W_{1B} main IMP compiled after Marcinek (1961) and Liedtke (1981). Hillshade based on SRTM data (Jarvis et al., 2008).

In some places the Saalian deposits are overlain by silt gyttja. Sometimes, this gyttja is intercalated with organogenic material which could be classified as Eemian (MIS 5e) by palynological analyses (Kühner et al., 2008). Recent OSL analyses of glaciofluvial material underlying the gyttja, confirm its Eemian age (Zöller and Schmidt, 2016).

Furthermore, the postglacial landscape development and the prehistorical land use were studied along the outcrops of this mine (Woithe, 2003; Nicolay et al., 2014).

The Weichselian sediment sequence, which overlays the Eemian layer discordantly, lacks detailed investigations, especially concerning the chronology. It is the aim of this case study to obtain numerical ages for the Weichselian glaciofluvial deposits, which were deposited in the direct surroundings of the main W_{1B} IMP.

At the time of sampling, in September 2011, the ongoing northward expansion of the opencast mine Jänschwalde exposed a complete sequence of Saalian, Eemian and Weichselian deposits at a width of ~400 m and a depth of 20 m. The stratigraphical interpretations were based on the previous findings presented above. Glaciofluvial deposits that are assumed to be Saalian and Weichselian were sampled in high resolution for luminescence dating. A lithological interpretation of the outcrop wall was kindly supplied by the mining operator (R. Kühner, Vattenfall Europe Mining AG; Fig. 45).

Recent geochronological analyses of glaciofluvial deposits at the W_{1B} IMP were reported by Lüthgens et al. (2010a, b). At two sites, Luckenwalde (Lüthgens et al., 2010a) and Beelitz (Lüthgens et al., 2010b), maximum ages of 34.4 ± 7 (Luckenwalde) and 34.1 ± 3 ka (Beelitz) were derived by quartz OSL dating. Revised analyses in Beelitz with single grain OSL resulted in ages of 30.6 ± 4 ka and 24.8 ± 2 ka (BEE-2 and BEE-3 in Lüthgens, 2011), giving an average age of 27.7 ± 4 ka (ibid.). Thus, Lüthgens and Böse (2011) concluded that the W_{1B} advance occurred in late MIS 3 to early MIS 2, which conflicts with the conventional model where the W_{1B} advance is correlated with the LGM at <24 - <20 ka (Litt et al., 2007).

The conventional ages of the W_{1B} phase are based on radiocarbon ages, which inhibit methodological drawbacks, as stated in the previous sections.

The Taubendorfer sandur is a key site with respect to the conflict between the different chronologies. Its morphology and sedimentology represent a “classical” lowland sandur. Its position between the W_1 maximum extent and the W_{1B} main IMP makes it peculiarly interesting for OSL dating. In addition to this, the underlying sediments of Eemian and Saalian age allow the establishment of a complete Saalian – Weichselian chronology at this site, which is an important step forward to a robust chronology for the W_{1B} phase in the region.

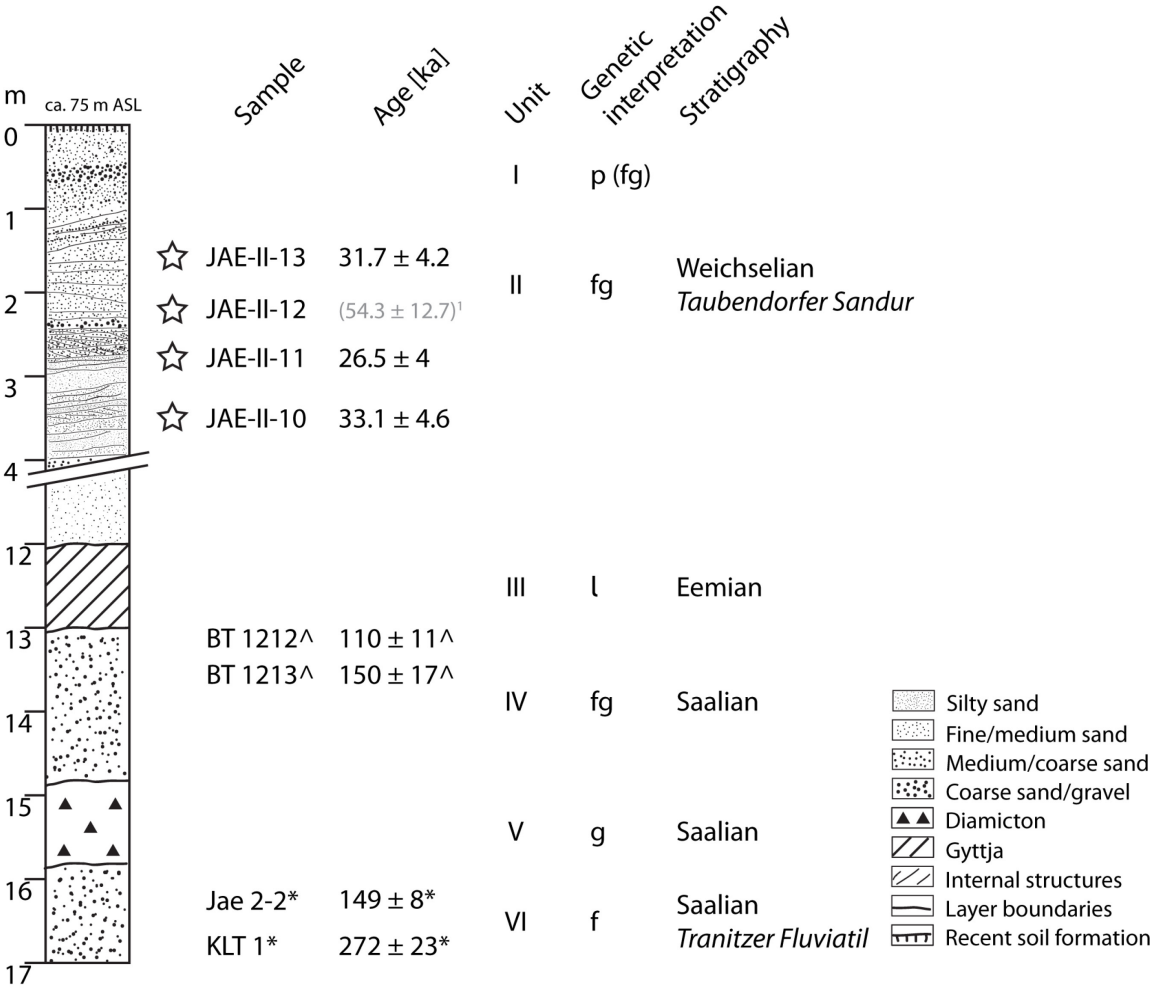

Fig. 45: Schematic profile log of the upper Jänschwalde open cast. The stars mark the position of the OSL samples analyzed in this study. [1] sample excluded from mean age calculation. * samples from Krbetschek et al. (2008). ^ samples from Zöller and Schmidt (2016): BT 1212 is an IRSL (feldspar) age, BT 1213 is an OSL (quartz) age; sample BT 1211 was excluded from this profile log because the original authors regard it as not representative. Codes for genetic interpretation: p – periglacial; fg – glaciofluvial; l – limnetic; g – glacial; f – fluvial. Sample JAE-II-12 is regarded as outlier (see text). The upper 4 m of the log are according to field notes and photographs of C. Lüthgens from the time of sampling. The lower part of the log is simplified according to sediment descriptions from the time of sampling supplied by R. Kühner (Vattenfall Europe Mining AG).

7.2 OSL Methods

The OSL measurements were performed at the Vienna Luminescence Laboratory. The samples were prepared as described in section 6.3.3.2 The SAR protocol was applied according to the settings explained in section 3.3 and section 6.3.3.3; the rejection criteria were also set accordingly. The used grain size fraction is different from the Ladeburg samples. The fraction from 170 – 250 µm was used (Ladeburg: 220 – 250 µm). As a result of a smaller minimum diameter, more grains per disc had to be expected. Thus, the aliquot size was reduced to 1 mm (Ladeburg: 2 mm). This results in an average of 15 grains per disc, as statistically estimated with the *calc_AliquotSize (Luminescence)* function in R Studio. Consequently, the measurements were performed on a quasi-single grain level as only a

proportion of around 3 – 5 % of the grains emits an appropriable luminescence signal (see section Ladeburg 6.3.3 for details and Lüthgens et al., 2010b).

The radionuclide content of the surrounding material was determined by high resolution gamma spectrometry (see section 6.3.3.4). The calculated dose rates range from 1.38 ± 0.09 Gy/ka to 0.9 ± 0.07 Gy/ka (Table 14). Zöller and Schmidt (2016) report similar dose rates for their samples from the Saalian and Eemian sections of the Jänschwalde outcrop.

Table 14: Summary of results from radionuclide analyses and dose rate calculations.

		Water content [%]	Radionuclide contents			Dose rate [Gy/ka]	
Sample	**Depth [m]**	**Estimated average**	**^{40}Ka [%]**	**^{232}Th [ppm]**	**^{238}U [ppm]**	**Quartz overall**	**Cosmic dose rate**
JAE-II-13	1.6	8 ± 4	0.562 ± 0.013	1.248 ± 0.048	0.480 ± 0.015	0.91 ± 0.07	0.17 ± 0.02
JAE-II-12	2.1	8 ± 4	0.660 ± 0.015	1.056 ± 0.043	0.409 ± 0.014	0.95 ± 0.07	0.16 ± 0.02
JAE-II-11	3.7	8 ± 4	0.631 ± 0.014	1.115 ± 0.043	0.395 ± 0.013	0.9 ± 0.07	0.1 ± 0.01
JAE-II-10	4.7	8 ± 4	1.213 ± 0.026	3.207 ± 0.072	1.091 ± 0.030	1.38 ± 0.09	0.1 ± 0.01

7.3 OSL RESULTS

A dose recovery test performed on all four samples returned satisfying results, with recovery ratios between 0.9 and 1 (Fig. 46). There is a slight trend of dose underestimation. Nevertheless, the obtained dose recovery ratios are well within the suggested range from 0.9 to 1.1 (Murray and Wintle, 2003) making the samples suitable for luminescence dating.

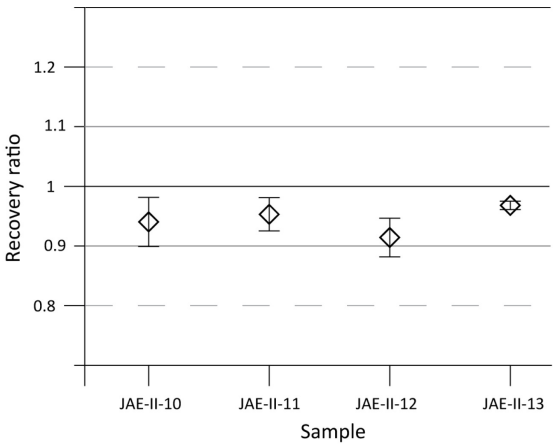

Fig. 46: Results of dose recovery test. Given dose: ~29 Gy. Error bars representative of 1σ standard error.

The results of the OSL analyses are displayed in Table 15 and Figure 47. ~43% and ~42% of the aliquots from sample JAE-II-11 and sample JAE-II-13, respectively, passed the rejection criteria. In contrast, only ~26% from sample JAE-II-10 and ~22% from sample JAE-II-12 could be accepted.

Overdispersion values range from 31.24 ± 9.36 % (JAE-II-12) to 52.65 ± 7.16 % (JAE-II-11) (Table 15). The samples JAE-II-10, JAE-II-11 and JAE-II-13 exhibit a significant positive skewness and scatter over

a wide D_e range. These characteristics, together with the relatively high overdispersion values, are indicative of incompletely bleached samples, which had to be expected in this geological setting (see section 3.3.4).

Owing to the low yield rate, only 11 D_es could be obtained from sample JAE-II-12. On this data basis, a reliable age calculation is not possible for this sample (Rodnight, 2008). Although there is a significant peak at around 60 Gy in the kernel density plot (Fig. 47), the plots of the other three samples indicate that there is a missing proportion of data in the lower and higher D_e ranges, which may be determined by further measuring. Nevertheless, there is one sample below and two samples above this sample from the same stratigraphical unit. JAE-II-12 is therefore excluded from age calculations and further interpretations.

Table 15: Results of OSL analyses and applied age models. * Sample JAE-II-12 excluded from mean age calculation.

Sample	Depth [m]	Aliquots measured/ accepted	Overdispersion (CAM) / σ_b [%]	Total dose rate [Gy]	MAM-3 (sigma_b 0.2)		Mean age [ka]*
					Equivalent dose [Gy]	Age [ka]	
JAE-II-13	1.6	120/50	51.12 ± 5.63	0.91 ± 0.07	28.8 ± 3.1	31.7 ± 4.2	30.4 ± 4.3
JAE-II-12	2.1	48/11	31.24 ± 9.36	0.95 ± 0.07	(51.6 ± 11.4)	(54.3 ± 12.7)	
JAE-II-11	3.7	72/31	52.65 ± 7.16	0.9 ± 0.07	23.9 ± 3.2	26.5 ± 4	
JAE-II-10	4.7	96/25	33.08 ± 5.84	1.38 ± 0.09	45.8 ± 5.5	33.1 ± 4.6	

Owing to the described sample characteristics, the three-parameter Minimum Age Model (MAM (Galbraith et al., 1999) was used for equivalent dose determination. Due to the absence of a well bleached sample, the sigma_b parameter (overdispersion) was set to 0.2 (20%), according to well bleached glaciofluvial samples examined by Lüthgens et al. (2011b) at sites in Althüttendorf and Macherslust. The ages were finally calculated with ADELE (Kulig, 2005).

The derived ages range from 26.5 ± 4 ka (JAE-II-11) to 33.1 ± 4.6 ka (JAE-II-13). The youngest age (26.5 ± 4 ka; JAE-II-11) was obtained at a depth of 3.7 m, the sample above yields an older age (31.7 ± 4.2 ka; JAE-II-13). The error ranges of both samples overlap by 3 ka. The lowermost sample yields an age of 33.1 ± 4.6 ka (JAE-II-13), representing the oldest age. Thus, the slight age inversion of sample JAE-II-12, which is not significantly different from both other ages, is probably neither of a

geological nature or a methodological issue but a statistical variance. This sample included, the arithmetic mean age for the formation of the Taubendorfer Sandur is 30.4 ± 4.3 ka.

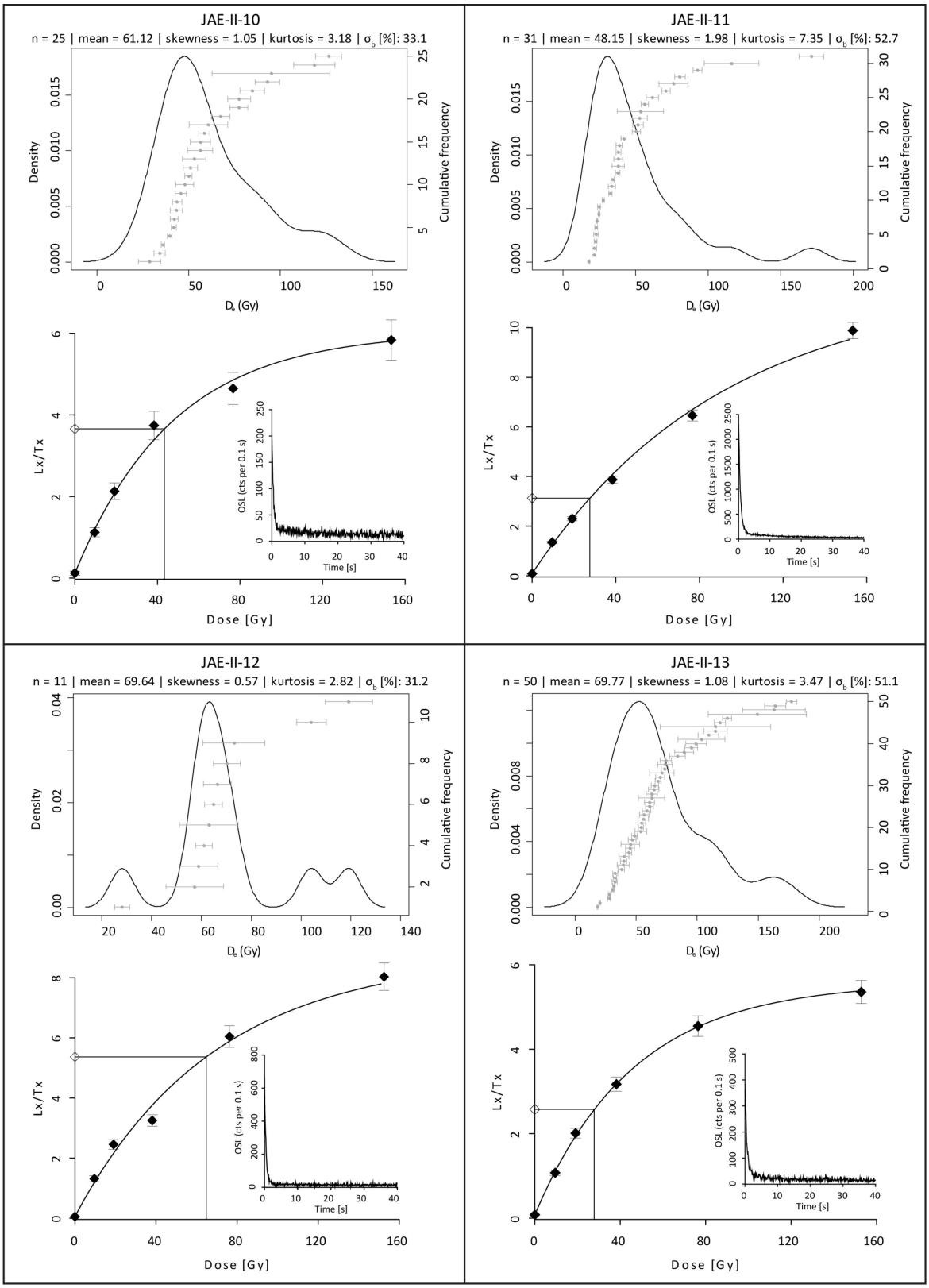

Fig. 47: Overview of statistical parameters and kernel density plots for each OSL sample. Dose recovery curves and shine down curves (inset) representative of a selected aliquot of the respective sample.

7.4 Discussion

Except for sample JAE-II-12, the sampled material turned out suitable for luminescence dating. Statistical analyses revealed incomplete bleaching of the material prior to last deposition. Although problematic for age determination, the bleaching characteristics go along with the glaciofluvial process regime and strengthen the sedimentological interpretation. The described statistical parameters justify the application of the minimum age model (Galbraith et al., 1999).

The derived mean age of 30.4 ± 4.3 ka proves the formation of the Taubendorfer Sandur in the Weichselian. Nevertheless, the new average age is considerably higher than the conventional age of the W_{1B} IMP, which ranges from <24 - <20 ka (Litt et al., 2007).

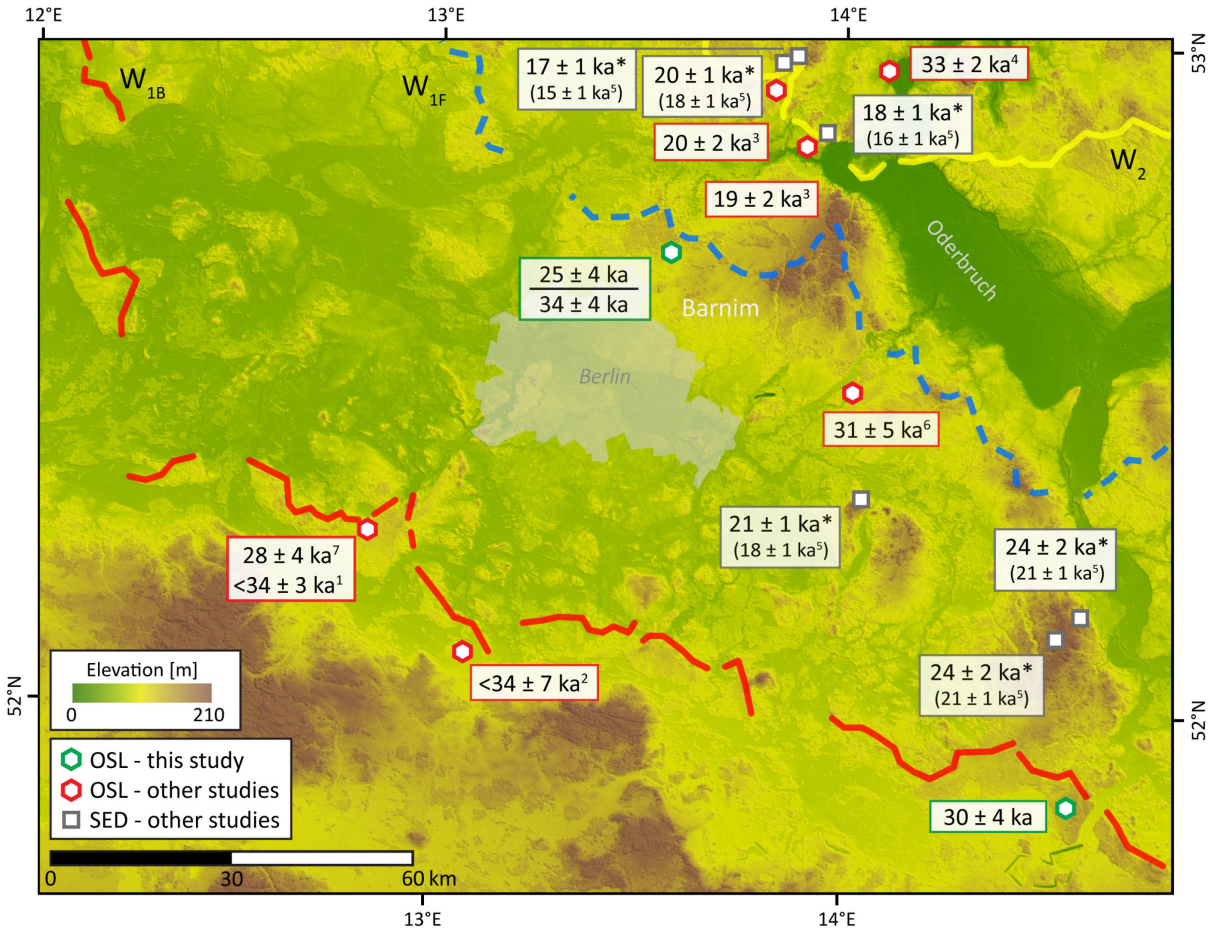

Fig. 48: Overview map showing ages from cosmogenic nuclide dating (SED) and OSL dating. 1 – Lüthgens et al. 2010a; 2 – Lüthgens et al. 2010b; 3 – Lüthgens et al. 2011; 4 – Brauer et al. 2005; 5 – Heine et al. 2009; 6 – Nitzsche 2015; 7 – Lüthgens 2011. *Recalculated ages (Hardt & Böse 2016) using CRONUS online (Balco et al. 2008) and the alternative calibration data set by Heyman (2014). Background map based on hillshaded SRTM data (Jarvis et al. 2008).

The relatively large error ranges do not allow for a differentiation of different phases during the sandur formation, e.g. the phase of the maximum extent cannot be distinguished from the formation of the main IMP – possibly because these processes occurred within some hundred or only few thousand years. Therefore, they cannot be resolved with OSL dating.

In context of the reported ages from the Jänschwalde site (Fig. 45), a chronology from the Lower Saalian (272 ± 23 ka, KLT1; Krbetschek et al., 2008) to the upper Weichselian (JAE-II-10 to JAE-II-13) could be compiled. Thus, the Saalian deposition of the lower till layer as well as the Eemian formation of the gyttja can be confirmed by numerical sediment dating.

The newly derived mean age (30.4 ± 4.3 ka) corresponds with results of other recent OSL studies at the W_{1B} IMP in Brandenburg (Fig. 48). In Beelitz and Luckenwalde, glaciofluvial deposits were dated with OSL to <34 ± 3 ka (Beelitz; Lüthgens et al., 2010b), 27.7 ± 4 ka (Beelitz; Lüthgens, 2011) and to <34 ± 7 ka (Luckenwalde; Lüthgens et al., 2010a). These results are discussed in more detail in section 8.

8 CONCLUDING DISCUSSION

The results of each study have already been discussed in sections 4, 5, and 6. In this section, the results are summarized and the overall outcome of this thesis is discussed. Some previously unpublished results (section 7; Appendix) are also included in this section.

8.1 BARNIM RIDGE STRUCTURES WITH NEW RESULTS

During the Frankfurt phase the Barnim ridges were formed on the Barnim plateau by an oscillation of the W_1 ice sheet. In Albertshof, it was found that the diamictic material (~5 m thick) assembling the ridge was deposited on top of more or less horizontally lying glaciofluvial deposits. The glaciofluvial material was most likely deposited during the advance ice of the W_{1B} phase (section 4; Hardt et al., 2015). A similar situation can be discovered in Ladeburg, where the diamictic material (on average ~ 7 m thick) is covered by a 1 – 2 m thick layer of aeolian and glaciofluvial deposits (Appendix 3; section 6; Hardt et al., 2016). Here, the OSL results proofed that the ridge was deposited on top of glaciofluvial material from the W_{1B} phase, whereas the overlying glaciofluvial material dates to the downwasting of the ice during the W_{1F} phase.

In Neulindenberg, a ridge was examined where the diamictic material exceeds a thickness of 10 m by far. The ERT tomogram (Appendix 2) shows a fairly homogeneous section with resistivity values below 50 Ωm. These values correspond with fine grained material or till. At this site, glacial till is present at the surface and additional drilling (end depth 10 m) confirmed that the upper 10 m of the ridge consist of till. According to Lippstreu and Zwirner (1972), up to 17 m of Weichselian till was deposited in the surroundings of Neulindenberg. It is followed by 2 m of gravel and then by another (Saalian) 8-m-thick till layer (Lippstreu and Zwirner, 1972). This situation (two superimposed individual till layers) is displayed in the ERT tomogram (Appendix 2). Only the gravel layer separating the two till layers is too thin to be resolved in the tomogram. Thus, the thickness of the Barnim ridge structures appears to be variable. At the investigated sites it ranges from ~5 to ~17 m.

However, this does not alter the outcome of section 4 (Hardt et al., 2015). The Barnim ridges are interpreted as ice marginal fans (after the definitions of Krzyszkowski and Zieliński, 2002). So far, no similar parallel arcuate ridges have been reported from formerly glaciated lowland areas. The increasing availability of LiDAR data to geomorphologists will help to find out whether the formation of the Barnim ridges was a unique event or not.

8.2 OSL DATING OF GLACIOFLUVIAL DEPOSITS

The dating of glaciofluvial sediments with quartz OSL proved as a reliable method. The reliability is documented in the consistency of the data itself and by the coherence with other ages from the surrounding regions – be it ages from OSL or cosmogenic exposure dating. All glaciofluvial samples from the W_{1F} and W_{1B} phase were affected by incomplete resetting of the signal. This is similar to the observations of Lüthgens et al. (2010a, b), who also report incomplete resetting of the material from the W_{1B} IMP. In contrast, at the W_2 IMP, well bleached material was observed (Lüthgens et al., 2011b). Thus, the similar poor bleaching characteristics also seem to indicate the close relationship of the W_{1B} and W_{1F} phases.

In comparison with single-grain dating, the small-diameter single-aliquot approach turned out to be time-effective and feasible. The decision not to measure single grains was based on preliminary investigations, which revealed that only a small number of grains had sufficient luminescence characteristics. Thus, measurements on a single-gran level were made possible also with 2 mm multigrain aliquots (220 – 250 µm).

Due to the incomplete bleaching, a minimum age model (Galbraith et al., 1999) was applied to determine D_e values representative for the last sedimentation. The sigma_b parameter was set in accordance with well bleached samples from the W_2 IMP, which is in line with the overdispersion value of an aeolian sample from the Ladeburg site.

8.3 GEOCHRONOLOGY AND AGE GAPS

An ice advance in late MIS 3 in Brandenburg was already discussed by Lüthgens and Böse (2011), who performed first OSL investigations of glaciofluvial sediments at the W_2 and W_{1B} IMP. Especially concerning the ages for the W_{1B} IMP, they remained unsure about the validity of the ages owing to the relatively large scatter of the data, and subsequent methodological improvements (single aliquots vs. single grains; Lüthgens, 2011). The relatively large age discrepancy of ~5 ka between boulders dated by cosmogenic exposure dating (the works of Heine et al., 2009; Rinterknecht et al., 2006a, 2012, 2014), and OSL were raising the question, *which of these ages are correct*.

Within this study, OSL was applied at one new site at the W_{1B} IMP (Jänschwalde; section 7) and, for the first time, at a site near the W_{1F} IMP (Ladeburg; section 6). Additionally, previously published datasets of cosmogenic exposure ages were critically reassessed and recalculated with an updated ^{10}Be global production rate (section 5). These investigations yielded essential results toward an answer of the question, *which the correct ages are*. Apparently, *both* are. It was shown, that the ages

obtained from both methods can corroborate each other, especially when taking the dated geomorphic processes into consideration.

After recalibration of the exposure ages, the age gap between both methods has decreased. It was explained in detail, why a recalibration of existent cosmogenic exposure data was valid and necessary (section 3.5; section 5). Possibly, with further progress in determining local production rates, the age gap will decrease even more in the future. Thus, as the resulting exposure ages depend on factors, which are still under development, it remains crucial to evaluate the source data used for exposure age calculation, and to recalibrate them if necessary.

Published OSL data also have to be critically evaluated, as there are many factors, which substantially influence the ages, apart from measurement errors. E.g., the determination of the water content, the dose rate calculation, and the bleaching characteristics should be assessed to verify the reliability of the ages.

With the new data from Jänschwalde and the previously published ages (Lüthgens et al., 2010a; Lüthgens et al., 2010b; Lüthgens, 2011), there is now strong evidence that the advance of the SIS toward the W_{1B} IMP took place already in late MIS 3 (Fig. 48). The subsequent downwasting phase lasted until early MIS 2, as documented by some exposure ages (reported ages in Heine et al., 2009; recalibrated ages in Hardt et al., 2016) and the results from Ladeburg (section 6). The advance during the LGM (in terms of ice volume) is represented by the W_2 IMP, as documented by OSL results from Lüthgens et al. (2011b) and strongly corroborated by the recalculated exposure ages. Thus, the largest ice extent in Brandenburg is not connected to the last global largest ice extent (which occurred significantly later in the Weichselian). Just recently the maximum ice coverage of the Eurasian ice-sheet complex was dated by ice-sheet-modeling to ~22.7 ka (Patton et al., 2016). Thus, the two-fold LGM in Brandenburg, as already discussed by Lüthgens (2011), is confirmed by the results of this study.

It remains questionable, whether this situation (an ice advance of the SIS in late MIS 3) is a unique situation, which occurred only in Brandenburg. In the surrounding regions geochronological records of this phase are scarce. A good correlation can be made with the so-called Klintholm advance, which was described by Houmark-Nielsen and Kjær (2003) and Houmark-Nielsen (2010). The Klintholm advance was reconstructed from sedimentological and geochronological analyses and is dated to 35 – 30 ka, which is in good agreement with the ages from the W_{1B} IMP and Ladeburg.

In northern middle Poland, a possible late MIS 3 ice advance is discussed by Marks (2012). Two glacigenic boulders located on the Lubawa elevation (LES-13 and LES-5) were dated by Rinterknecht et al. (2005). The recalculated ages range from 37 ± 3.2 ka to 41.9 ± 3.3 ka (Hardt and Böse, 2016).

On basis of the reported ages (32.2 ± 2.2 and 36.4 ± 2.2 ka; Rinterknecht et al., 2005), Marks (2012) assumed that these boulders might have been transported by an ice advance correlating to the Klintholm advance. Owing to the raised position of the Lubawa elevation, he proposed the area was ice free during later advances, thus preserving the boulders. Further research is necessary to gain more insights in this possible advance into northern middle Poland. Thus, the presumed late MIS 3 ice sheet limits presented in Fig. 49 are still subject to debate and have to be labelled with question marks outside Denmark and Brandenburg.

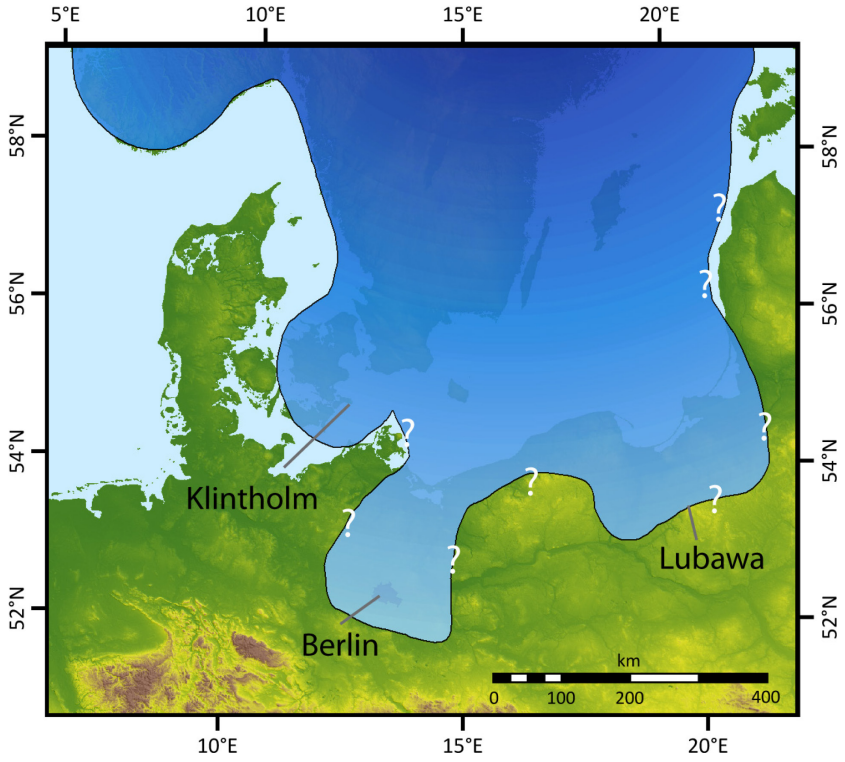

Fig. 49: Presumed late MIS 3 ice sheet limits in the study area and neighboring regions. Ice sheet limits modified after Houmark-Nielsen and Kjær (2003), Marks (2012), and Hughes et al. (2015). 250 m SRTM base map (Jarvis et al., 2008).

Kenzler et al. (2015, 2016) did not find evidence for a Weichselian ice advance prior to 23 ± 2 ka at several cliff sections on the Rügen Island. Thus, the SIS might have moved around Rügen when advancing into Brandenburg in MIS 3. The landforms associated with the W_1 advance are generally relatively weakly expressed and strongly influenced by the pre-existing relief. End moraines are widely missing and mostly glaciofluvial deposits, which cover older landforms, are representative of this advance – in contrast to, e.g., the W_2 advance. As stated in section 2, the thickness of the W_1 ice advance must have been relatively thin and its velocity was relatively high (Liedtke, 1992; Brose, 1995). The movement of this thin ice sheet was possibly stronger influenced by the preexisting relief than the succeeding W_2 advance. Thus, higher elevated areas – such as the Jasmund peninsula of Rügen - could have been ice-free (in the sense of nunataks) while they were surrounded by the active ice sheet.

A correlation of the late MIS 3 ice advance with *Heinrich (H) events* 4 and 3, which occurred at 38 ka and ~31 ka, respectively (Hemming, 2004), is theoretically conceivable. Heinrich events – characterized by an enormous discharge of icebergs from the Laurentide ice sheets in the North Atlantic (Bard et al., 2000) – had a great impact on the earth's climate. Along the eastern North Atlantic margin, these events are connected to colder glacial conditions (Hemming, 2004). Thus, H4 and H3 might have contributed to the late MIS 3 ice advance. The average duration of H events has been calculated to ~500 years (ibid.). However, given the relatively short duration of H events and the error incorporated in the presented OSL ages (several thousand years), the precision of the OSL data is too low to establish a reliable connection between H events and the ice advance in the study area at this point.

8.4 The Frankfurt phase revisited

For the first time, OSL ages of glaciofluvial deposits of the W_{1F} phase were presented. Do these new data change the picture of this Weichselian phase? It is widely accepted from sedimentological and geomorphological investigations, that the W_{1F} phase represents a recessional halt of the downwasting W_{1B} ice masses. The mean age of unit III (Ladeburg site; section 6) of 26.3 ± 3.7 ka stands for the deposition of sediments, which are typically assigned to the Frankfurt phase (Gärtner, 1993). The 'classic', uncalibrated, radiocarbon age of 18.8 ka (Kozarski, 1995) for this phase is considerably younger. Its calibration (Reimer at al., 2013) results in an age of 22.8 – 22.4 cal ka BP, thus there is an overlap within the error of the OSL data. However, the nature of the radiocarbon age is not clear, as it is extrapolated from material underlying glacial deposits (Litt et al., 2007). Hence, it has to be seen as a maximum age. Additionally, it originates from a site in Poland, which could not exactly be traced and which could be several hundred km away. As shown in Fig. 49, this site was probably ice free at the time the glaciofluvial material was deposited in Brandenburg.

The dynamics of the SIS require more regional studies to be better understood. Long distance correlations of single ages do not sufficiently represent the past glacial processes. Thus, it is not surprising that the new data are inconsistent with the classical chronology.

A continuous W_{1F} ice marginal position could not be detected, at least in northern Germany, and the theoretical connection of outwash plains that might resemble an IMP, needs further revision.

If there is no specific W_{1F} IMP, then what is the reason to maintain the W_{1F} phase as a distinct stratigraphical unit? The formation of the Barnim ridges illustrate, that at least on the Barnim plateau, particular glacial processes occurred as the ice generally wasted down from the W_{1B} IMP. It remains questionable, whether this was a sole situation or whether other small oscillations can be

detected in the adjoining areas, and if these are a characteristic of this downwasting phase. Thus, at the moment it appears plausible to maintain the W_{1F} phase and interpret it as the downwasting phase of the W_{1B} advance. However, the concept of a single stationary IMP during the W_{1F} phase remains questionable and needs further revision. At least in the Barnim region the W_{1F} IMP needs to be redrawn. Only the Barnim ridges are remnants of stationary ice margins.

8.5 UPDATED GEOCHRONOLOGY

In the following, the results of this study and other recent works are integrated into an updated geochronological model of Brandenburg (see Fig. 48 for an overview map):

- Upper Saalian (148.6 ± 10.4 ka): presence of an active ice margin, deposition of glaciofluvial deposits in the Barnim region (unit VIII of the Ladeburg site). Saalian glaciofluvial deposits were also reported for the south of Brandenburg (Lüthgens et al., 2010b; Zöller and Schmidt, 2016).

- MIS 5e: Widespread deposition of limnetic sediments in Brandenburg indicate interglacial vegetational succession (Hermsdorf and Strahl, 2008).

- W_{1B} phase: First indications of Weichselian glaciofluvial processes at ~34 ± 5 ka (unit V of the Ladeburg site) in the Barnim region. Deposition of glaciofluvial material of the advancing W_{1B} ice at 33 ± 2 ka in the northeast of Brandenburg (Brauer et al., 2005), and at 31 ± 5 ka in the Lebus region (Nitzsche, 2015). Formation of the W_{1B} IMP at 30 ± 4 ka (Jänschwalde), <34 ± 7 ka (Luckenwalde; Lüthgens et al., 2010b), and <34 ± 3 – 28 ± 4 ka (Beelitz; Lüthgens et al., 2010a; Lüthgens, 2011).

- W_{1F} phase: Deposition of glaciofluvial material during the downwasting of the W_{1B} ice at ~26.3 ± 3.7 ka (unit III of the Ladeburg site). At the same time formation of the Barnim ridges by oscillation of an ice lobe on the Barnim plateau.

- Late W_{1F} phase until early W_2 phase (23.9 ± 1.8 ka – 20.6 ± 1.4 ka): landscape stabilization as indicated by recalibrated surface exposure ages in the area between W_{1B} and W_2 IMP.

-W_2 phase: Formation of the W_2 IMP in the north of Brandenburg at ~20 ka, according to OSL results (Lüthgens et al., 2011b) and recalibrated cosmogenic exposure ages (Heine et al., 2009 - recalibrated in this study).

- After termination of the W_2 downwasting phase: landscape stabilization in the hinterland of the W_2 IMP between 20 and ~15 ka, as indicated by recalibrated cosmogenic exposure ages (Rinterknecht et al., 2014 – recalibrated in this study).

- Under periglacial climatic conditions: periglacial reworking of the surficial deposits, formation of the 'Geschiebedecksand' (e.g., unit II of the Ladeburg site).

- Around 1 ka: phase of aeolian activity around Ladeburg, possibly due to medieval human impact, formation of cover sand (unit I of the Ladeburg site).

Table 16 summarizes the geochronological results of the Weichselian processes.

Table 16: Summary of recent cosmogenic exposure (SED) and OSL data of Weichselian processes in the study area.

Phase	Process	Age	Method	Reference
Pomeranian W_2	landscape stabilization	20 - ~15 ka	SED	Rinterknecht et al., 2014 → recalibrated in Hardt & Böse 2016
	formation of the W_2 IMP	~20 ka	OSL	Lüthgens et al., 2011b
		~20 – ~17 ka	SED	Heine et al., 2009 → recalibrated in Hardt & Böse 2016
Frankfurt W_{1F}	landscape stabilization	~24 - ~21 ka	SED	Heine et al., 2009 → recalibrated in Hardt & Böse 2016
	downwasting of the W_{1B}-ice and formation of Barnim ridges	~26 ± 4 ka	OSL	Hardt et al., 2016
Brandenburg W_{1B}	formation of the W_{1B} IMP	30 ± 4 ka	OSL	this study
		<34 ± 7 ka	OSL	Lüthgens et al, 2010b
		<34 ± 3 – 28 ± 4 ka	OSL	Lüthgens et al., 2010a; Lüthgens 2011
	W_{1B} ice advance	~34 ± 5 ka	OSL	Hardt et al., 2016
		33 ± 2 ka	OSL	Brauer et al., 2005
		31 ± 5 ka	OSL	Nitzsche 2015

8.6 Outlook

To further improve the chronology presented above, it will be necessary to date several more sites, which are correlated to the Frankfurt phase. The sites should be situated to the east and to the west of the Barnim plateau. To the east, it remains interesting whether the morphostratigraphical correlation of Frankfurt and Poznan phase can be confirmed by sediment dating. The combination of OSL and cosmogenic exposure dating proved to be useful and should be extended. It also needs to be investigated how far the late MIS 3 ice advance extended towards the east and west of the study area.

The further analysis of LiDAR DEM will certainly provide many more yet unrecognized geomorphological details relevant for Quaternary research in the lowland areas.

9 OVERALL REFERENCES

Adamiec, G., Aitken, M., 1998: Dose-rate conversion factors: update. Ancient TL 16, 37-50.

Aitken, M., 1998: An Introduction to Optical Dating. Oxford University Press, Oxford.

Akçar, N., Ivy-Ochs, S., Kubik, P.W., Schlüchter, C., 2011: Post-depositional impacts on 'Findlinge' (erratic boulders) and their implications for surface-exposure dating. Swiss Journal of Geosciences 104, 445-453.

Ampel, L., Wohlfarth, B., Risberg, J., Veres, D., 2008: Paleolimnological response to millennial and centennial scale climate variability during MIS 3 and 2 as suggested by the diatom record in Les Echets, France. Quaternary Science Reviews 27, 1493-1504.

Arnold, L.J., Roberts, R.G., 2009: Stochastic modelling of multi-grain equivalent dose (D_e) distributions: Implications for OSL dating of sediment mixtures. Quaternary Geochronology 4, 204-230.

Bailey, R.M., 2010: Direct measurement of the fast component of quartz optically stimulated luminescence and implications for the accuracy of optical dating. Quaternary Geochronology 5, 559-568.

Bailey, R.M., Arnold, L.J., 2006: Statistical modelling of single grain quartz D_e distributions and an assessment of procedures for estimating burial dose. Quaternary Science Reviews 25, 2475-2502.

Balco, G., Briner, J., Finkel, R.C., Rayburn, J.A., Ridge, J.C., Schaefer, J.M., 2009: Regional beryllium-10 production rate calibration for late-glacial northeastern North America. Quaternary Geochronology 4, 93-107.

Balco, G., Stone, J.O., Lifton, N.A., Dunai, T.J., 2008: A complete and easily accessible means of calculating surface exposure ages or erosion rates from ^{10}Be and ^{26}Al measurements. Quaternary Geochronology 3, 174-195.

Ballantyne, C.K., 2012: Chronology of glaciation and deglaciation during the Loch Lomond (Younger Dryas) Stade in the Scottish Highlands: implications of recalibrated ^{10}Be exposure ages. Boreas 41, 513-526.

Ballarini, M., Wallinga, J., Wintle, A.G., Bos, A.J.J., 2007: A modified SAR protocol for optical dating of individual grains from young quartz samples. Radiation Measurements 42, 360-369.

Bard, E., 2004: Greenhouse effect and ice ages: historical perspective. Comptes Rendus Geoscience 336, 603-638.

Bard, E., Rostek, F., Turon, J.-L., Gendreau, S., 2000: Hydrological Impact of Heinrich Events in the Subtropical Northeast Atlantic. Science 289, 1321-1324.

Beckenbach, E., Müller, T., Seyfried, H., Simon, T., 2014: Potential of a high-resolution DTM with large spatial coverage for visualization, identification and interpretation of young (Würmian) glacial geomorphology: a case study from Oberschwaben (southern Germany). E&G - Quaternary Science Journal 63, 107-129.

Benn, D.I., Evans, D.J.A., 2010: Glaciers & Glaciation, 2. ed. Hodder Education, London.

Berendt, G., 1882: Geologische Karte von Preussen 1:25000, Sect. Biesenthal 3247. Königl. Preuss. Generalstab.

Berendt, G., Gagel, C., 1898: Geologische Karte von Preußen 1:25000, Freienwalde 3250. Königl. Preuss. Generalstab.

Berger, A., 1988: Milankovitch Theory and climate. Reviews of Geophysics 26, 624-657.

Berner, K., 2010: Grundwasserflurabstand, in: Stackebrandt, W., Andreae, A., Strahl, J. (Eds.), Atlas zur Geologie von Brandenburg, 4. ed. LBGR, Cottbus, pp. 114-115.

Bernhardi, A., 1832: Wie kamen die aus dem Norden stammenden Felsbruchstücke und Geschiebe, welche man in Norddeutschland und den benachbarten Ländern findet, an ihre gegenwärtigen Fundorte? Jahrbuch für Mineralogie, Geognosie, Geologie und Petrefaktenkunde 3, 257-267.

Bierman, P.R., Nichols, K.K., 2004: Rock to sediment - slope to sea with ^{10}Be - rates of landscape change. Annual Review of Earth and Planetary Sciences 32, 215-255.

Błaszkiewicz, M., 2011: Timing of the final disappearance of permafrost in the central European Lowland, as reconstructed from the evolution of lakes in N Poland. Geological Quarterly 55, 361–374.

Błaszkiewicz, M., Piotrowski, J.A., Brauer, A., Gierszewski, P., Kordowski, J., Kramkowski, M., Lamparski, P., Lorenz, S., Noryśkiewicz, A.M., Ott, F., Słowiński, M., Tyszkowski, S., 2015: Climatic and morphological controls on diachronous postglacial lake and river valley evolution in the area of Last Glaciation, northern Poland. Quaternary Science Reviews 109, 13-27.

BLDAM, 2015: Denkmalliste des Landes Brandenburg (monument register of Brandenburg). Brandenburgisches Landesamt für Denkmalpflege und Archäologisches Landesmuseum (State Office for preservation of historical monuments Brandenburg) http://www.bldam-brandenburg.de/images/05-BAR-Internet-15.pdf (last accessed: 05.07.2016).

Börner, A., 2007: Vergleich der quartärstratigraphischen Gliederungen von Nordost-Deutschland und Polen. Brandenburgische Geowissenschaftliche Beiträge 14, 15-24.

Böse, M., 1995: Problems of dead ice and ground ice in the central part of the North European Plain. Quaternary International 28, 123-125.

Böse, M., Lüthgens, C., Lee, J.R., Rose, J., 2012: Quaternary glaciations of northern Europe. Quaternary Science Reviews 44, 1-25.

Bøtter-Jensen, L., Andersen, C.E., Duller, G.A.T., Murray, A.S., 2003a: Developments in radiation, stimulation and observation facilities in luminescence measurements. Radiation Measurements 37, 535-541.

Bøtter-Jensen, L., McKeever, S.W.S., Wintle, A.G., 2003b: Optically Stimulated Luminescence Dosimetry. Elsevier.

Bøtter-Jensen, L., Thomsen, K.J., Jain, M., 2010: Review of optically stimulated luminescence (OSL) instrumental developments for retrospective dosimetry. Radiation Measurements 45, 253-257.

Boulton, G.S., 1986: Push-moraines and glacier-contact fans in marine and terrestrial environments. Sedimentology 33, 677-698.

Brauer, A., Tempelhoff, K., Murray, A.S., 2005: OSL Dating of Fine-Grained Sand Deposits and its Implications for Glacial Stratigraphy and Landscape Evolution: Research Results from Stolzenhagen, Northeastern Brandenburg. Die Erde 136, 20.

Briner, J.P., Young, N.E., Goehring, B.M., Schaefer, J.M., 2012: Constraining Holocene ^{10}Be production rates in Greenland. Journal of Quaternary Science 27, 2-6.

Brodzikowski, K., Loon, A.J., 1991: Glacigenic sediments. Elsevier, Amsterdam.

Brose, F., 1995: Erscheinungen des weichselzeitlichen Eisrückzuges in Ostbrandenburg (in German, with English summary). Brandenburgische Geowissenschaftliche Beiträge 2, 3-11.

Brose, F., Marcinek, J., 1995: Brandenburger Eisrandlage und Baruther Urstromtal, in: Schroeder, J.H., Nowel, W. (Eds.), Führer zur Geologie von Berlin und Brandenburg Nr. 3: Lübbenau – Calau. Geowissenschaftler in Berlin und Brandenburg, Berlin, pp. 189 - 195.

Bussemer, S., 1993: Genese, Verteilungsmuster und Stoffbestand periglaziärer Deckserien auf dem Barnim: ein Beitrag zur weichselspätglazialen Landschaftsentwicklung im älteren Jungmoränengebiet Norddeutschlands (Dissertation), Geographisches Institut. Humboldt-Universität zu Berlin.

Bussemer, S., 1994: Geomorphologische und bodenkundliche Untersuchungen an periglaziären Deckserien des mittleren und östlichen Barnim. Fachbereich Geographie der Humboldt-Universität zu Berlin.

Bussemer, S., 1995: Relief, Pleistozänsedimente und Böden des Barnims zwischen Berlin und Bad Freienwalde, in: Hofmeister, B., Voss, F. (Eds.), Berliner Geographische Studien. Technische Universität Berlin, pp. 221-230.

Bussemer, S., 2002: Quartäre Entwicklung und Gliederung der Binnenentwässerungsgebiete auf der Barnimhochfläche (NE-Brandenburg). Greifswalder Geographische Arbeiten 26, 23-26.

Bussemer, S., Michel, J., 2006: Die Hirschfelder Heide als typische Niedertaulandschaft des nordöstlichen Barnims (NE-Brandenburg). Brandenburgische Geowissenschaftliche Beiträge 13, 27-34.

Bussemer, S., Michel, J., Schlaak, N., Luckert, J., 2007: Geologisch-morphologisches Profil durch den nordöstlichen Barnim (Brandenburg). Brandenburgische Geowissenschaftliche Beiträge 14, 37-49.

Buylaert, J.P., Jain, M., Murray, A.S., Thomsen, K.J., Lapp, T., 2012: IR-RF dating of sand-sized K-feldspar extracts: A test of accuracy. Radiation Measurements 47, 759-765.

Cameron, D., 1965: Goethe-discoverer of the ice age. Journal of Glaciology 5, 751-754.

Candy, I., Schreve, D.C., Sherriff, J., Tye, G.J., 2014: Marine Isotope Stage 11: Palaeoclimates, palaeoenvironments and its role as an analogue for the current interglacial. Earth-Science Reviews 128, 18-51.

Cepek, A.G., 1965: Die Stratigraphie der pleistozänen Ablagerungen im Norddeutschen Tiefland (in German), in: Gellert, J.F. (Ed.), Die Weichsel-Eiszeit im Gebiet der Deutschen Demokratischen Republik. Akademie-Verl., Berlin.

Cepek, A.G., Hellwig, D., Nowel, W., 1994: Zur Gliederung des Saale-Komplexes im Niederlausitzer Braunkohlereviert. Brandenburgische Geowissenschaftliche Beiträge 1, 43-83.

Chrobok, S.M., Markuse, G., Nitz, B., 1982: Abschmelz- und Sedimentationsprozesse im Rückland weichselhoch- und spätglazialer Marginalzonen des Barnims und der Uckermark (mittlere DDR). Petermanns Geographische Mitteilungen 126.

Clark, C.D., Hughes, A.L.C., Greenwood, S.L., Jordan, C., Sejrup, H.P., 2012: Pattern and timing of retreat of the last British-Irish Ice Sheet. Quaternary Science Reviews 44, 112-146.

Clifford, N.J., Richards, K.S., Brown, R.A., Lane, S.N., 1995: Scales of Variation of Suspended Sediment Concentration and Turbidity in a Glacial Meltwater Stream. Geografiska Annaler. Series A, Physical Geography 77, 45-65.

Cockburn, H.A.P., Summerfield, M.A., 2004: Geomorphological applications of cosmogenic isotope analysis. Progress in Physical Geography 28, 1-42.

Cohen, K.M., Gibbard, P., 2011: Global chronostratigraphical correlation table for the last 2.7 million years. Subcommission on Quaternary Stratigraphy (International Commission on Stratigraphy), Cambridge, England.

Cunningham, A.C., Wallinga, J., 2010: Selection of integration time intervals for quartz OSL decay curves. Quaternary Geochronology 5, 657-666.

Cunningham, A.C., Wallinga, J., 2012: Realizing the potential of fluvial archives using robust OSL chronologies. Quaternary Geochronology 12, 98-106.

Dansgaard, W., Johnsen, S.J., Clausen, H.B., Dahl-Jensen, D., Gundestrup, N.S., Hammer, C.U., Hvidberg, C.S., Steffensen, J.P., Sveinbjornsdottir, A.E., Jouzel, J., Bond, G., 1993: Evidence for general instability of past climate from a 250-kyr ice-core record. Nature 364, 218-220.

Degering, D., Krbetschek, M.R., 2007: 11. Dating of interglacial sediments by luminescence methods, in: Sirocko, F., Claussen, M., Fernanda, M., Goñi, S., Litt, T. (Eds.), Developments in Quaternary Sciences. Elsevier, pp. 157-171.

Dietze, M., Kreutzer, S., Fuchs, M.C., Burow, C., Fischer, M., Schmidt, C., 2013: A practical guide to the R package Luminescence. Ancient TL 31, 11-18.

Duller, G.A.T., 2003: Distinguishing quartz and feldspar in single grain luminescence measurements. Radiation Measurements 37, 161-165.

Duller, G.A.T., 2004: Luminescence dating of Quaternary sediments: recent advances. Journal of Quaternary Science 19, 183-192.

Duller, G.A.T., 2007: Assessing the error on equivalent dose estimates derived from single aliquot regenerative dose measurements. Ancient TL 25, 15-24.

Duller, G.A.T., 2008: Single-grain optical dating of Quaternary sediments: why aliquot size matters in luminescence dating. Boreas 37, 589-612.

Duller, G.A.T., Bøtter-Jensen, L., Murray, A.S., 2000: Optical dating of single sand-sized grains of quartz: sources of variability. Radiation Measurements 32, 453-457.

Dunai, T.J., 2010: Cosmogenic Nuclides: Principles, Concepts and Applications in the Earth Surface Sciences. Cambridge University Press.

Ehlers, J., Astakhov, V., Gibbard, P.L., Mangerud, J., Svendsen, J.I., 2013: Glaciations | Late Pleistocene in Eurasia, in: Elias, S.A., Mock, C.J. (Eds.), Encyclopedia of Quaternary Science (Second Edition). Elsevier, Amsterdam, pp. 224-235.

Ehlers, J., Gibbard, P.L., 2004: Preface, in: Ehlers, J., Gibbard, P.L. (Eds.), Developments in Quaternary Sciences. Elsevier, pp. VII-VIII.

Ehlers, J., Grube, A., Stephan, H.-J., Wansa, S., 2011: Chapter 13 - Pleistocene Glaciations of North Germany—New Results, in: Jürgen Ehlers, Gibbard, P.L., Hughes, P.D. (Eds.), Developments in Quaternary Sciences. Elsevier, pp. 149-162.

Eissmann, L., 2002: Quaternary geology of eastern Germany (Saxony, Saxon–Anhalt, South Brandenburg, Thüringia), type area of the Elsterian and Saalian Stages in Europe. Quaternary Science Reviews 21, 1275-1346.

Evans, D.J.A., 2003: Ice-marginal terrestrial landsystems: Active temperate glacier margins, in: Evans, D.J.A. (Ed.), Glacial Landsystems. Arnold, London, pp. 12-43.

Evans, I.S., 2012: Geomorphometry and landform mapping: What is a landform? Geomorphology 137, 94-106.

Fenton, C.R., Hermanns, R.L., Blikra, L.H., Kubik, P.W., Bryant, C., Niedermann, S., Meixner, A., Goethals, M.M., 2011: Regional ^{10}Be production rate calibration for the past 12 ka deduced from the radiocarbon-dated Grøtlandsura and Russenes rock avalanches at 69° N, Norway. Quaternary Geochronology 6, 437-452.

Franz, H.-J., 1965: Weichseleiszeitliche Eisrandlagen auf dem Territorium der Deutschen Demokratischen Republik (in German), in: Gellert, J.F. (Ed.), Die Weichsel-Eiszeit im Gebiet der Deutschen Demokratischen Republik. Akademie-Verl., Berlin.

Franz, H.-J., Schneider, R., Scholz, E., 1970a: Erläuterungen für die Kartenblätter Berlin-Potsdam und Frankfurt-Eberswalde (in German). Haack, Gotha.

Franz, H.-J., Schneider, R., Scholz, E., 1970b: Geomorphologische Übersichtskarte Berlin-Potsdam, in: Gellert, J.F., Scholz, E. (Eds.). Haack, Gotha.

Fritze, W.H., 1987: Zu Deutung und ursprünglicher Beziehung des Landnamens "Barnim". Jahrbuch für Brandenburgische Landesgeschichte 37, 41-50.

Fuchs, M., Owen, L.A., 2008: Luminescence dating of glacial and associated sediments: review, recommendations and future directions. Boreas 37, 636-659.

Fuchs, M.C., Kreutzer, S., Burow, C., Dietze, M., Fischer, M., Schmidt, C., Fuchs, M., 2015: Data processing in luminescence dating analysis: An exemplary workflow using the R package ‘Luminescence’. Quaternary International 362, 8-13.

Galbraith, R.F., 2010: On plotting OSL equivalent doses. Ancient TL 28, 1-10.

Galbraith, R.F., Roberts, R.G., Laslett, G.M., Yoshida, H., Olley, J.M., 1999: Optical dating of single and multiple grains of quartz from Jinmium rock shelter, Northern Australia: Part I, experimental design and statistical models. Archaeometry 41, 339-364.

Gärtner, P., 1993: Beiträge zur Landschaftsgeschichte des westlichen Barnim. Berliner Geographische Arbeiten 77.

Gärtner, P., 2004: Niederungen des Westlichen Barnims, in: Schroeder, J.H. (Ed.), Nordwestlicher Barnim - Eberswalder Urstromtal. Führer zur Geologie von Berlin und Brandenburg. Selbstverlag Geowissenschaftler in Berlin und Brandenburg e.V., Berlin.

Geikie, J., 1874: The Great Ice Age and its Relation to the Antiquity of Man. D. Appleton & Co., New York.

Gemmell, A.M.D., 1985: Special Issue: Thermoluminescence and Electron-Spin-Resonance DatingZeroing of the TL signal of sediment undergoing fluvial transportation: A laboratory experiment. Nuclear Tracks and Radiation Measurements (1982) 10, 695-702.

Geyh, M.A., Müller, H., 2005: Numerical ^{230}Th/U dating and a palynological review of the Holsteinian/Hoxnian Interglacial. Quaternary Science Reviews 24, 1861-1872.

Goehring, B.M., Lohne, Ø.S., Mangerud, J., Svendsen, J.I., Gyllencreutz, R., Schaefer, J., Finkel, R., 2012: Late glacial and holocene ^{10}Be production rates for western Norway. Journal of Quaternary Science 27, 89-96.

Gosse, J.C., Phillips, F.M., 2001: Terrestrial in situ cosmogenic nuclides: theory and application. Quaternary Science Reviews 20, 1475-1560.

Granger, D.E., 2013: Cosmogenic Nuclide Dating | Landscape Evolution in: Elias, S.A., Mock, C.J. (Eds.), Encyclopedia of Quaternary Science (Second Edition). Elsevier, Amsterdam, pp. 440-445.

Greenwood, S.L., Clark, C.D., 2008: Subglacial bedforms of the Irish Ice Sheet. Journal of Maps 4, 332-357.

Greenwood, S.L., Clark, C.D., 2009: Reconstructing the last Irish Ice Sheet 2: a geomorphologically-driven model of ice sheet growth, retreat and dynamics. Quaternary Science Reviews 28, 3101-3123.

Greinwald, S., Thierbach, R., 1997: Elektrische Eigenschaften der Gesteine, in: Beblo, M. (Ed.), Umweltgeophysik. Ernst & Sohn, Berlin.

Griffiths, D.H., Barker, R.D., 1993: Two-dimensional resistivity imaging and modelling in areas of complex geology. Journal of Applied Geophysics 29, 211-226.

Grimmel, E., 1973: Bemerkungen zum Geschiebedecksand. E&G - Quaternary Science Journal 23/24.

Grün, R., Schwarcz, H.P., 2000: Revised open system U-series/ESR age calculations for teeth from Stratum C at the Hoxnian Interglacial type locality, England. Quaternary Science Reviews 19, 1151-1154.

Gustavson, T.C., Boothroyd, J.C., 1987: A depositional model for outwash, sediment sources, and hydrologic characteristics, Malaspina Glacier, Alaska: A modern analog of the southeastern margin of the Laurentide Ice Sheet. Geological Society of America Bulletin 99, 187-200.

Hallet, B., Putkonen, J., 1994: Surface Dating of Dynamic Landforms: Young Boulders on Aging Moraines. Science 265, 937-940.

Hannemann, M., 2005: Der Bad Freienwalde–Frankfurter Stauchungszug und die Entstehung der Oderbruchdepression. Brandenburgische Geowissenschaftliche Beiträge 12, 143-152.

Hardt, J., Böse, M., 2016: The timing of the Weichselian Pomeranian ice marginal position south of the Baltic Sea: A critical review of morphological and geochronological results. Quaternary International (in press).

Hardt, J., Hebenstreit, R., Lüthgens, C., Böse, M., 2015: High-resolution mapping of ice-marginal landforms in the Barnim region, northeast Germany. Geomorphology 250, 41-52.

Hardt, J., Lüthgens, C., Hebenstreit, R., Böse, M., 2016: Geochronological (OSL) and geomorphological investigations at the presumed Frankfurt ice marginal position in northeast Germany. Quaternary Science Reviews 154, 85-99.

Heine, K., Reuther, A.U., Thieke, H.U., Schulz, R., Schlaak, N., Kubik, P.W., 2009: Timing of Weichselian ice marginal positions in Brandenburg (northeastern Germany) using cosmogenic in situ Be-10. Zeitschrift für Geomorphologie N.F. 53, 433-454.

Hemming, S.R., 2004: Heinrich events: Massive late Pleistocene detritus layers of the North Atlantic and their global climate imprint. Reviews of Geophysics 42.

Hermanowski, P., 2015: Substratum morphology and significance during the Weichselian Odra ice lobe advance in northeast Germany and northwest Poland. Geologos 21, 241-248.

Hermsdorf, N., Lippstreu, L., Sonntag, A., 1998: Geologische Übersichtskarte 1:200000, CC 3942 Berlin. Bundesanstalt für Geowissenschaften und Rohstoffe, Hannover.

Hermsdorf, N., Strahl, J., 2008: Karte der Eem-Vorkommen des Landes Brandenburg (Eemian deposits in the Brandenburg area). Brandenburgische Geowissenschaftliche Beiträge 15, 1-57.

Heyman, J., 2014: Paleoglaciation of the Tibetan Plateau and surrounding mountains based on exposure ages and ELA depression estimates. Quaternary Science Reviews 91, 30-41.

Heyman, J., Stroeven, A.P., Harbor, J.M., Caffee, M.W., 2011: Too young or too old: Evaluating cosmogenic exposure dating based on an analysis of compiled boulder exposure ages. Earth and Planetary Science Letters 302, 71-80.

Hibbert, F.D., Austin, W.E.N., Leng, M.J., Gatliff, R.W., 2010: British Ice Sheet dynamics inferred from North Atlantic ice-rafted debris records spanning the last 175 000 years. Journal of Quaternary Science 25, 461-482.

Hirsch, F., Schneider, A., Nicolay, A., Błaszkiewicz, M., Kordowski, J., Noryskiewicz, A.M., Tyszkowski, S., Raab, A., Raab, T., 2015: Late Quaternary landscape development at the margin of the Pomeranian phase (MIS 2) near Lake Wygonin (Northern Poland). Catena 124, 28-44.

Houmark-Nielsen, M., 2010: Extent, age and dynamics of Marine Isotope Stage 3 glaciations in the southwestern Baltic Basin. Boreas 39, 343-359.

Houmark-Nielsen, M., Björck, S., Wohlfarth, B., 2006: 'Cosmogenic ^{10}Be ages on the Pomeranian Moraine, Poland': Comments. Boreas 35, 600-604.

Houmark-Nielsen, M., Kjær, K.H., 2003: Southwest Scandinavia, 40–15 kyr BP: palaeogeography and environmental change. Journal of Quaternary Science 18, 769-786.

Houmark-Nielsen, M., Linge, H., Fabel, D., Schnabel, C., Xu, S., Wilcken, K.M., Binnie, S., 2012: Cosmogenic surface exposure dating the last deglaciation in Denmark: Discrepancies with

independent age constraints suggest delayed periglacial landform stabilisation. Quaternary Geochronology 13, 1-17.

Hughes, A.L.C., Gyllencreutz, R., Lohne, Ø.S., Mangerud, J., Svendsen, J.I., 2015: The last Eurasian ice sheets – a chronological database and time-slice reconstruction, DATED-1. Boreas 45, 1-45.

Huntley, D.J., Godfreysmith, D.I., Thewalt, M.L.W., 1985: Optical Dating of Sediments. Nature 313, 105-107.

Ivy-Ochs, S., Kober, F., 2008: Surface exposure dating with cosmogenic nuclides. E&G - Quaternary Science Journal 57, 179-209.

Ivy-Ochs, S., Kober, F., 2013: Cosmogenic Nuclide Dating | Exposure Geochronology, in: Elias, S.A., Mock, C.J. (Eds.), Encyclopedia of Quaternary Science (Second Edition). Elsevier, Amsterdam, pp. 432-439.

Jakobsen, P.R., 2012: Rock-cored drumlins on Bornholm, Denmark. Geological Survey of Denmark and Greenland Bulletin 26, 17-20.

Jarvis, A., Reuter, H.I., Nelson, A., Guevara, E., 2008: Hole-filled seamless SRTM data V4, International Centre for Tropical Agriculture (CIAT), available from http://srtm.csi.cgiar.org.

Johnsen, S.J., Clausen, H.B., Dansgaard, W., Fuhrer, K., Gundestrup, N., Hammer, C.U., Iversen, P., Jouzel, J., Stauffer, B., steffensen, J.P., 1992: Irregular glacial interstadials recorded in a new Greenland ice core. Nature 359, 311-313.

Junge, F.W., Eissmann, L., 2000: Postsedimentäre Deformationsbilder in mitteldeutschen Vorstoßbändertonen - Hinweise auf den Bewegungsmechanismus des quartären Inlandeises. Brandenburgische Geowissenschaftliche Beiträge 7, 21-28.

Jurgaitis, A., Juozapavicius, G., 1989: Genetic classification of glaciofluvial deposits and criteria for their recognition, in: Goldthwaith, R.P., Matsch, C.L. (Eds.), Genetic classification of glacigenic deposits. Balkema, Rotterdam.

Juschus, O., 2003: Das Jungmoränenland südlich von Berlin: Untersuchungen zur jungquartären Landschaftsentwicklung zwischen Unterspreewald und Nuthe. Dissertation, Geographisches Institut der Humboldt-Universität zu Berlin.

Juschus, O., 2010: Der maximale Vorstoß des weichselzeitlichen Inlandeises am Nordrand des Lausitzer Grenzwalls und des Flämings. Brandenburgische Geowissenschaftliche Beiträge 17, 63-73.

Juschus, O., Schlaak, N., Bauriegel, A., Kowalski, S., Bussert, R., 2011: Geologische und bodenkundliche Untersuchungen entlang der Erdgasleitung OPAL in Brandenburg – erste Ergebnisse. Brandenburgische Geowissenschaftliche Beiträge 18, 29-70.

Kalm, V., 2012: Ice-flow pattern and extent of the last Scandinavian Ice Sheet southeast of the Baltic Sea. Quaternary Science Reviews 44, 51-59.

Kearey, P., Brooks, M., Hill, I., 2002: An Introduction to Geophysical Exploration. Blackwell Science.

Keilhack, K., 1909: Begleitworte zur Karte der Endmoränen und Urstromtäler Norddeutschlands. Jahrbuch der Königlich Preussischen geologischen Landesanstalt und Bergakademie zu Berlin 30, 507-510.

Kelly, M.A., Lowell, T.V., Applegate, P.J., Phillips, F.M., Schaefer, J.M., Smith, C.A., Kim, H., Leonard, K.C., Hudson, A.M., 2015: A locally calibrated, late glacial ^{10}Be production rate from a low-latitude, high-altitude site in the Peruvian Andes. Quaternary Geochronology 26, 70-85.

Kenzler, M., Tsukamoto, S., Meng, S., Frechen, M., Hüneke, H., 2016: New age constraints from the SW Baltic Sea area – implications for Scandinavian Ice Sheet dynamics and palaeo-environmental conditions during MIS 3 and early MIS 2. Boreas (in press).

Kenzler, M., Tsukamoto, S., Meng, S., Thiel, C., Frechen, M., Hüneke, H., 2015: Luminescence dating of Weichselian interstadial sediments from the German Baltic Sea coast. Quaternary Geochronology 30, Part B, 251-256.

Koster, E.A., 2009: The "European Aeolian Sand Belt": Geoconservation of Drift Sand Landscapes. Geoheritage 1, 93-110.

Kozarski, S., 1995: Deglacjacja Pólnocno-Zachodniej Polski: Warunki srodowiska i transformacja geosystemu (~20 ka - 10 ka BP). Polska Akademia NAUK, Wroclaw.

Krbetschek, M., Degering, D., Alexowsky, W., 2008: Infrarot-Radiofluoreszenz-Alter (IR-RF) unter-saalezeitlicher Sedimente Mittel- und Ostdeutschlands. Zeitschrift der deutschen Gesellschaft für Geowissenschaften 159, 133-140.

Kreutzer, S., Schmidt, C., Fuchs, M.C., Dietze, M., Fischer, M., Fuchs, M., 2012: Introducing an R package for luminescence dating analysis. Ancient TL 30, 1-8.

Krzyszkowski, D., Zieliński, T., 2002: The Pleistocene end moraine fans: controls on their sedimentation and location. Sedimentary Geology 149, 73-92.

Kühner, R., 2003: Ausbildung und Gliederung des saalezeitlichen Sedimentkomplexes im Bereich der Hornoer Hochfläche (Arrangement and structure of the Saalian sediment sequence in the area of the upland plain of Horno). Brandenburgische Geowissenschaftliche Beiträge 10, 111-121.

Kühner, R., 2013: Die Faltenzone Radewiese-Briesnig im Tagebau Jänschwalde (Südbrandenburg) – eine warthezeitliche Eisrandlage? (The Radewiese-Briesnig fault zone in the Jänschwalde opencast mine (South Brandenburg) – a Warthian ice marginal position?). Brandenburgische Geowissenschaftliche Beiträge 20, 109-116.

Kühner, R., Strahl, J., 2008: Die Eem-Vorkommen am Außenrand der warthestadialen Vereisung im Tagebau Welzow-Süd, Niederlausitz. Zeitschrift der deutschen Gesellschaft für Geowissenschaften 159, 191-204.

Kühner, R., Strahl, J., Süssmilch, P., Thieke, H., Meng, S., 2008: Lithologische und pollenanalytische Befunde aus dem saalefrühglazialen Fluviatilkomplex (Tranitzer Fluviatil) und dem Eem-Interglazial im Tagebau Jänschwalde, Südbrandenburg (Lithological and palynological results to the Early Saalian Fluvialtile Complex (Tranitzer Fluviatil) and the Eemian in the Jänschwalde opencast mine, South Brandenburg). Brandenburgische Geowissenschaftliche Beiträge 15, 1-12.

Kulig, G., 2005: Erstellung einer Auswertesoftware zur Altersbestimmung mittels Lumineszenzverfahren unter spezieller Berücksichtigung des Einflusses radioaktiver Ungleichgewichte in der 238-U-Zerfallsreihe. Bakkalaureusarbeit Network Computing, TU Freiberg.

Lal, D., 1991: Cosmic ray labeling of erosion surfaces: in situ nuclide production rates and erosion models. Earth and Planetary Science Letters 104, 424-439.

Laufer, E., 1881: Geologische Karte von Preußen 1:25000, Sect. Bernau 3347. Königl. Preuss. Generalstab.

Laufer, E., Keilhack, K., 1882: Geologische Karte von Preußen 1:25000, Sect. Wandlitz 3246. Königl. Preuss. Generalstab.

Leberl, F., Irschara, A., Pock, T., Meixner, P., Gruber, M., Scholz, S., Wiechert, A., 2010: Point Clouds: Lidar versus 3D Vision. Photogrammetric Engineering and Remote Sensing 76, 1123-1134.

Lepper, K., McKeever, S.W.S., 2002: An Objective Methodology for Dose Distribution Analysis. Radiation Protection Dosimetry 101, 349-352.

Lian, O.B., 2013: Luminescence Dating | Optical Dating, in: Editor-in-Chief: Scott, A.E. (Ed.), Encyclopedia of Quaternary Science (Second Edition). Elsevier, Amsterdam, pp. 653-666.

Lian, O.B., Roberts, R.G., 2006: Dating the Quaternary: progress in luminescence dating of sediments. Quaternary Science Reviews 25, 2449-2468.

Liedtke, H., 1981: Die nordischen Vereisungen in Mitteleuropa, 2. erw. Aufl., Zentralausschuß für Dt. Landeskunde, Trier.

Liedtke, H., 1992: Die Entwicklung der Ostsee als Folge ehemaliger Inlandeisbedeckung und anhaltender Hebung Skandinaviens. Geographische Rundschau 42, 620-625.

Lifton, N., Sato, T., Dunai, T.J., 2014: Scaling in situ cosmogenic nuclide production rates using analytical approximations to atmospheric cosmic-ray fluxes. Earth and Planetary Science Letters 386, 149-160.

Lippstreu, L., 1995a: Brandenburg (in German), in: Benda, L. (Ed.), Das Quartär Deutschlands. Borntraeger, Berlin, Stuttgart, pp. 116-147.

Lippstreu, L., 1995b: Geologische Übersichtskarte von Berlin und Umgebung 1:100000, in: Stackebrandt, W., Frey, W. (Eds.). Landesamt für Geowissenschaften und Rohstoffe Brandenburg.

Lippstreu, L., Hermsdorf, N., Sonntag, A., Strahl, J., 2015: Pleistozän, in: Stackebrandt, W., Franke, D. (Eds.), Geologie von Brandenburg. Schweizerbart'sche Verlagsbuchhandlung, Stuttgart, pp. 333-419.

Lippstreu, L., Hermsdorf, N., Strahl, J., 2010: Die Gliederung des Pleistozäns in Brandenburg, in: Stackebrandt, W., Andreae, A., Strahl, J. (Eds.), Atlas zur Geologie von Brandenburg, 4. ed., LBGR, Cottbus, p. 134.

Lippstreu, L., Sonntag, A., Horna, F., Badura, J., Przybylski, B., 2001: Geologische Übersichtskarte 1:200 000, Blatt CC 4750 Cottbus. Bundesanstalt für Geowissenschaften und Rohstoffe, Hannover.

Lippstreu, L., Stackebrandt, W., 2003: Jänschwalde und die Gliederung des Saale-Komplexes - ein Kommentar zum Beitrag von Werner Nowel. E&G - Quaternary Science Journal 52, 84-90.

Lippstreu, L., Zwirner, R., 1972: Lithofazieskarten Quartär 1:50000, Berlin NO 1968, in: Cepek, A.G. (Ed.). Zentrales Geologisches Institut (GDR), Berlin.

Litt, T., Behre, K.-E., Meyer, K.-D., Stephan, H.-J., Wansa, S., 2007: Stratigraphical Terms for the Quaternary of the North German Glaciation Area. E&G - Quaternary Science Journal 56, 7-65.

Litt, T., Gibbard, P., 2008: Definition of a Global Stratotype Section and Point (GSSP) for the base of the Upper (Late) Pleistocene Subseries (Quaternary System/Period). Episodes 31, 260-263.

Liu, X., 2008: Airborne LiDAR for DEM generation: some critical issues. Progress in Physical Geography 32, 31-49.

Livingstone, S.J., Evans, D.J.A., Cofaigh, C.O., 2010: Re-advance of Scottish ice into the Solway Lowlands (Cumbria, UK) during the Main Late Devensian deglaciation. Quaternary Science Reviews 29, 2544-2570.

Loke, M.H., 2014: Electrical Resistivity Surveys and Data Interpretation, in: Gupta, H. (Ed.), Encyclopedia of Solid Earth Geophysics. Springer Netherlands, pp. 276-283.

Loke, M.H., Barker, R.D., 1995: Least-squares deconvolution of apparent resistivity pseudosections. Geophysics 60, 1682-1690.

Loke, M.H., Barker, R.D., 1996: Rapid least-squares inversion of apparent resistivity pseudosections by a quasi-Newton method. Geophysical Prospecting 44, 131-152.

Lowe, J.J., Walker, M.J.C., 2014: Reconstructing Quaternary Environments, 3. ed. Routledge.

Lukas, S., Rother, H., 2016: Moränen versus Till: Empfehlungen für die Beschreibung, Interpretation und Klassifikation glazialer Landformen und Sedimente. E&G - Quaternary Science Journal 65, 95-112.

Lüthgens, C., 2011: The age of Weichselian main ice marginal positions in north-eastern Germany inferred from Optically Stimulated Luminescence (OSL) dating (Dissertation), Department of Earth Sciences. Freie Universität Berlin.

Lüthgens, C., Böse, M., 2011: Chronology of Weichselian main ice marginal positions in north-eastern Germany. E&G - Quaternary Science Journal 60, 236-247.

Lüthgens, C., Böse, M., 2012: From morphostratigraphy to geochronology – on the dating of ice marginal positions. Quaternary Science Reviews 44, 26-36.

Lüthgens, C., Böse, M., Krbetschek, M., 2010a: On the age of the young morainic morphology in the area ascribed to the maximum extent of the Weichselian glaciation in north-eastern Germany. Quaternary International 222, 72-79.

Lüthgens, C., Böse, M., Lauer, T., Krbetschek, M., Strahl, J., Wenske, D., 2011a: Timing of the last interglacial in Northern Europe derived from Optically Stimulated Luminescence (OSL) dating of a terrestrial Saalian–Eemian–Weichselian sedimentary sequence in NE-Germany. Quaternary International 241, 79-96.

Lüthgens, C., Böse, M., Preusser, F., 2011b: Age of the Pomeranian ice-marginal position in northeastern Germany determined by Optically Stimulated Luminescence (OSL) dating of glaciofluvial sediments. Boreas 40, 598-615.

Lüthgens, C., Krbetschek, M., Böse, M., Fuchs, M.C., 2010b: Optically stimulated luminescence dating of fluvioglacial (sandur) sediments from north-eastern Germany. Quaternary Geochronology 5, 237-243.

Lyell, C., 1853: Principles of Geology, 9. ed. D. Appleton & Co., New York.

Lytwyn, J., 2010: Remote sensing and GIS investigation of glacial features in the region of Devil's Lake State Park, South-Central Wisconsin, USA. Geomorphology 123, 46-60.

Marks, L., 2002: Last Glacial Maximum in Poland. Quaternary Science Reviews 21, 103-110.

Marks, L., 2011: Chapter 23 - Quaternary Glaciations in Poland, in: Jürgen Ehlers, P.L.G., Philip, D.H. (Eds.), Developments in Quaternary Sciences. Elsevier, pp. 299-303.

Marks, L., 2012: Timing of the Late Vistulian (Weichselian) glacial phases in Poland. Quaternary Science Reviews 44, 81-88.

Marrero, S.M., Phillips, F.M., Borchers, B., Lifton, N., Aumer, R., Balco, G., 2016: Cosmogenic nuclide systematics and the CRONUScalc program. Quaternary Geochronology 31, 160-187.

Meyer, H., 1974: Pollenanalytische Untersuchungen und Jahresschichtenzählungen an der holstein-zeitlichen Kieselgur von Hetendorf. Geologisches Jahrbuch A 21, 87-105.

Michas, U., 2003: Die Eroberung und Besiedlung Nordostbrandenburgs. Gesellschaft zur Erforschung der Märkischen Eiszeitstraße e.V., Eberswalde.

Müller, U., 2004: Weichsel-Frühglazial in Nordwest-Mecklenburg. Meyniana 56, 81-115.

Murray, A.S., Wintle, A.G., 2000: Luminescence dating of quartz using an improved single-aliquot regenerative-dose protocol. Radiation Measurements 32, 57-73.

Murray, A.S., Wintle, A.G., 2003: The single aliquot regenerative dose protocol: potential for improvements in reliability. Radiation Measurements 37, 377-381.

Nicolay, A., Raab, A., Raab, T., Rösler, H., Bönisch, E., Murray, A.S., 2014: Evidence of (pre-) historic to modern landscape and land use history near Jänschwalde (Brandenburg, Germany). Zeitschrift für Geomorphologie 58, 7-31.

Nishiizumi, K., Kohl, C.P., Arnold, J.R., Dorn, R., Klein, I., Fink, D., Middleton, R., Lal, D., 1993: Role of in situ cosmogenic nuclides ^{10}Be and ^{26}Al in the study of diverse geomorphic processes. Earth Surface Processes and Landforms 18, 407-425.

Nitz, B., 2004: Biesenthaler Becken (in German), in: Schroeder, J.H. (Ed.), Nordwestlicher Barnim - Eberswalder Urstromtal. Führer zur Geologie von Berlin und Brandenburg. Selbstverlag Geowissenschaftler in Berlin und Brandenburg e.V., Berlin.

Nitzsche, C., 2015: Zur Geochronologie der Sedimentablagerung im Bereich des Müncheberger Sanders (unpublished master thesis), Department of Geosciences, Physical Geography. Freie Universität Berlin.

Nowel, W., 2003a: Nochmals zur Altersstellung des Tranitzer Fluviatils (Anmerkungen zum „Kommentar" von Lippstreu & Stackebrandt). E&G - Quaternary Science Journal 53, 114-123.

Nowel, W., 2003b: Zur Korrelation der Glazialfolgen im Saale-Komplex Nord- und Mitteldeutschlands am Beispiel des Tagebaus Jänschwalde in Brandenburg. E&G - Quaternary Science Journal 52, 47-83.

Oguchi, T., Hayakawa, Y.S., Wasklewicz, T., 2011: Chapter Seven - Data Sources, in: Mike J. Smith, P.P., James, S.G. (Eds.), Developments in Earth Surface Processes. Elsevier, pp. 189-224.

Olley, J., Caitcheon, G., Murray, A., 1998: The distribution of apparent dose as determined by Optically Stimulated Luminescence in small aliquots of fluvial quartz: Implications for dating young sediments. Quaternary Science Reviews 17, 1033-1040.

Olley, J.M., Caitcheon, G.G., Roberts, R.G., 1999: The origin of dose distributions in fluvial sediments, and the prospect of dating single grains from fluvial deposits using optically stimulated luminescence. Radiation Measurements 30, 207-217.

Otepka, J., Ghuffar, S., Waldhauser, C., Hochreiter, R., Pfeifer, N., 2013: Georeferenced Point Clouds: A Survey of Features and Point Cloud Management. ISPRS International Journal of Geo-Information 2, 1038.

Paillard, D., 2015: Quaternary glaciations: from observations to theories. Quaternary Science Reviews 107, 11-24.

Patton, H., Hubbard, A., Andreassen, K., Winsborrow, M., Stroeven, A.P., 2016: The build-up, configuration, and dynamical sensitivity of the Eurasian ice-sheet complex to Late Weichselian climatic and oceanic forcing. Quaternary Science Reviews 153, 97-121.

Penck, A., 1879: Die Geschiebeformation Norddeutschlands. Zeitschrift der Deutschen Geologischen Gesellschaft 31, 117-203.

Penck, A., Brückner, E., 1909: Die Alpen im Eiszeitalter. C.H. Tauchnitz, Leipzig.

Pillans, B., Gibbard, P., 2012: Chapter 30 - The Quaternary Period, The Geologic Time Scale. Elsevier, Boston, pp. 979-1010.

Prescott, J.R., Hutton, J.T., 1994: Cosmic ray contributions to dose rates for luminescence and ESR dating: Large depths and long-term time variations. Radiation Measurements 23, 497-500.

Preusser, F., Blei, A., Graf, H., Schlüchter, C., 2007: Luminescence dating of Würmian (Weichselian) proglacial sediments from Switzerland: methodological aspects and stratigraphical conclusions. Boreas 36, 130-142.

Preusser, F., Chithambo, M.L., Götte, T., Martini, M., Ramseyer, K., Sendezera, E.J., Susino, G.J., Wintle, A.G., 2009: Quartz as a natural luminescence dosimeter. Earth-Science Reviews 97, 184-214.

Preusser, F., Degering, D., Fuchs, M., Hilgers, A., Kadereit, A., Klasen, N., Krbetschek, M.R., Richter, D., Spencer, J.Q.G., 2008: Luminescence dating: basics, methods and applications. E&G - Quaternary Science Journal 57, 95-149.

Przybylski, B., 2008: Geomorphic traces of a Weichselian ice stream in the Wielkopolska Lowland, western Poland. Boreas 37, 286-296.

Putkonen, J., Swanson, T., 2003: Accuracy of cosmogenic ages for moraines. Quaternary Research 59, 255-261.

Putnam, A.E., Schaefer, J.M., Barrell, D.J.A., Vandergoes, M., Denton, G.H., Kaplan, M.R., Finkel, R.C., Schwartz, R., Goehring, B.M., Kelley, S.E., 2010: In situ cosmogenic ^{10}Be production-rate calibration from the Southern Alps, New Zealand. Quaternary Geochronology 5, 392-409.

Raymo, M.E., Ruddiman, W.F., 1992: Tectonic forcing of late Cenozoic climate. Nature 359, 117-122.

Reimann, T., 2012: "The riddle of the sands" - Luminescence dating of coastal sediments from the southern Baltic Sea and southern North Sea coast, Department of Geosciences. Freie Universität Berlin.

Reimer, P.J., Bard, E., Bayliss, A., Beck, J.W., Blackwell, P.G., Ramsey, C.B., Buck, C.E., Cheng, H., Edwards, R.L., Friedrich, M., Grootes, P.M., Guilderson, T.P., Haflidason, H., Hajdas, I., Hatte, C., Heaton, T.J., Hoffmann, D.L., Hogg, A.G., Hughen, K.A., Kaiser, K.F., Kromer, B., Manning, S.W., Niu, M., Reimer, R.W., Richards, D.A., Scott, E.M., Southon, J.R., Staff, R.A., Turney, C.S.M., van der Plicht, J., 2013: Intcal13 and Marine13 Radiocarbon Age Calibration Curves 0-50.000 Years Cal Bp. Radiocarbon 55, 1869-1887.

Reineck, H.-E., Singh, I.B., 1980: Depositional sedimentary environments: with reference to terrigenous clastics, 2., rev.and updated ed. Springer, Berlin.

Rendell, H.M., Webster, S.E., Sheffer, N.L., 1994: Underwater bleaching of signals from sediment grains: new experimental data. Quaternary Science Reviews 13, 433-435.

Rhodes, E.J., 2011: Optically Stimulated Luminescence Dating of Sediments over the Past 200,000 Years. Annual Review of Earth and Planetary Sciences 39, 461-488.

Rinterknecht, V., Börner, A., Bourlès, D., Braucher, R., 2014: Cosmogenic ^{10}Be dating of ice sheet marginal belts in Mecklenburg-Vorpommern, Western Pomerania (northeast Germany). Quaternary Geochronology 19, 42-51.

Rinterknecht, V., Braucher, R., Böse, M., Bourles, D., Mercier, J.L., 2012: Late Quaternary ice sheet extents in northeastern Germany inferred from surface exposure dating. Quaternary Science Reviews 44, 89-95.

Rinterknecht, V.R., Bitinas, A., Clark, P.U., Raisbeck, G.M., Yiou, F., Brook, E.J., 2008: Timing of the last deglaciation in Lithuania. Boreas 37, 426-433.

Rinterknecht, V.R., Clark, P.U., Raisbeck, G.M., Yiou, F., Bitinas, A., Brook, E.J., Marks, L., Zelcs, V., Lunkka, J.P., Pavlovskaya, I.E., Piotrowski, J.A., Raukas, A., 2006a: The last deglaciation of the southeastern sector of the Scandinavian Ice Sheet. Science 311, 1449-1452.

Rinterknecht, V.R., Marks, L., Piotrowski, J.A., Raisbeck, G.M., Yiou, F., Brook, E.J., Clark, P.U., 2005: Cosmogenic Be-10 ages on the Pomeranian Moraine, Poland. Boreas 34, 186-191.

Rinterknecht, V.R., Marks, L., Piotrowski, J.A., Raisbeck, G.M., Yiou, F., Brook, E.J., Clark, P.U., 2006b: Cosmogenic Be-10 ages on the Pomeranian moraine, Poland': Reply to comments. Boreas 35, 605-606.

Rinterknecht, V.R., Pavlovskaya, I.E., Clark, P.U., Raisbeck, G.M., Yiou, F., Brook, E.J., 2007: Timing of the last deglaciation in Belarus. Boreas 36, 307-313.

Rodnight, H., 2008: How many equivalent dose values are needed to obtain a reproducible distribution? Ancient TL 26, 8.

Rutzinger, M., Höfle, B., Vetter, M., Pfeifer, N., 2011: Chapter Eighteen - Digital Terrain Models from Airborne Laser Scanning for the Automatic Extraction of Natural and Anthropogenic Linear Structures, in: Mike J. Smith, P.P., James, S.G. (Eds.), Developments in Earth Surface Processes. Elsevier, pp. 475-488.

Salcher, B.C., Hinsch, R., Wagreich, M., 2010: High-resolution mapping of glacial landforms in the North Alpine Foreland, Austria. Geomorphology 122, 283-293.

Samouëlian, A., Cousin, I., Tabbagh, A., Bruand, A., Richard, G., 2005: Electrical resistivity survey in soil science: a review. Soil and Tillage Research 83, 173-193.

Schaefer, J.M., Lifton, N., 2013: Cosmogenic nuclide dating | Methods, in: Elias, S.A., Mock, C.J. (Eds.), Encyclopedia of Quaternary Science (Second Edition). Elsevier, Amsterdam, pp. 410-417.

Schneider, R., 1965: Die Frankfurter Staffel (in German), in: Gellert, J.F. (Ed.), Die Weichsel-Eiszeit im Gebiet der Deutschen Demokratischen Republik. Akademie-Verl., Berlin.

Scholz, E., 1970: Geomorphologische Übersichtskarte Frankfurt-Eberswalde, in: Gellert, J.F., Scholz, E. (Eds.). Haack, Gotha.

Schrott, L., Sass, O., 2008: Application of field geophysics in geomorphology: Advances and limitations exemplified by case studies. Geomorphology 93, 55-73.

Scourse, J., 2006: Comment on: Numerical ^{230}Th/U dating and a palynological review of the Holsteinian/Hoxnian Interglacial by Geyh and Müller. Quaternary Science Reviews 25, 3070-3071.

Scourse, J.D., Haapaniemi, A.I., Colmenero-Hidalgo, E., Peck, V.L., Hall, I.R., Austin, W.E.N., Knutz, P.C., Zahn, R., 2009: Growth, dynamics and deglaciation of the last British–Irish ice sheet: the deep-sea ice-rafted detritus record. Quaternary Science Reviews 28, 3066-3084.

Shackleton, N.J., Sánchez-Goñi, M.F., Pailler, D., Lancelot, Y., 2003: Marine Isotope Substage 5e and the Eemian Interglacial. Global and Planetary Change 36, 151-155.

Silverman, B.W., 1986: Density Estimation for Statistics and Data Analysis. Chapman & Hall, London.

Słowiński, M., Błaszkiewicz, M., Brauer, A., Noryśkiewicz, B., Ott, F., Tyszkowski, S., 2015: The role of melting dead ice on landscape transformation in the early Holocene in Tuchola Pinewoods, North Poland. Quaternary International 388, 64-75.

Smith, A.G., Pickering, K.T., 2003: Oceanic gateways as a critical factor to initiate icehouse Earth. Journal of the Geological Society 160, 337-340.

Smith, M.J., 2011: Chapter Eight - Digital Mapping: Visualisation, Interpretation and Quantification of Landforms, in: Mike J. Smith, P.P., James, S.G. (Eds.), Developments in Earth Surface Processes. Elsevier, pp. 225-251.

Smith, M.J., Clark, C.D., 2005: Methods for the visualization of digital elevation models for landform mapping. Earth Surface Processes and Landforms 30, 885-900.

Smith, M.J., Wise, S.M., 2007: Problems of bias in mapping linear landforms from satellite imagery. International Journal of Applied Earth Observation and Geoinformation 9, 65-78.

Smith, R.C., Sjogren, D.B., 2006: An evaluation of electrical resistivity imaging (ERI) in Quaternary sediments, southern Alberta, Canada. Geosphere 2, 287-298.

Stackebrandt, W., 2009: Subglacial channels of Northern Germany – a brief review. Zeitschrift der deutschen Gesellschaft für Geowissenschaften 160, 203-210.

Stackebrandt, W., Lippstreu, L., 2010: Brandenburg – Landescharakter und geologischer Bau, in: Stackebrandt, W., Andreae, A., Strahl, J. (Eds.), Atlas zur Geologie von Brandenburg, 4. ed. LBGR, Cottbus, pp. 10-16.

Standke, G., 2015: Tertiär - Einführung, in: Stackebrandt, W., Franke, D. (Eds.), Geologie von Brandenburg. Schweizerbart'sche Verlagsbuchhandlung, Stuttgart, pp. 259-262.

Stephan, H.-J., Müller, U., 2010: Frankfurt (Oder)-Formation, In: LithoLex online database. Hannover: BGR. Available from: http://www.bgr.bund.de/litholex.

Stephan, H.-J., Müller, U., 2012: Brandenburg-Formation. In: LithoLex online database. Hannover: BGR. Available from: http://www.bgr.bund.de/litholex.

Stephan, H.J., 2011: Ellund-Formation, In: LithoLex online database. Hannover: BGR. Available from: http://www.bgr.bund.de/litholex.

Stone, J.O., 2000: Air pressure and cosmogenic isotope production. Journal of Geophysical Research: Solid Earth 105, 23753-23759.

Stroeven, A.P., Hättestrand, C., Kleman, J., Heyman, J., Fabel, D., Fredin, O., Goodfellow, B.W., Harbor, J.M., Jansen, J.D., Olsen, L., Caffee, M.W., Fink, D., Lundqvist, J., Rosqvist, G.C., Strömberg, B., Jansson, K.N., 2016: Deglaciation of Fennoscandia. Quaternary Science Reviews 147, 91-121.

Stroeven, A.P., Heyman, J., Fabel, D., Björck, S., Caffee, M.W., Fredin, O., Harbor, J.M., 2015: A new Scandinavian reference 10Be production rate. Quaternary Geochronology 29, 104-115.

Szymanek, M., 2016: Stable isotope composition of the Holsteinian (MIS 11) freshwater snail Valvata piscinalis (O. F. Müller, 1774) from eastern Poland and its palaeoenvironmental implications. Journal of Quaternary Science 31, 622-630.

Tarolli, P., 2014: High-resolution topography for understanding Earth surface processes: Opportunities and challenges. Geomorphology 216, 295-312.

Tarolli, P., Tarboton, D.G., 2006: A new method for determination of most likely landslide initiation points and the evaluation of digital terrain model scale in terrain stability mapping. Hydrol. Earth Syst. Sci. 10, 663-677.

Thieke, H., 2010: Mittelpleistozäner Berliner Elbelauf 1:1 000 000, in: Stackebrandt, W., Andreae, A., Strahl, J. (Eds.), Atlas zur Geologie von Berlin und Brandenburg, 4 ed. LBGR, Cottbus, pp. 50-51.

Thrasher, I.M., Mauz, B., Chiverrell, R.C., Lang, A., 2009: Luminescence dating of glaciofluvial deposits: A review. Earth-Science Reviews 97, 133-146.

Torell, O., 1875: Über einen gemeinschaftlich mit den Herren Berendt und Orth nach den Rüdersdorfer Kalkbergen unternommenen Ausflug. Zeitschrift der Deutschen Geologischen Gesellschaft 27, 961-962.

Tye, G.J., Sherriff, J., Candy, I., Coxon, P., Palmer, A., McClymont, E.L., Schreve, D.C., 2016: The δ18O stratigraphy of the Hoxnian lacustrine sequence at Marks Tey, Essex, UK: Implications for the climatic structure of MIS 11 in Britain. Journal of Quaternary Science 31, 75-92.

Van der Wateren, F.M., 2003: Ice-marginal terrestrial landsystems: Southern Scandinavian Ice Sheet margin, in: Evans, D.J.A. (Ed.), Glacial Landsystems. Arnold, London, pp. 166-203.

Van Meerbeeck, C.J., Renssen, H., Roche, D.M., 2009: How did Marine Isotope Stage 3 and Last Glacial Maximum climates differ? – Perspectives from equilibrium simulations. Clim. Past 5, 33-51.

Vandenberghe, D., De Corte, F., Buylaert, J.P., Kučera, J., Van den haute, P., 2008: On the internal radioactivity in quartz. Radiation Measurements 43, 771-775.

Vermeesch, P., 2012: On the visualisation of detrital age distributions. Chemical Geology 312–313, 190-194.

Wehr, A., Lohr, U., 1999: Airborne laser scanning—an introduction and overview. ISPRS Journal of Photogrammetry and Remote Sensing 54, 68-82.

Wintle, A.G., 2008: Luminescence dating: where it has been and where it is going. Boreas 37, 471-482.

Wintle, A.G., Murray, A.S., 2006: A review of quartz optically stimulated luminescence characteristics and their relevance in single-aliquot regeneration dating protocols. Radiation Measurements 41, 369-391.

Woithe, F., 2003: Untersuchungen zur postglazialen Landschaftsentwicklung in der Niederlausitz, Mathematisch-Naturwissenschaftliche Fakultät. Christian-Albrechts-Universität zu Kiel.

Woldstedt, P., 1925: Die großen Endmoränenzüge Norddeutschlands. Zeitschrift der Deutschen Geologischen Gesellschaft 77, 172-184.

Woodward, J., 2014: The Ice Age: A Very Short Introduction. Oxford University Press.

Wysota, W., Molewski, P., Sokołowski, R.J., 2009: Record of the Vistula ice lobe advances in the Late Weichselian glacial sequence in north-central Poland. Quaternary International 207, 26-41.

Young, N.E., Schaefer, J.M., Briner, J.P., Goehring, B.M., 2013: A ^{10}Be production-rate calibration for the Arctic. Journal of Quaternary Science 28, 515-526.

Zhang, W., Montgomery, D.R., 1994: Digital elevation model grid size, landscape representation, and hydrologic simulations. Water Resources Research 30, 1019-1028.

Zöller, L., Schmidt, C., 2016: OSL-Altersbestimmungen an den spätsaale- bis eemzeitlichen Ablagerungen von Jänschwalde. Sonderband Brandenburgische geowissenschaftliche Beiträge / Arbeitsberichte zur Bodendenkmalpflege in Brandenburg 22 / 28, 191-197.

VIII APPENDIX

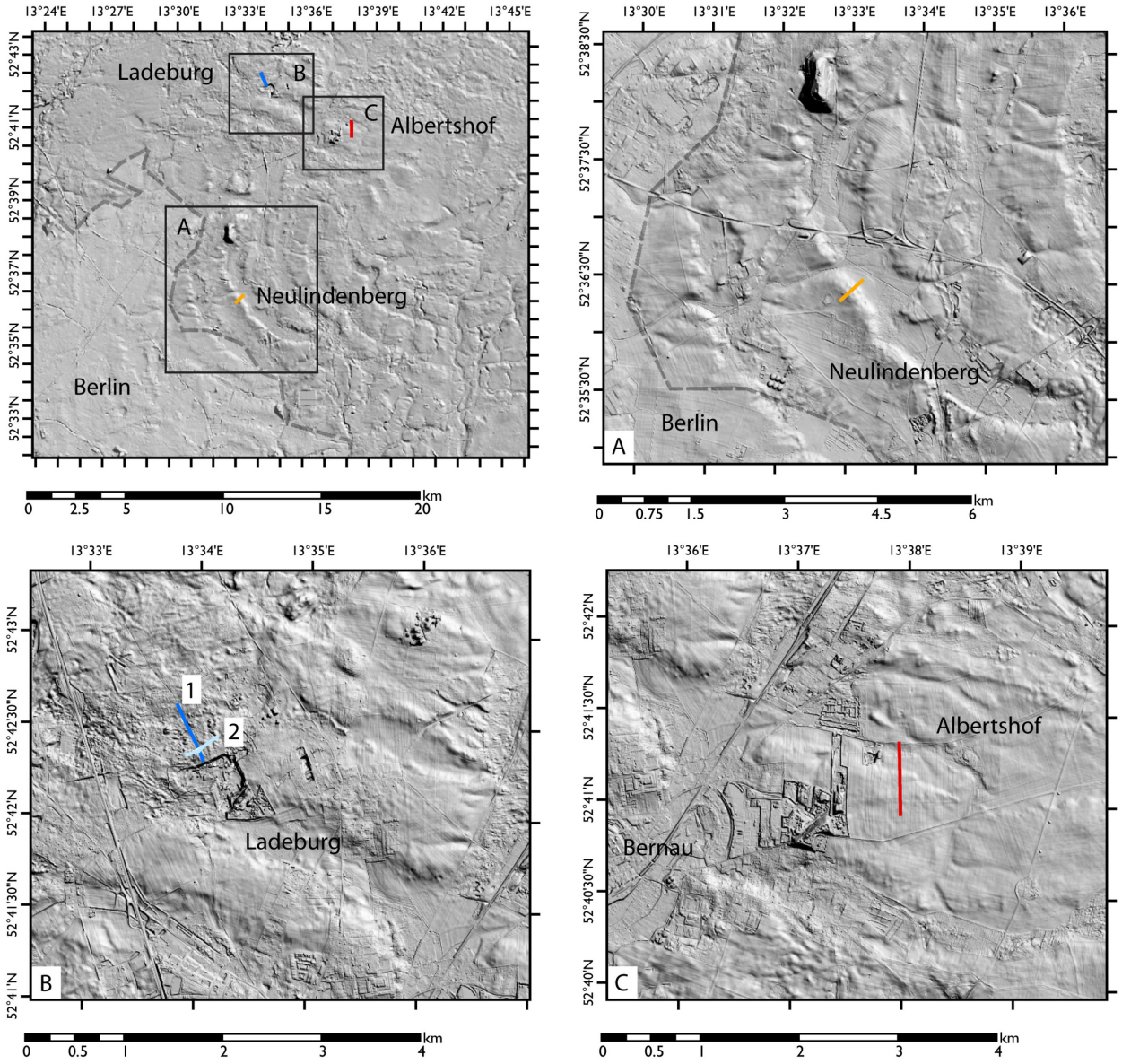

Appendix 1: Location of ERT profile sections in the middle Barnim area. B: Profile 1 is presented in Appendix 2; Profile 2 is presented in Hardt et al. (2016) and in section 6.

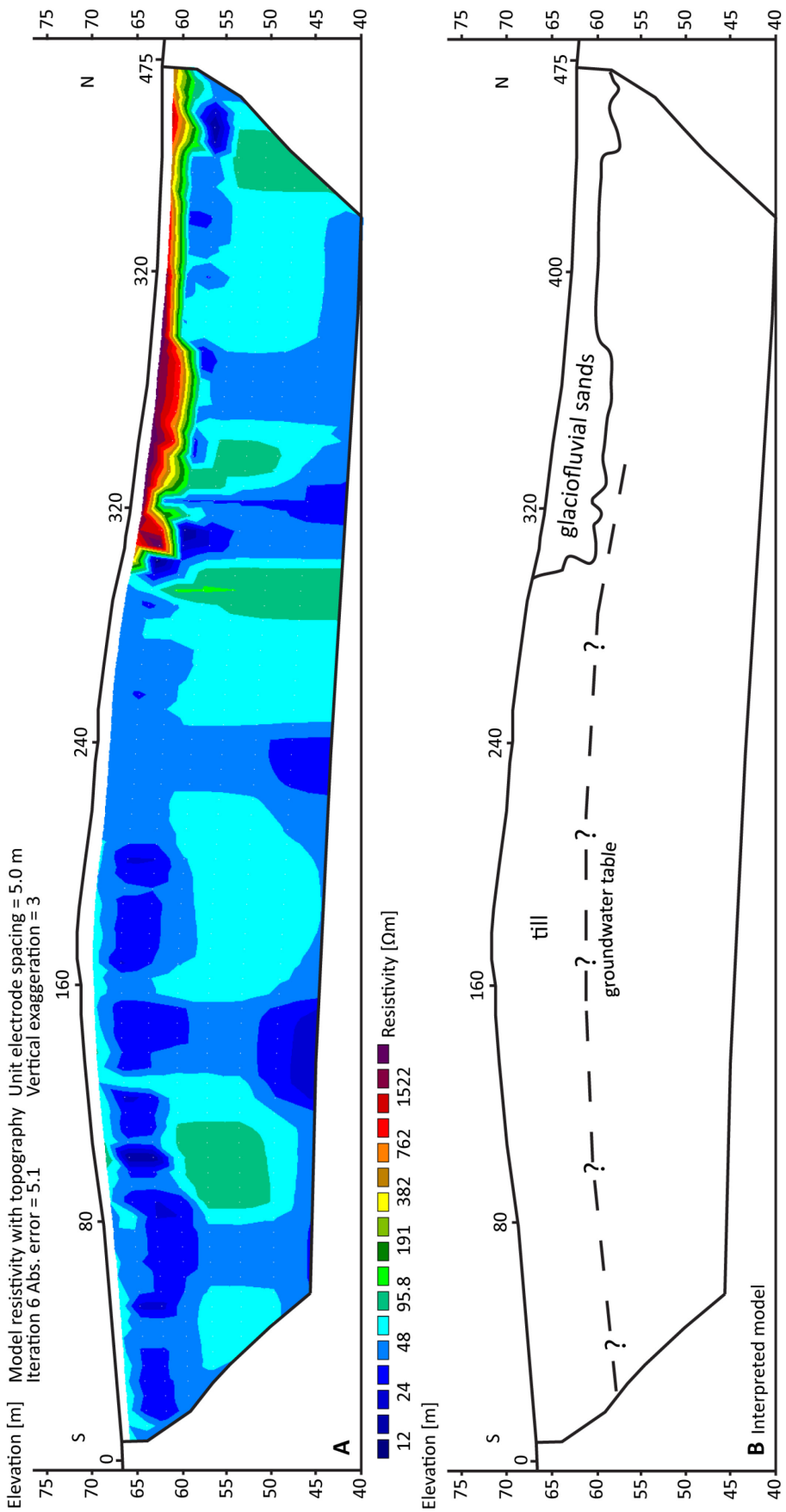

Appendix 2: ERT results from ridge structure Neulindenberg (A in Appendix 1). Wenner array with 5 m electrode distance. Data recorded on 9 September 2015.

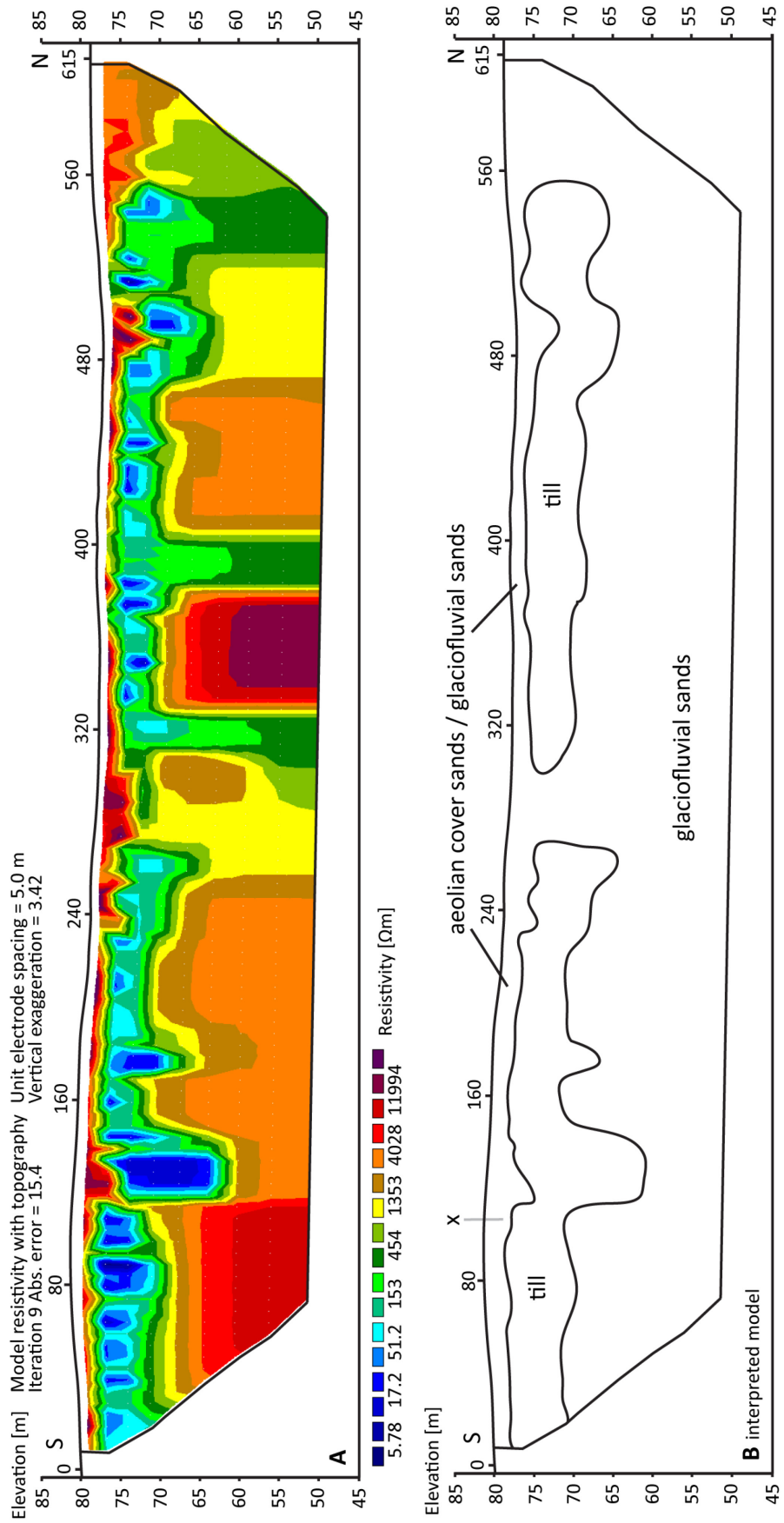

Appendix 3: Additional ERT results from Ladeburg (B 1 in Appendix 1). Wenner array with 5 m electrode distance. Data recorded on 9 March 2016. X: Intersection with ERT profile of section 6.4.2.

IX LIST OF PUBLICATIONS

Publications in international peer-reviewed journals (with reference to the dissertation project):

- **Hardt, J.**, Lüthgens, C, Hebenstreit, R., Böse, M., (2016). Geochronological (OSL) and geomorphological investigations at the presumed Frankfurt ice marginal position in northeast Germany. *Quaternary Science Reviews* 154, 85-99.
- **Hardt, J.**, Böse, M., 2016. The timing of the Weichselian Pomeranian ice marginal position south of the Baltic Sea: A critical review of morphological and geochronological results. *Quaternary International (in press)*.
- **Hardt, J.**, Hebenstreit, R., Lüthgens, C., Böse, M., 2015. High-resolution mapping of ice-marginal landforms in the Barnim region, northeast Germany. *Geomorphology* 250, 41-52.

Publications in international peer-reviewed journals (independent of the dissertation project):

- Böse, M., Hebenstreit, R., **Hardt, J.**, 2014. A deformation till at Hohuan Shan, Taiwan. *Quaternary International* 321, 55-58.

X LIST OF CONFERENCE CONTRIBUTIONS

Oral presentations (with reference to the dissertation project):

- **Hardt, J.**, Lüthgens, C, Böse, M., 2016. Geomorphologische und Geochronologische Studien zur Frankfurt-Phase im Raum Barnim (Brandenburg, NE-Deutschland). DEUQUA 2016, 38. Hauptversammlung der deutschen Quartärvereinigung, 25.-30.09.2016, Dresden.
- **Hardt, J.**, Böse, M., 2015: Geomorphologische und Geochronologische Untersuchungen der lobusförmigen Rückenstrukturen im Bereich des mittleren Barnim (Brandenburg) - neue Einsichten in den Eisrückzug während der Frankfurt-Phase. 79. Tagung der Arbeitsgemeinschaft Norddeutscher Geologen, 26.-29.05.2015, Güstrow.
- **Hardt, J.**, Böse, M., 2014: Hochaufgelöste Geländemodelle als Werkzeug zur Neubewertung von Glaziallandschaften – das Beispiel der Frankfurter Eisrandlage im Raum Barnim (NO-Deutschland). DEUQUA 2014, 37. Hauptversammlung der deutschen Quartärvereinigung, 24.-29.09.2014, Innsbruck.
- **Hardt, J.**, Böse, M., 2014: Late Quaternary ice sheet dynamics in northeastern Germany – new insights in the formation of the Frankfurt ice marginal position based on the analysis of a high resolution LiDAR digital elevation model. INQUA Peribaltic working group symposium, 16.-22.08.2014, Latvia.
- **Hardt, J.**, 2014: The Frankfurt ice marginal position in the Barnim area - reinterpretation of the genesis of a glacial landscape on basis of the interpretation of a high resolution LiDAR-DEM. 8th Young Geomorphologists Workshop, 23.-25.05.2014, Usedom.

Poster presentations (with reference to the dissertation project):

- **Hardt, J.**, Lüthgens, C., Böse, M., 2016: The Frankfurt phase - Geomorphological and geochronological investigations to reassess a "classical" ice marginal position in NE Germany. 10th International Young Geomorphologists Workshop, 27.-29.05.2016, Werbellinsee.

- **Hardt, J.**, Nitzsche, C., Lüthgens, C., Böse, M., 2015: OSL-Dating of glaciofluvial sediments in the Barnim region (Brandenburg) - new insights in the Frankfurt ice marginal position. German Luminescence- and ESR-Meeting, 06.-08.11.2015, Berlin.
- **Hardt, J.**, Lüthgens, C., Böse, M., 2015: Geomorphologische und Geochronologische (OSL) Studien in der Umgebung der Frankfurter Eisrandlage im Raum Barnim (Brandenburg). Arbeitskreis Geomorphologie 2015, 03.10.-04.10.2015, Berlin.
- Böse, M., **Hardt, J.**, 2015: About Weichselian Ice-Marginal Positions South of the Baltic Sea - Stratigraphy and Critical Discussion of Age Estimates. EGU General Assembly 2015, Vienna.
- **Hardt, J.**, Lüthgens, C, Böse, M., 2014: Geochronological analyses (OSL) of glaciofluvial sediments in the proximity of the Frankfurt ice marginal position on the Barnim till plain (Brandenburg). German Luminescence- and ESR-Meeting, 14.-16.11.2014, Gießen.
- **Hardt, J.**, Böse, M., Hebenstreit, R., Lüthgens, C., 2014: New insights into palaeoglaciological processes in northeastern Germany by analysis of a LiDAR DEM: using high-resolution elevation data to reassess the geomorphology of the Barnim till plain. EGU General Assembly 2014, Vienna.

Poster presentations (independent of the dissertation project):

- Hebenstreit, R., **Hardt, J.**, Böse, M., 2015: New evidence for Quaternary glaciations in Taiwan and a recalculation of the equilibrium line altitude. XIX INQUA Congress, Nagoya.

Public presentations:

- **Hardt, J.**, 2016: Geomorphologische, geochronologische und fernerkundliche Untersuchungen der Glaziallandschaft Barnim. Oder: Vom Sandkorn zur Landschaft. Vortragsreihe des Vereins Märkische Eiszeitstraße, Eberswalde, 20.01.2016.
- **Hardt, J.**, 2014: Untersuchungen zur Neubewertung der Glaziallandschaft in der Umgebung Frankfurter Eisrandlage im Raum Barnim. Colloquium der Geomorphologie des Geographischen Instituts der Humboldt-Universität zu Berlin, 17.12.2014.

XI CURRICULUM VITAE

For privacy reasons, the curriculum vitae is not included in the online version of this thesis.

EIDESSTATTLICHE ERKLÄRUNG

Hiermit erkläre ich, Jacob Hardt, dass ich die vorliegende Dissertation selbständig verfasst und keine anderen als die von mir angegebenen Quellen und Hilfsmittel verwendet habe.

Ich erkläre, dass die Arbeit nicht schon einmal in einem früheren Promotionsverfahren eingereicht wurde.

Berlin, 13.12.2016 _____